The Performance of Double Skin Façade Window Systems by Experimental Methods

By

Suzie Jaimie Mkandawire

B.S. Mechanical Engineering, 2000

Massachusetts Institute of Technology

Submitted to the Department of Mechanical Engineering
in partial fulfillment of the requirements for the Degree of
Masters of Science in Mechanical Engineering

at the

Massachusetts Institute of Technology

February 2002

Signature of Author.....
Department of Mechanical Engineering
January 18,2002

Certified by.....
Leon Glicksman
Professor of Mechanical Engineering
Thesis Supervisor

Accepted by.....
Ain A. Sonin
Chairman, Department Committee on Graduate Students

The Performance of Double Skin Façade Window Systems by Experimental Methods

by

Suzie J. Mkandawire

Submitted to the Department of Mechanical Engineering
on January 18, 2002 in Partial Fulfillment of the
Requirements for the Masters of Science in Mechanical Engineering

ABSTRACT

Double Skin Façade (DSF) window systems have been used in Europe for over thirty years. They have changed the face of building architecture as well as cut down operating costs of Heating, Ventilation, and Air Condition (HVAC). The DSF window is defined has having an interior and exterior windowpane. The cavity between the panes is where air circulates from outside to inside. A shading device, located in the cavity, is used to help dissipate or store the excess energy depending on the weather conditions. The technology is new to the United States. However, by thoroughly testing the system many questions can be answered, which may change building codes to allow these window systems to be implemented in the US. Ultimately, the US will incorporate the DSF window system into all sorts of buildings.

There are three main goals for testing the performance of the Double Skin Façade window system. These goals are to record an extensive amount of data, to verify the mathematical model and experimental data taken from a life-size model created by Permasteelisa (DSF manufacturer), and to apply the model to large-scale applications.

Extensive Data

There is very little data to back up the claim that the Double Skin Façade window system is efficient. The companies who make the windows are not too forthcoming with publishing their data. There are many parameters involved in the system, and it is important to find out how each of these parameters effects the overall performance. Four parameters will be the focus of this research. They are heat source, air velocity, air cavity dimension and position of blinds. The data will be valuable because it will corroborate the facts of the DSF window system as well as validate the mathematical model, which is the second goal of this thesis.

Verify Mathematical Model

A mathematical model was created to predict the performance of the DSF window system. However, the accuracy of the model as yet to be determined. Ultimately, the model will be available on the World Wide Web for anyone to use. The data is needed at this point to determine the accuracy of the model, as well as compare the data from Permasteelisa.

Apply Model to Large Scale Application

Once the model has been validated, it can be used to model life size buildings. The value of the program is that a variety of window facades can be modeled without building a full-scale experiment. Time and money is not wasted testing different

scenarios by using the mathematical model. Architects and other professionals involved in the preliminary stages of constructing a building can use this model to double-check the thermal efficiency of the structure. The long-term savings in terms of heating and cooling the building are worth the extra effort in the beginning.

Thesis Supervisor: **Leon Glicksman**
Title: Professor of Mechanical Engineering

Acknowledgements

I would like to thank friends and family who helped me through out this research project. I would especially like to thank Professor Leon Glicksman who made the thesis work interesting and challenging. Daniel Arons and Matthew Lehar for their contributions and advice. The Permasteelisa Company for their financial support, which gave me the opportunity to explore this field of research. The research project did make graduate school a fulfilling experience. Thank you.

Biographic Note

I completed my Bachelors of Science June 2000 at the Massachusetts Institute of Technology (MIT) in Mechanical Engineering. I published an undergraduate thesis which was titled, "". I will be finishing a Masters of Science at MIT upon completing a thesis as well in Mechanical Engineering. I have presented my research to a building technology conference at Harvard. I received a GEM Fellowship for the 2000-2001 academic years to attend graduate school. I have interned at Dupont and Ford Motor Companies in addition to being a design tutor for a summer program on MIT campus. I have volunteered to tutor children in math, reading, and writing in the Cambridge Community.

Table of Contents

List of Figures

Chapter One: Introduction

1.1 History and Background of Double Skin Facades

A Swedish company, ECKNO, first patented the Double Skin Façade (DSF) window system in 1957 [Arons, 1999]. They were one of the first companies to realize the great potential and need for such a device. By the late sixties, the company had constructed the first DSF or airflow window building. They brought a new technology to the engineering and architectural fields, which would soon change how buildings were constructed and operated. The introduction of the new airflow building brought double skin façade windows into mass-production.

Commerzbank in Frankfurt, Germany is one of the well-known double skin façade buildings, which was erected in the nineties. The DSF window system was chosen for this building because of the cost savings. It is said that the building uses up 30% less energy than a comparable traditional high rise [Pearson, 1997]. The reduction was possible because of the high heat insulation quality of the facades and glazing (quality of glass), combined with the accurate measuring of the performance. The efficiency of the building definitely influenced engineers, who were looking to cut costs, and architects, who were looking for a change of façade design. Figure 1 is a photograph of the Commerzbank taken from different views. The building is definitely not a traditional high rise.

Figure 1 Side View of Commerzbank

Briarcliff House at Faranbourough is yet another famous DSF building, which is noted for managing solar loads and noise impact well for low-rise buildings. How is it possible for the DSF

buildings: to decrease the amount of energy it uses to operate, to decrease the amount of noise coming from the outside, and to look appealing to architects? The double skin façade window is a specialized system, which addresses the issues of heat gain in buildings, while representing the new façade technology.

Figure 2 Front view of Commerzbank

Double Skin Façade window systems are distinguished from other window configurations because of its unique design. DSF consists of an interior and exterior windowpane set anywhere from 10 centimeters to a meter apart. The distance between the two windows creates an air cavity, which acts as a buffer. It filters out noise and stale air, which plague city buildings. The inner windowpane is usually operable; it can open to let in the fresh circulating air without the treacherous winds of tall buildings. In addition to the air cavity, a solar shading device, usually a Venetian Blind, is located between the windows. The shading device has the ability to rotate to let in very little or a lot of sunshine. It facilitates the removal of any excess heat and can store heat as well. The DSF window system is defined as a dynamic process because air is allowed to move through the cavity. The two methods of air movement are natural ventilation, where air can flow in from outside or forced convection, where fans move the air. When the DSF windows are integrated into a building, the joined air cavities create an envelope. The double skin façade buildings are sometimes referred to as building envelopes because the exterior windowpane of the DSF forms a pocket around the building. Figure 2 is another photograph of the Commerzbank in Germany.

1.2 Types of Double Skin Facades and Design Configurations

There are three distinct types of double skin façade window systems: Double Skin Façade, Airflow Façade, and Airflow Window. The Double Skin Façade is defined as two planar elements that allow interior or exterior air to move through them. DSF is also referred to as "twin skins"[Arons, 1999]. The Air Flow Façade consists of two parallel

windowpanes, which are the height of at least one story of the building. The air inlet is at or below the floor level below one story and the exhaust is at or above the floor level above one story. Finally, the Airflow window is a shorter version of the airflow façade.

The type of airflow ventilation is also important. Depending on the weather conditions, different ventilation patterns are favored over others. For example, if it is cold and you want to choose a type of ventilation for the DSF window system, picking an airflow pattern, which keeps the circulating air warm is favored over a ventilation pattern where the air goes from hot to cold. The ventilation patterns are broken down into four categories: inside ventilation, outside ventilation, hybrid supply, and hybrid exhaust. Logically, the inside ventilation enters from the inside and exhausts to the interior. Conversely, outside ventilation inlets from the outside and exits to the exterior. The hybrid supply is a combination of the inside and outside ventilation. The modified air path is defined as pulling air from the exterior and exiting inside. The hybrid exhaust does the exact opposite. It pulls air from the inside and exits outside. It is possible to have quite a few different variations of double skin facades, because of the air flow patterns and window structure. Figure 3 visually describes the types of air ventilation pattern. The Commerzbank façade is an inside ventilation scheme. The DSF window system represented in this research most resembles an airflow window with inside ventilation. The window setup will be illustrated in greater detail in the next chapter.

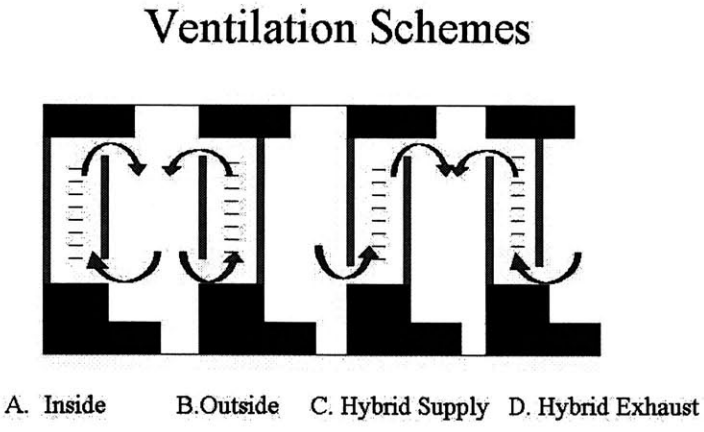

Figure 3. Air Flow Patterns

1.3 The Advantages of Double Skin Facades

The operating costs of building are high mainly because of the heating loads, which consist of computers, lighting, and people. Cooling a building may be required all year just because of the high heating loads. The type of window used in a building can

greatly effect how much energy is used to heat or cool the building. For example, if a building has single pane windows, in hot weather, tremendous amounts of heat will be generated near the window. The heat is due to radiation from the sun. In an office with a controlled climate, the air condition would be on constantly to remove the heat from the window. It may create a difference of temperature in the room. The air away from the window would be colder than the air near the window. Cooling the office would be costly if the air conditioning was running all the time. The Double Skin Façade window system has many advantages over the traditional single pane windows.

The Double Skin Façade system is an integrated approach used to combine building components where the result is energy savings. During the cooling season, air enters the cavity between to the two windows and carries away heat that would most likely collect on the blinds and near the window inside the room. The temperature of the interior window is relatively lower than if a single windowpane was used. Conversely, in the heating season, there are two scenarios.

Scenario One: The air is stagnant and warmed by the sun. The air blanket acts as a buffer and reduces the amount of heat loss by the building. Less heat is required to warm the building because the air in the cavity is optimizing the heat transfer from the sun.

Scenario Two: The air is moving through the cavity much like the cooling season process but the air is warmer. One issue that arises with this setup is how does the air maintain a warm temperature when it interacts with the cool surface of the exterior window? The air can have a ventilation pattern where it comes from inside and exhausts outside (i.e. hybrid exhaust).

By reducing the heating and cooling loads of a DSF building envelope, the usage of the heating, ventilation, and air conditioning (HVAC) system can be reduced. One component, the shading device, contributes to the reduction of the heating and cooling loads by acting as a heat sink and temporarily holds the unwanted energy until it can be removed by convection. The air moves across the shading device and takes away the heat in this convection process. Figure 4 depicts the heat transfer of the DSF window.

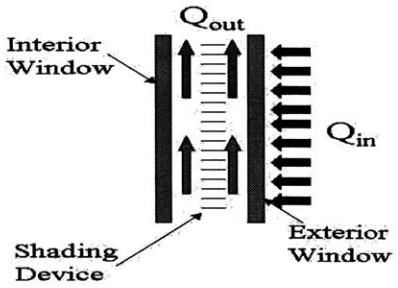

Figure 4 Heat Transfer Model

The heat is transferred through the exterior window, and the air blowing in the vertical direction in the cavity moves the heat away from the interior window. The speed of the air controls how fast the extra heat is dissipated. The shading device also blocks unwanted sunlight, which may create visual discomfort in the room. The occupants of the building also are satisfied because they can control their environment in terms of the amount of sunlight that enters the room.

Double Skin Façade window systems not only reduce the amount of heat transfer to rooms but reduce the amount of noise and air pollution as well. The city can be a very noisy place to work, because of the sounds generated from the street are very boisterous and distracting. The air cavity is a buffer, which filters out the noise so that the building occupants are not disturbed. Office buildings with climate controls are one extreme, which does not allow windows to open. The office can often become stuffy without fresh air. Building envelopes have the option of operable interior windows, which can receive air from the outside to get rid of the stale air of the office. Noise and air pollutes are reduced with the use of a DSF design. Designers are concerned with these issues (removal of toxins from office environment) and usually solve it with mechanical ventilation (i.e. fans), however DSF windows can achieve the same goal with its unique style. The air cavity is often described as a barrier to interaction with the outside, which is how it reaches the goal of reducing noise from the city.

The cost savings of the building is not only dependent on the one-time construction costs but also the operating costs. Many of the buildings economic and ecological needs are realized through facility management [Fischer, Gruneis, 1997]. DSF buildings are beneficial because of the improved thermal performance over time. The costs of heating and cooling the building decrease as the thermal performance increases.

The environmental quality of the air is enhanced over time. The operating costs of lighting a building can be reduced by taking advantage of daytime lighting. All of these factors contribute to energy savings of the building.

A study was conducted in California where Venetian Blinds were used to control the amount of light entering the office. Just enough light was let in so that the occupants of the building could work comfortably. The electrical lights were dimmed in times of bright day lighting. The lights were more of a back up to the day lighting. This research was a proof of concept test that was designed to work out bugs and refine the Venetian Blind and lighting system. The study was conducted for about a year and the results were: 1% – 22% lighting energy savings, 13% - 28% cooling load reduction, and 13% - 28% peak cooling load reduction were achieved. The day lighting and Venetian Blind system was compared to a static blind under clear sky and overcast year round conditions [Lee, DiBartolomeo, Vine, Selkowitz, 1998].

Double Skin Façade windows have many advantages over the traditional window configurations. Some of the key benefits are reduction of air conditioning loads in the summer, and heating loads in the winter. The building envelope reduces the amount of noise and air pollution as well as the amount of discomfort near the window. The energy savings are realized in the operating costs of a building, which come from lower electrical and HVAC costs.

1.4 Scope of Research

Background

The focus of this research is to test the thermal performance of double skin façade window systems. Presently, there is little if any data available on the thermal performance of Double Skin Facades. One group of researchers in Belgium under the lead of Hugo Hens and Dirk Saelens has done some performance measurements of DSF, and have lab model as well.

Hens' and Saelens' research is focused around actual case studies of double skin façade buildings in Brussels. They discuss the relationships between air velocity of cavity vs. energy and overall thermal resistance. By analyzing the behavior of airflow windows of an office building in Downtown Brussels, an analytical model is formed from their experimental data to prove if the airflow window is energy efficient [Hens, Saelens,

1999]. Their goal is to prove the DSF window concept rather than put effort in improving a mathematical model, which can predict the thermal performance. Moreover, future researchers would not have to rely heavily on experimental data.

The difference between Hens' and Saelens' research and the recent work is that the data recorded is analyzed with a mathematical model, which was not created to fit the experimental data, but to predict it. The motivation for this research was to verify a model created in Excel by Daniel Arons in 1999. The model takes input parameters and returns a temperature profile among other outputs, which describe the thermal performance of Double Skin Façade. The mathematical model will be described in greater detail in the results chapter.

The data collected is primarily used to verify a program, which predicts the performance of various DSF windows. The program, Design Advisor, is java based and available on the MIT web. The website is part of an effort to introduce the double skin façade window systems to companies involved in construction of buildings in America. The technology was developed in Europe and became popular because of the many benefits. American construction companies are hesitant to follow behind the Europeans and start incorporating the technology into their designs. The American building codes are different from those of Europeans so it is harder to get the DSF windows approved for construction. However, by thoroughly testing the window system many questions can be answered, which may change building codes to allow these window systems to be constructed in the US. Ultimately, it is expected that the United States construction companies will incorporate the DSF window system into all sorts of buildings.

Building Envelopes Organization

The Design Advisor program is a small part of a larger entity called Building Envelopes Organization (BEO). This organization is comprised of individuals in academia as well as professionals involved in the building construction business. The Building Envelopes Organization has a website called **buildingenvelopes.org**, where engineers, architects, designers, contractors, HVAC companies, building code officials, and anyone who has interests in this area can interact and discuss various DSF projects. People who are not to familiar with DSF window systems can access the site and find out information.

The Building Envelopes Organization has partners at MIT, Harvard, Permasteelisa (an Italian window making company, who is sponsoring this research), and about forty companies in Europe and America who have interests in Double Skin Facades. The BEO website acts as portal between people of diverse backgrounds. The website facilitates the transfer of information from members of the group, because it is difficult to send huge files via email. Members can post material on the web where others can download it.

The organization meets twice a year to present new findings in the building technology field. The results of the recent work were presented at the last meeting held at Harvard University. The experiment and preliminary results from May 2001 were described. It was a unique opportunity because companies and institutions from all over Europe were represented and were vocal about their concerns with the DSF window systems. The members had good suggestions on how to improve the buildingenvelopes.org website as well as the Design Advisor and this experiment.

The Design Advisor can be accessed through the BEO website. For the most part, the Design Advisor does not give absolute numbers; it compares various facades with each other. However for energy consumption values are calculated in W/m^2. This tool has been developed to give preliminary estimates for the performance of building facades. Double skin facades may be compared to conventional facades, while the location, occupancy and depth of the perimeter space may be adjusted and the effects viewed.

The Design Advisor is for any one who has some knowledge about or interest of DSF windows. The user does not have to have a technical background to understand the results. The program is user friendly and the information that it asks for is standard, for example the height of the room, the location of the site, and the occupancy. For the more experienced user there are advanced options to model their particular project. The depth of the air cavity as well as the type of glass used can be added for complexity. If the user is having problems understanding the effects of the variables, there is help available through the Buildingenevelopes.org website. The Design Advisor as the capability of running up to four cases simultaneously. For instance, if a user is curious about an inside ventilation versus an outside ventilation for hot weather conditions in Africa and Europe,

the program can manage it. When the program runs it generates three types of results: comfort, energy, and day lighting.

Comfort refers to the how occupants feel at various locations in the room. The comfort is illustrated through colors: red is too hot, blue is too cold, and amber is just right. The comfort of the building in Europe can be compared to the comfort of the building in Africa. The comfort level near the window is dependant on the inside window temperature, one of the key quantities measured in the experiment. Similarly, the energy results (series of bar graphs), which are broken down in to monthly or yearly energy usage are related to each other. The energy savings of one scenario over the other is realized by analyzing the results. Finally, the day lighting result, which is a 3D virtual model of the room, illustrates how comfortable the room is with the weather conditions. If it were a sunny day, the room would be very bright due to the sun. The visual comfort is monitored with the day lighting result. If a scenario has too much day lighting than the shading device can be easily adjusted to compensate for the sun. The user has the option of generating a report, which summarizes the results. The user can choose any combination of results for the report. The Design Advisor has much potential in the building technology field. The software can be used to influence users that the double skin façade technology is important to the future building construction.

1.5 Goals of Research

There are three main goals for testing the performance of the double skin façade window system. These goals are to record an extensive amount of data, and use that data to verify the mathematical model, Design Advisor, and the experimental data taken from a life-size model created by Permasteelisa (DSF manufacturer), and to apply the model to large-scale application. To this date there has not been a validated program, which predicts the performance of DSF window systems. The data collected for this research is crucial for supporting both the Design Advisor and Permasteelisa research.

Extensive Data

There is very little data to back up the claim that the double skin façade window system is efficient. The companies who make the windows are not too forthcoming with publishing their data. There are many parameters involved in the system, and it is

important to find out how each of these parameters affects the overall performance. Four parameters, which control the output: are type of heat source (i.e. lamp or heater), air velocity, air cavity dimension and position of blinds. The data will be valuable because it will corroborate the facts of the DSF window system as well as validate the Design Advisor and Permasteelisa Data, which is the second goal of this thesis.

Verify Design Advisor and Permasteelisa Research

A mathematical model, Design Advisor, was created to predict the performance of the DSF window system. However, the accuracy of the model is yet to be determined. The data is needed at this point to determine the accuracy of the model, as well as compare the data from Permasteelisa. This research will be one of the first to have published data from a model and experiment, which prove that the DSF window system is efficient in terms of energy usage.

Apply Model to Large Scale Application

Once the model has been validated, it can be used to model life size buildings. The value of the program is that a variety of window facades can be modeled without building a full-scale experiment. By using Design Advisor, time and money is not wasted testing different scenarios. Architects and other professionals involved in the preliminary stages of constructing a building can use this model to double-check the thermal efficiency of the structure. The long-term savings with respect to heating and cooling buildings are worth the extra effort in the beginning.

1.6 Summary

Double Skin Facades were developed over forty years ago in Europe, yet they have very little popularity in America. They are attractive because of their unique style and significant energy savings. The Commerzbank in Germany was one of the first building envelopes erected and it was documented that building with a traditional façade (single window pane) of its size consumes 30 % more energy. In the long run that energy savings adds up to a substantial amount of money.

The Building Envelopes Organization is a group of people interested in spreading the knowledge of DSF to professionals and scholars with interests or curiosities in

building construction. They have many resources available to members including the Design Advisor, a mathematical model, which compares the performance of one DSF window configuration to another, where the similarities and contrasts of the scenarios are generated. The goals of the research are to record an extensive amount of data, to verify the mathematical model and the experimental data taken from a life-size model created by Permasteelisa (DSF manufacturer), and to apply the model to large-scale application.

The next chapter, experimental setup, will discuss the components, which define the Double Skin Façade window system. The details of the instrumentation and parameters are also described in that section. Chapter three is about the procedures and focuses on the beginning of the experimental phase. Many of the unforeseen kinks are discussed and solved to record the most useful data. The results chapter follows the procedure chapter where the actual comparison of the model and data is performed. The accuracy of the mathematical model is also determined. Finally, the research is concluded in the last chapter.

Chapter Two: Experimental Setup

In order to collect data on the performance of double skin façade window systems a small scale DSF window system was constructed. The primary materials used were plywood, gypsum (dry wall), dexion steel, storm glass window, and duct metal. The apparatus was designed and completed with in one semester. Minor machining was required (i.e. milling and sawing). Many of the materials were bought ready for assembly, because function was more important than form. The five main components to the experimental apparatus are: frame, heated box, duct, windows and shading device, and insulation.

2.1 Experiment Components

Frame

One of the critical issues in designing the apparatus was how was it going to stay together? Dexion was implemented to support the experiment components because of its durability. Figure 5 shows the frame structure, before other components were added. The drawing depicts the frame as parallelepiped with different area base and top.

Figure 5 Frame of DSF Window

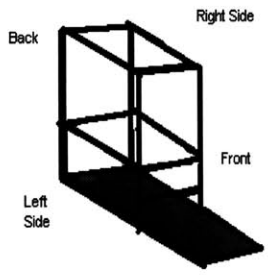

Heated Box

A temperature difference had to be created to simulate outside weather conditions versus room temperature. An enclosed area was needed to achieve this goal. The most convenient method of isolating the space was to create a box out of plywood. The box is located 1 ft. from the back end of the frame. Since the box is 2 ft. in length, a foot of the box sticks out from the frame.

The box sits flush to the exterior window and is enclosed with a door on the other end. The door allows easy access to the contents in the box in case parameters have to change. Inside the box, a layer of gypsum commonly known as dry wall protects the wood. One concern with using hot metal objects enclosed in wood was fire safety.

Usually, experiments were run in succession, which means the heat source could be on for eight hours. In that time the wood can heat to very high temperatures, and the possibility of an accident happening would increase. To eliminate the possibility of a fire the gypsum, which is fire retardant, was incorporated into the heat box design.

Duct System

In the center or body of the frame, the two parallel windows are suspended (see Figure 6a). The Duct system was built directly above and below the windows. The duct, in conjunction with the windows, forms the path for the airflow pattern. The mock DSF window system has inside ventilation airflow, which means the air is entering and exhausting inside the room. In a life size model, the air would enter below the floor level and exit above the ceiling.

The top section of the duct consists of a plate and rectangular shaft. The shaft has a ventilation (exhaust) fan attached 6“ from the top. The fan's face fits snug in the shaft. The dimensions of the shaft and plate were both governed by the fan's dimensions. The fan has the capacity of creating air speeds as low as .1 m/s up to on the order of 1 m/s within the spaces between the windows.

The bottom section of the duct system is simply three rectangular plates that cover up the exposed cavity regions and a louver. The louver minimizes turbulent airflow by its smooth curved surface. The louver is the point of entry of the air coming into the double skin façade system.

Windows and Shading Device

The windows and shading device complete the cavity. The windows are made of clear storm glass which has a thickness of 1/8 “, and have dimensions 2 ft. by 4 ft. The exterior window is fixed 12” from the rear of the frame. The interior window is movable so it does not have an exact location. The interior window can move out to 1.5ft from the exterior window. The shading device, a Hunter Douglass white aluminum Venetian Blind (The exact part name is Decor® 1" Mini Blind) is suspended to the frame 4.5” from the exterior window. The blind has the same dimensions of the windows, 2ft. by 4ft. Each blind is spaced 1” apart when it is in the open position. The width of each blind is also 1”.

Insulation

One of the concerns of using dexion (because of its many holes) as the frame was how to prevent the heat loss due to poor insulation. The critical area, which had to be completely sealed, was the cavity. The air flowing in the cavity had to enter from one source, the louver below the window, and exit through the exhaust fan. Many types of insulation were used ranging from duct tape and plywood to sheet metal and foam pipe covers.

Doors of dimension 3 ft. by 4 ft. were made from plywood to cover the sides of the frame. All of the major heat losses were eliminated, however a 1" gap formed between the doors and windows. In addition, above and below the doors there were gaps created by the dexion. Insulation material was needed to fill in the holes. The ¼" foam tape was extremely helpful in closing the gap between the doors and the frame. Sheet metal was cut in 1.5 ft. strips to line the frame at the top and bottom of the door. This prevented air to escape from the holes created by the dexion. The foam insulation tape was then applied to the sheet metal. The doors closed snuggly to the frame. The door/frame problem was solved, but the door/ window contact was poor. The windows should have been flush to the door, but there was about an inch gap between the two. A combination of ¼" gasket material and 1" pipe foam cover reduced the gap so that the windows and doors had contact. To finish insulating the cavity, duct tape was used to eliminate any minor leaks.

A series of figures 6a-6c illustrate the final experiment set up before the addition of any instrumentation. Each component is color-coded. The doors are not shown so that the inside cavity can be visible. The key dimensions mentioned in this chapter are also included (dimensions have been converted to SI units). While the experiment is running the windows can only be viewed from the front of the experiment set up. The five components: the frame, the heated box, the duct system, the windows and shading device, and the insulation are the bare essentials needed to produce the double skin façade windows. However, a few design iterations were preformed until the right combination of materials was achieved. A few of the key design considerations, which affected the insulation, the windows and shading device components, will be highlighted.

Figure 6a Experiment Setup side view

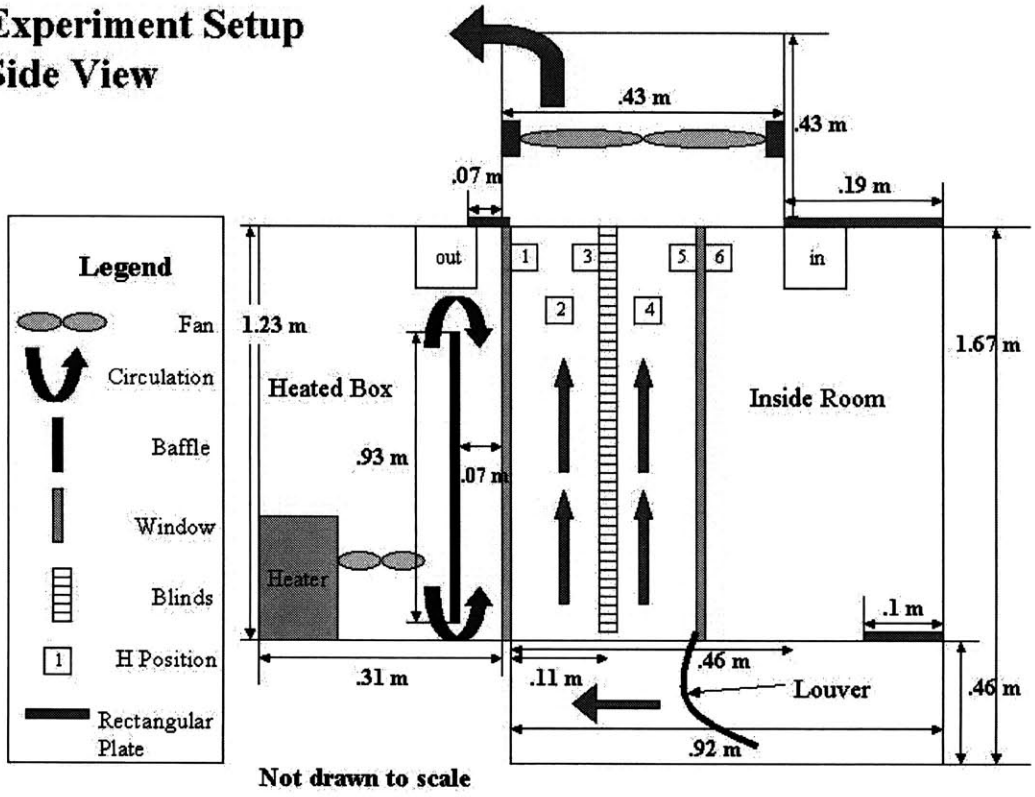

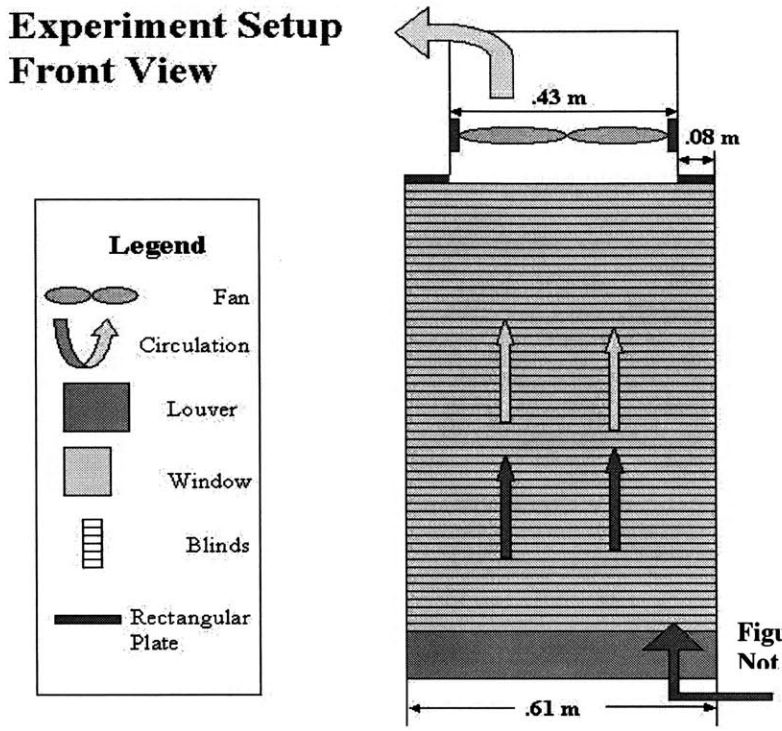

Figure 6b Experiment Setup front view Not drawn to scale

2.2 Design Considerations

The insulation of the DSF system was a concern from the start of the design phase. The use of the dexion left many passages for air to escape, so additional material

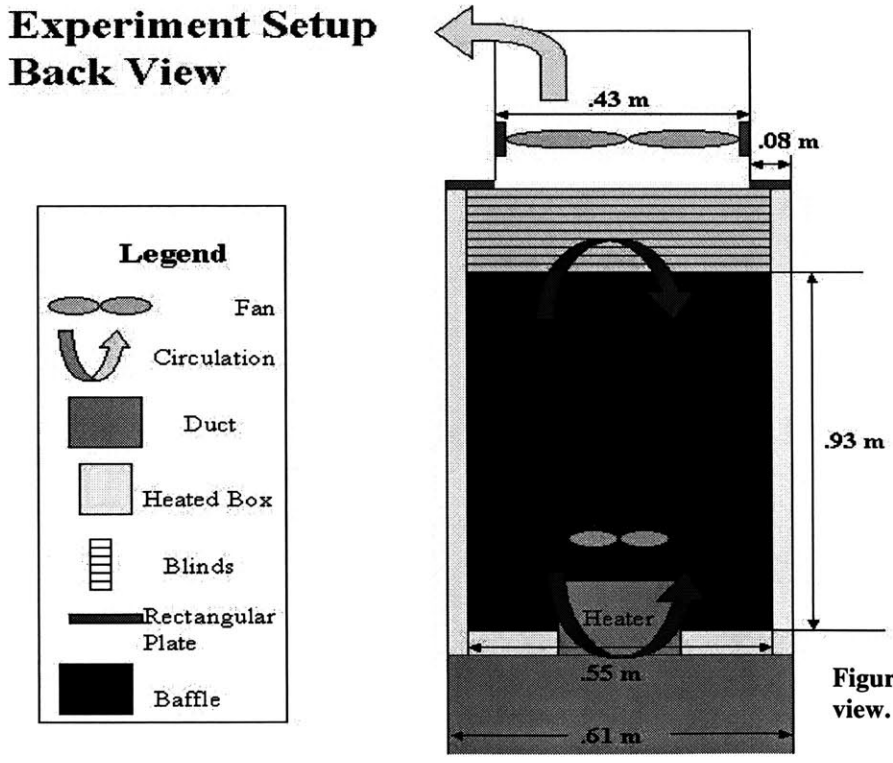

Figure 6c. Experiment Setup back view. Not drawn to scale.

was need near the air cavity to seal up the spaces. Before the insulation was added, a gap existed between the doors that enclosed the DSF and the windows. The windows should have been flush to the doors, and this problem was not realized until after the system was constructed. The insulating material used, 1" foam pipe cover, was not traditionally used as gasket material but served its purpose: eliminate the gap between the windows and door. The use of the foam and sheet metal greatly improved the effort to insulate the DSF window system.

A minor design change was the material used for the doors that covered the side of the frame. Originally a foam PVC was used because of its weight. The foam lost its stiffness for large square footages, so a 3ft. by 4ft. piece would bend easily at the midpoint. The door needed to remain stiff to fit flush against the window, but the foam PVC bulged out instead of pushing against the window to close the gap. It was apparent that the foam PVC was not working well so wood, which is extremely stiff was used. The wood was heavier but it performed the function of enclosing the air cavity well.

The final design consideration, which took a lot of re-thinking, was the sliding mechanism. One of the key goals of the experiments was to compare different sized cavities to one another. It would be frustrating to install and remove one window at a different position from the other every time the cavity dimension had to change. I approached the problem by thinking of already made devices that could achieve the same sliding mechanism. Drawer slides for large metal cabinets came to mind because they have the capacity of holding up to 100 lbs easily. The tricky part was attaching the glass to the drawer slide. After a few iterations, four ¼" holes were drilled into the frame of the window and L-shaped brackets attached the frame to the drawer slide. The solution was very effective and the interior window now had the capability of moving with very little effort.

2.3 Parameters of the Experiment

The output of the experiments is affected by four governing parameters. These parameters, which control the efficiency of the double skin façade window system, are: the heat source, air velocity, air cavity dimension, and position of the blinds.

Heat Source

The heat source was initially controlled by a modified space heater. It was located in the heat box fixed to the back of the experiment apparatus. Inside the box there was a baffle to separate the heated air from the cooler air and a fan to help mix the air and keep it at a uniform temperature. The modified heater is controlled by two variacs, which determine the low and high temperatures (The function of the variac is to vary the amount of voltage that an electric device uses). The initial problem with the heater was that its internal thermostat would shut off the heater if it exceeded the set high design temperature.

The purpose of implementing the two variacs was to bypass the internal thermostat and use the variacs to control the high and low design temperatures. So for example, if the temperature in the heated box falls below the set low temperature (approximately 98 °F) the heater will turn on because the internal thermostat is triggered and signals the variac to increase the amount of power going to the heater. Similarly, if the temperature rises too much (approximately 102°F), the heater will shut off, because the internal thermostat is triggered and signals the variac to decrease the amount of power going to the heater. This is done to ensure that the temperature remains uniform inside the heated box. Usually, the variacs,

Figure 6d Heated Box Configuration (not drawn to scale)

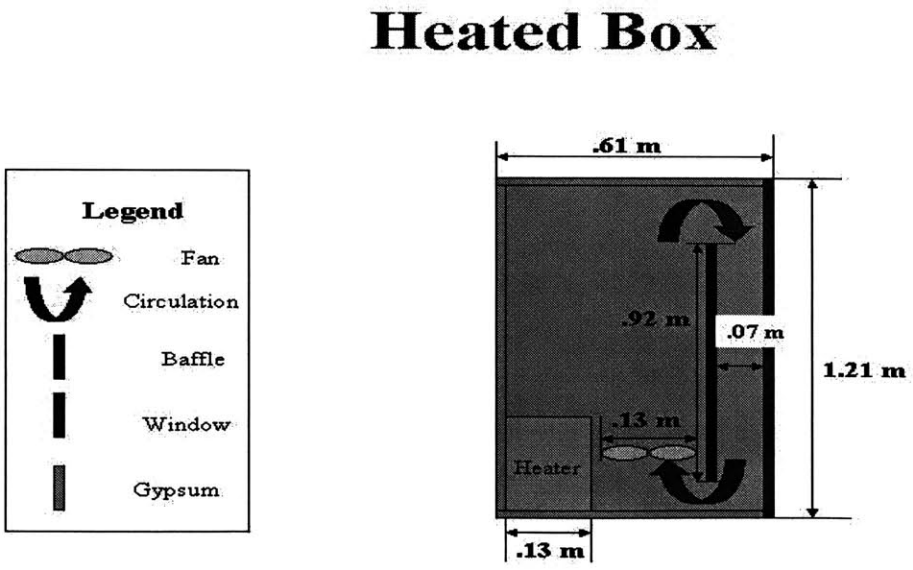

which control the heater, are set to about 50 volts on the high side and 40 volts on the low

side. Figure 6d illustrates in greater detail the heated box with the heater and baffle location. The temperature in the box, which was controlled by the variacs, was about 37.78° C (100° F) for this research.

Currently, the heated box configuration is set up to simulate a sunny day. The heater was removed and a powerful sun lamp replaced it. The product line used is Sun System™ and is manufactured by Sunlight Supply, Inc, who sells high-quality supplementary lighting systems for the retail garden and commercial growing industry. The 400 W bulb has a supplementary power source to control the lights output. At first the sun lamp remained in the box about 1 ft away from the exterior windowpane. The results were not desirable, because the lamp was too close to the bottom of the window. The concentrated heat of the lamp was focused on the bottom of the window and did not hit the entire window with the same intensity. In a high-rise building the sun will hit the window with approximately a uniform heat flux. A new set up was created, where the lamp is clamped to a stool directly outside the heated box. Reflectors were made out of plywood and painted white. They extend from the sides of lamp to close the air gap between the lamp and heated box. Insulating plastic covers the lamp and heated box so that heat is not lost to the surrounding air. The fan remains inside the box to facilitate the mixing of air. Figure 6e and 6f illustrate the lamp out of the heated box from the side and top view.

Figure 6e Side view of Sun Lamp and Heated Box

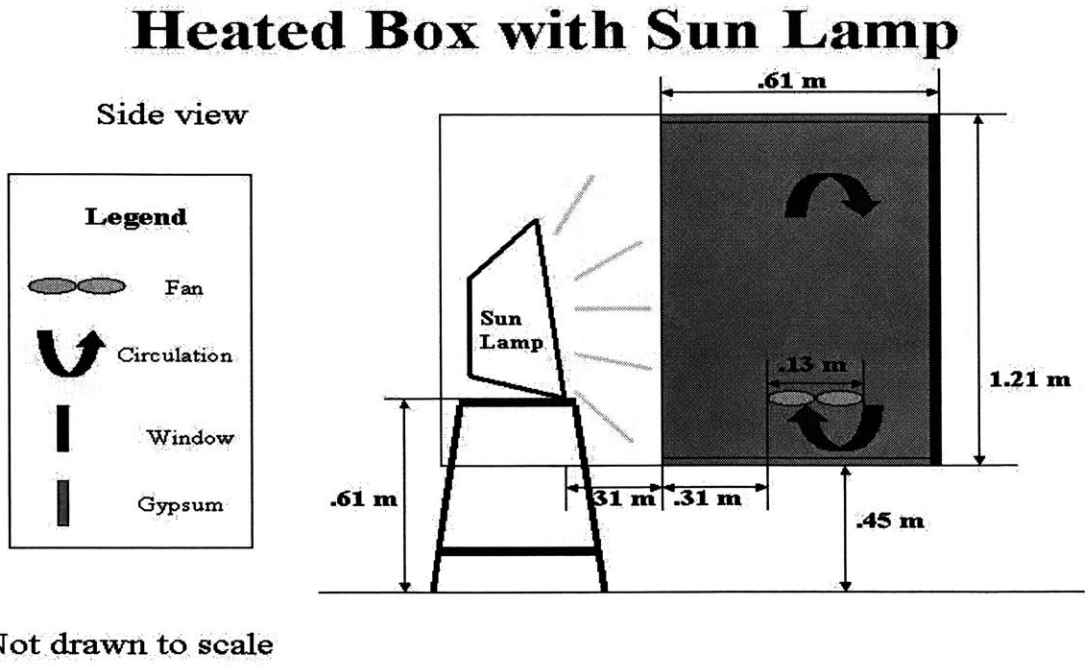

Figure 6f Top view of Sun Lamp and Heated Box

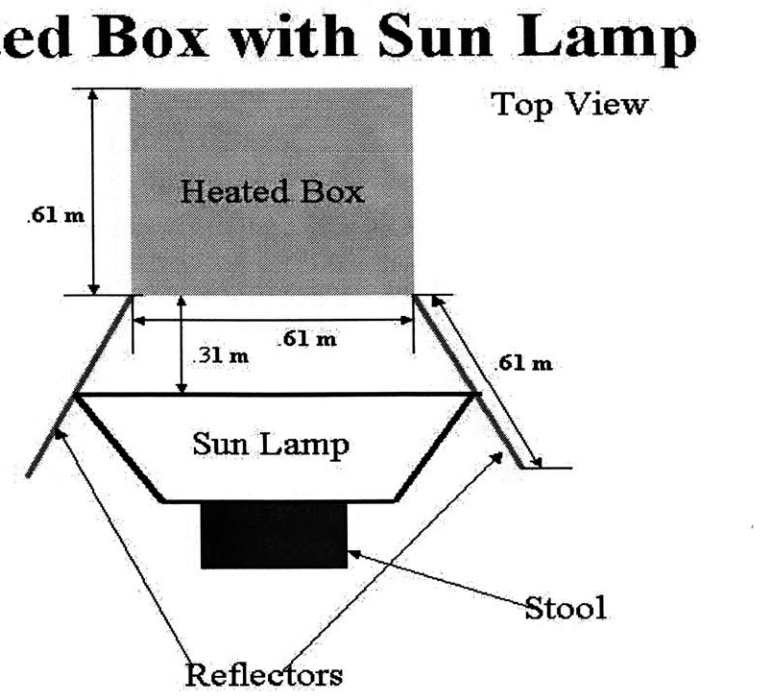

Not drawn to scale

The Air Velocity

The air velocity is the second parameter, which controls the efficiency of the DSF window system. There is an exhaust duct fan installed above the window system. The range of the air velocity it can produce is on the order of 1 m/s to .1 m/s inside the air cavity. For the most part, the air velocity has been set at about .3 m/s. The duct fan has two speed settings (high and low) but those settings are too powerful for the window cavity. Therefore, the duct fan is controlled by a separate variac. The velocities on the high setting are unrealistic for an actual DSF system so the low speed fan setting is used.

Air Cavity Dimension

The air cavity dimension is the third parameter. The smallest air cavity dimension is 9". The blind is suspended half way between the windows. The interior window is initially 4.5" away from the blind, but it can move out to make the cavity dimension 1'6". The calibration of the cavity dimension is based on the length between the exterior window and the midpoint of the blind. This distance is 4.5", and is referred to as the Exterior Cavity Length (ECL). The starting position of the interior window is also 4.5" and is referred to as the Interior Cavity Length (ICL), however it can move out to length of 9" from the blind or a the length 13.5" from the blind, which is three times the length of the ECL.

The Shading Device

The Blind Position is the final parameter governing the outcome of the results. There are two blind positions, open and closed. The angle theta, which determines the

blind position is measured off of the horizontal axis, such that a theta of zero represents blinds open and a theta of 90 represents blinds closed. When the blind is open or in the horizontal orientation, the temperature trends are slightly different from when it is closed.

2.4 Instrumentation

The mock double skin façade window with inside ventilation has been defined in terms of the physical components and parameters. The instrumentation of the DSF window is the element missing which completes the definition of the entire system. The instrumentation controls the parameters as well as records the system's response. The instrumentation is broken down into two categories hardware and software, which work together to manage the experiment apparatus. The hardware consists of physical components, which measure or control the temperature, air velocity, and heat flux. There are four main elements to the hardware instrumentation: a control box and variacs for heater and fan, thermocouples, a hot film anemometer, and Keithley's 2700 multimeter and data acquisition system. The software handles the recording and collecting of the data. Xlinx is a custom-made software program for the Keithley multimeter, which records the time dependant data. Microsoft Excel is the other software used for the storing and analyzing of data.

Control Box and Variacs

The control box and variacs for the heater and fan are used to control the temperature and air velocity. The control box is connected to the fan in the duct system. Increasing or decreasing the air velocity can significantly alter the overall temperature trends. The control box has a high setting which ranges in air velocities of .5 m/s to about 4 m/s. The low setting air velocities range from .1 m/s to 2 m/s. For the purpose of this experiment the lower air velocities regimes are more germane. The high setting velocities would only be used for rare extreme cases.

The three variacs incorporated in the experiment apparatus control the modified heater and fan. The variacs enhance the performance of the instruments by varying the output so that a range is created. For instance, the duct fan with out the variac can only generate two speeds, however with the variac attached a wide range is introduced. For the heater configuration, the exact opposite is desired. The heater should maintain a constant

temperature so that the temperature of the heated box does not fluctuate. As described in section 2.3 the variacs control the heater such that the heated box does not fluctuate in temperature, which the thermocouples in the heated box do not detect. The ultimate goal of a uniform heated box temperature is achieved within +/- 1°C.

Thermocouples

The thermocouples are a product of the Omega Company and they consist of yellow and red wires chromium (+), aluminum (-) respectively. The thermocouples are type K and have a diameter on the order of 1^{-4} m. The thermocouples are located through out the experiment apparatus at varying heights and lengths away from the heat source. There are 39 thermocouples used in the experiment and they are grouped by location. The groups are: thermocouples #1-4 measure the temperature in the cavity, thermocouples #5-8 measure the temperature on the blinds, thermocouples #9-15 measure the temperature on window 6, thermocouples #16-25 measure the temperature on window 5, thermocouple # 26-35 measure the temperature on window 1, and thermocouples #36-#39 measure the temperature in the box.

Figures 7 and 8 illustrate the position of the thermocouples with respect to each

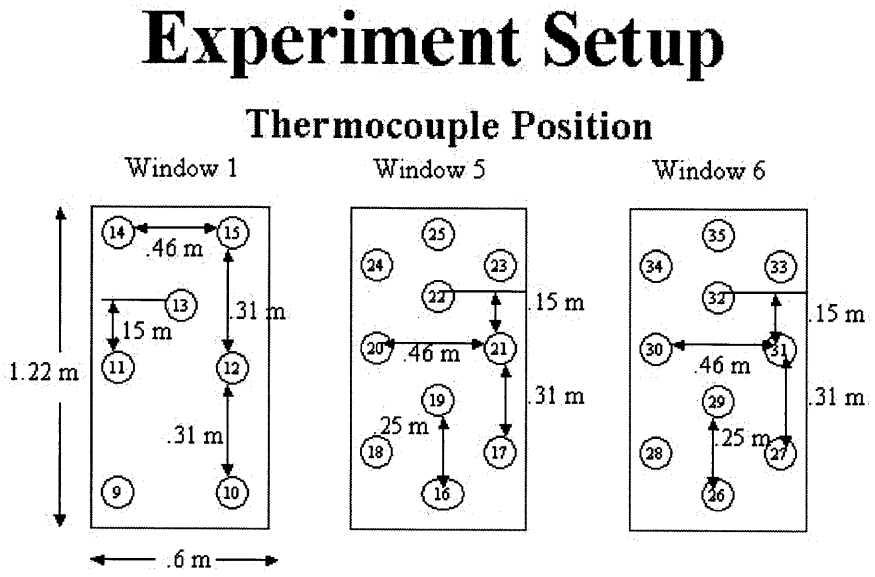

4 Thermocouples are located in the heated box near window 3.

4 Thermocouples are placed on the blinds 8 -12 in apart.

4 Thermocouples are located in the window envelope.

Figure 7 Thermocouple Positions on Windows

other. Window 1 is the exterior window and window 5 and 6 and represent both sides of the interior window. The thermocouples are attached to the windows and blinds with a very strong adhesive, which can with stand high temperature. The thermocouple tape strips are a product of Keithley Instruments.

About 1.5 feet separate thermocouples at the same height, thermocouples on window 2 and 3 are separated in the vertical direction by 6", and the thermocouples on window 1 are separated in the vertical direction by 12", except for #13 which is located 6" below #14. The 8 thermocouples, which are not taped to the windows and blinds, are suspended on wooden dowels and pointed into the air stream. As drawn in figure 8, thermocouples 1-4 are in the air cavity on both sides of the blind. The location of thermocouples 1 and 2 is about 8" the bottom of the windows, where the air enters. The location of 3 and 4 is about 12" from the top of the windows. All thermocouples point towards the center of the air cavity. Thermocouples 5 –8 are roughly 10 inches apart on

Figure 8 Thermocouple Positions in Cavity

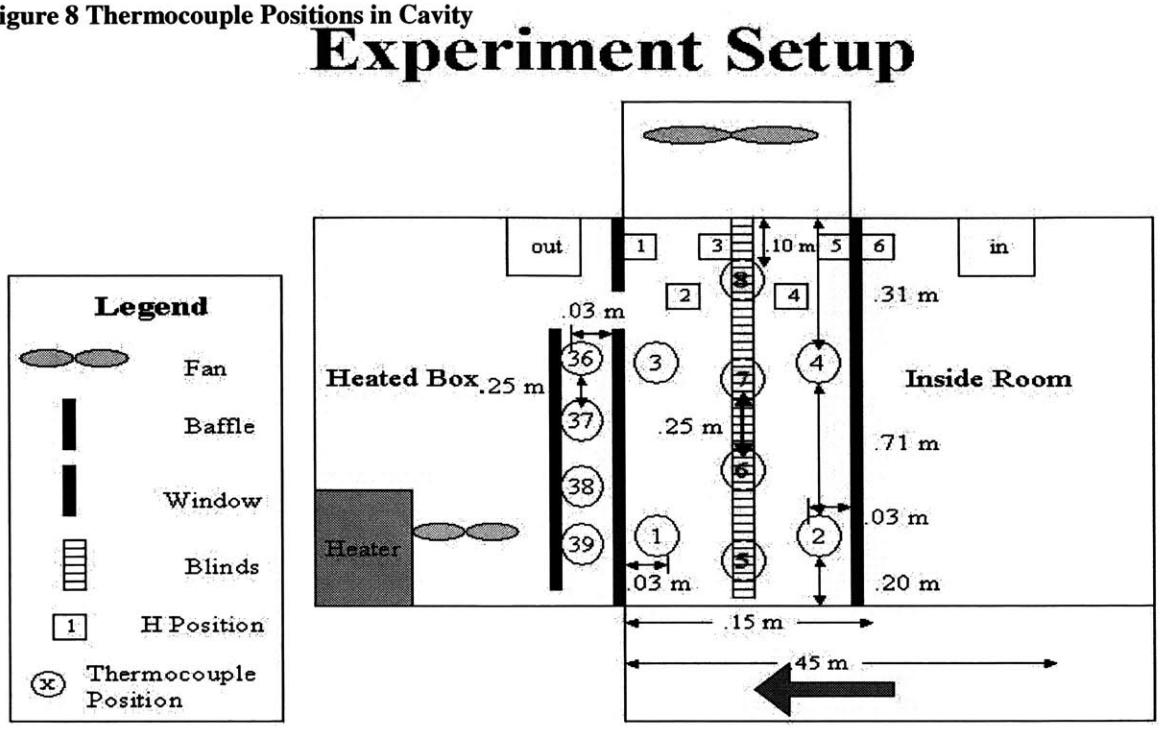

the blinds, starting from 4 inches from the top. Thermocouples 36-39 are located approximately 10" apart along the length of the exterior window and are shielded with aluminum foil. They are attached on the side of the heated box and point towards the center of the window. All of the thermocouples are dipped in aluminum paint to improve the accuracy of the measurements.

Probe

The hot film anemometer is a probe, which works by being placed directly in the path of what it is measuring. The probe differs from the thermocouples because they continuously take data, where as the hot film anemometer takes one measurement for a set of data. The parameter, which the probe measures, is constant so continuous data collection, becomes redundant. The hot film anemometer measures the air velocity by the slight change of temperature across the hot film as the air blows across it. The hot film is a thin wire with a diameter on the order of a few microns and a length of about 3 mm. The hot film anemometer measures the velocity by the amount of voltage it generates, which is then converted to a velocity by using calibration curve. The voltage is read through and recorded by the Keithley 2700 Multimeter.

Data Acquisition System

The Keithley Instruments 2700 multimeter and data acquisition system is the bulk of the hardware. It is designed as a mini-computer, which can read up to 80 channels of information. The channels are the lines of data, for example one thermocouple is a channel. The channels each have a +/- terminal where the instruments are connected. The multimeter reads voltages and converts then to either: temperature, DC current or voltage, AC current and voltage, resistance, or frequency. The 2700 Multimeter is connected to the hard drive of the computer so that data can be transferred from the hardware to the software. The actual instruments such as the thermocouples and hot-film anemometer are connected to the 7708 data card, which can hold up to 40 channels. The card is then fit into the back of the 2700 Multimeter, and the system is initialized with the software. It is important for the thermocouple to have a cold-junction were the two wires are emerged in $0^{o}C$ water and ice bath. Conveniently the 7708 card simulates the cold-junction or ice bath for each channel. The 2700 and 7708 are the interface between the instruments and the measurements for the temperature profile and air velocities.

The other half to the instrumentation is the software. The Xlinx software controls the 2700 Multimeter such that channels can be grouped by location, and the frequency of the data collection can be set. The 39 thermocouples are easily managed in groups rather than individually, the six groups that were outlined in the thermocouple description are used in data collecting. The Xlinx software allows the user to read all channels or selected groups so that memory is not wasted collecting unwanted data. The rate of the data collection can also be arranged, for example the 2700 can collect data every second from the selected channels one at a time and can average the data every 50 readings. Once all the data has been collected, it is transferred from Xlinx to Microsoft Excel.

2.5 Summary

The combination of the hardware and software complete the instrumentation of the experiment. The instrumentation is the final component of the definition of the experiment apparatus, which also consists of the physical setup: frame, heated box, duct, windows and shading device, and insulation, and the experiment parameters: the heat source, air velocity, cavity dimension and blind position. There were a few design considerations such as type of insulation and the drawer slides that were implemented.

These choices facilitated in insulating the system and the sliding motion of the interior window. The experiment setup creates the foundation of the research goals, which will be built upon with the next chapter, procedures.

Chapter Three: Procedures

One of the goals of this research is to test the mathematical model and compare it to the experimental data. Many questions arise with regard to the right technique for testing the mock double skin façade window. For instance, how long should experiments run, or how to determine that the heat source is at a constant temperature? Some of the questions answered themselves through trial and error, and others took some re-engineering of the experimental apparatus. The experiments have to maintain a certain consistency such that the variations are minimized in the results.

3.1 How to Determine Steady State

Each experiment run time was determined by how it took the experiment to reach equilibrium. When looking at energy savings for long periods of time, the transient or immediate responses to the system are not important. The transient responses die off and the steady state result remains. The experiments had to run long enough so that a steady state system is reached. To identify the steady state regime, the heat source was turned on and the temperature was taken every few seconds for about two hours. Figure 9 was the temperature vs. time curve for the heated box. The numbers along the side

Figure 9 Time to steady state graph

Procedure

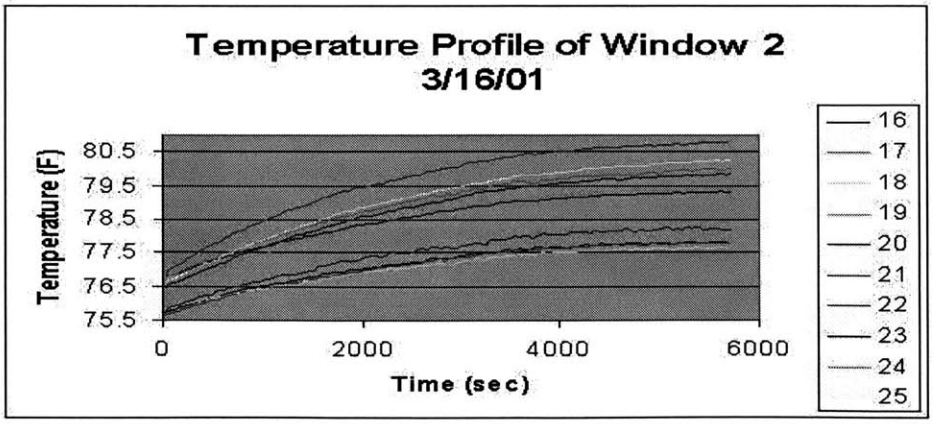

- About an hour to reach steady state

represent the thermocouple channel, which was defined in chapter 2 (refer to figure 7).

From looking at the graph equilibrium was reached at about an hour from turning on the heat source. One part of the question was answered, but after steady state how long should the experiment collect data to get an accurate steady state value.

After the window system reached steady state, it was determined from a few trials that a time period of two hours was a good length of each experiment. The data acquisition system would measure the temperature every second moving from channel to channel. After every fifty measurements of a single channel the 2700 Keithley Instrument would average the data and store it. After two hours a sufficient amount of data was collected from each channel. An accurate temperature profile of the steady state regime was recorded with the 2700. At the end of the experiment, the user as an option of transferring the data from the data acquisition system to Excel spreadsheets where the data is analyzed.

3.2 Fan Calibration

One of the key parameters is the velocity of the air, because it is one of the factors that control the rate of heat transfer, which affects the temperature schemes of the DSF window system. In order to model the air velocity accurately in the mathematical model the velocity would have to be physically measured. The air velocity was measured using a hot film anemometer. The probe is a product of TSI inc, and is similar to the model 1237 standard flush surface sensor. The probe outputs voltage, which must be converted to velocity. Fortunately, there is a correlation between voltage and velocity of the device. The calibration curve of the hot film anemometer is located in Appendix A. The square root of velocity is plotted against square voltage, which generates a linear relationship.

The calibration of the fan using the hot film anemometer is the first part, which relates the fan speeds to the actual air velocity. The velocity readings were taken on both sides of the blind near the center of the windows. The duct fan used in the apparatus has two settings, low and high. There was not much variation with just those two air velocities settings so a variac that controls the AC voltage into the fan was incorporated into the system. The dial range of the variac is 0 – 260 volts. For the range of 0-35 volts there was no response from the duct fan, however from 35-260 volts created a wide range of velocities. A detailed curve had to be created to illustrate the air velocity equivalents

for the range of voltages (the range increased because of high and low settings of duct fan).

Many voltage readings were taken with the hot film anemometer every 20-voltage partition on the variac. These voltage readings were then converted to air velocities via the hot film anemometer calibration curve. The results were calibration curves for the low and high setting of the duct fan. Figure 10 shows the AC voltage of the variac vs. the air velocity in the cavity of the window system. The curve that represents the relationship between the air velocity and the AC voltage is close to linear. The curve allows the user to input the correct velocity into the mathematical model.

Figure 10 Voltage vs. Velocity

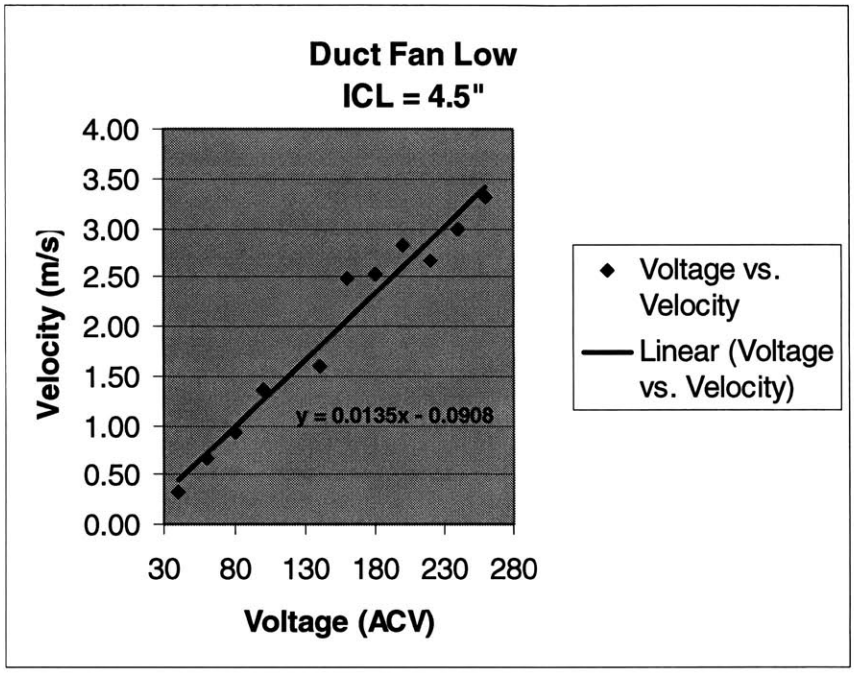

Similarly the air velocity, which the heated box fan generates, is also computed. It is imperative that the air inside the heated box is well mixed to ensure the uniformity of the heated box temperature. The heat source is simulating the outside temperature during the summer, which radiates evenly so uniformity of temperature is needed. The closer the experiment setup achieves the uniform heat source, the more accurate the results. Figure 11 represents the three speeds of the heated box fan vs. the air velocity. It is obvious that setting one is low and setting

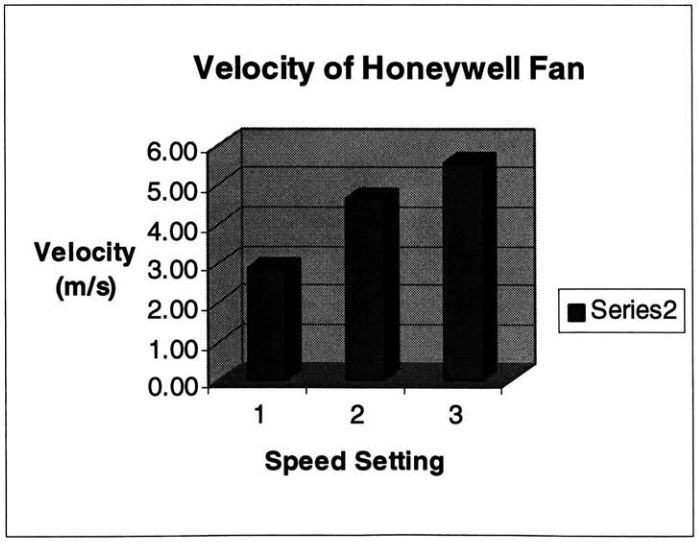

Figure 11: Fan Speed Options

two and three are medium and high respectively. The fan is consistently on setting three for the duration of the experiment. In addition to measuring the air velocity at different variac voltages, the air velocity was also measured at different horizontal positions in the cavity to ensure that the air velocity was uniform. Figure 11a illustrates the air velocity vs. horizontal distance. Velocity A is measured in the interior cavity window and velocity B is measured from the exterior cavity at about of .6 meters from bottom of the system.

Figure 11a. Velocity Profile in the Cavity

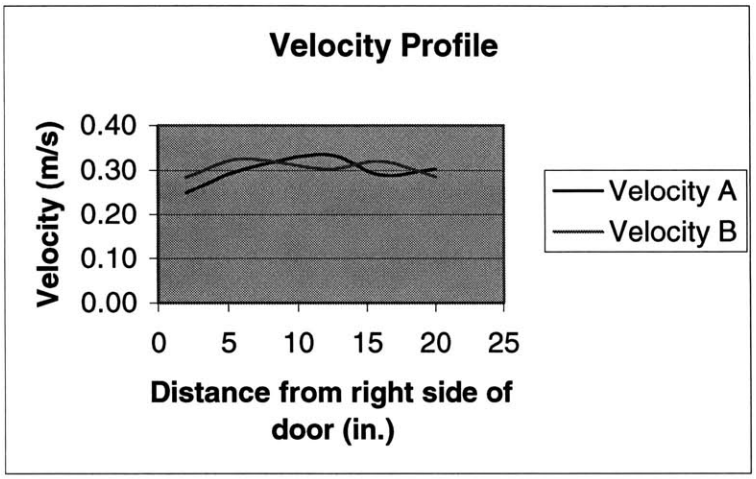

The air in the box is well mixed as seen from the graph in Appendix A, where the temperature in box is plotted vs. time and the average temperature is plotted vs. vertical height. The numbers represent the thermocouple channels; thermocouple 39 is located at the bottom and thermocouple 36 at the top. They are spaced roughly 10 inches apart near the exterior window. The temperature curves are with in a degree Celsius of each other at steady state. The fan ensures that the air is mixed well in the heated box.

3.3 Modifications to the Double Skin Façade System

The beginning of the experimentation period was a time for trial and error. The response of the mock DSF window system was not easily predictable. The type of heat source used and the method of air velocity measurements created a few issues. These minor problems had to be addressed before the data could be collected. The two problem areas were the heated box and the air cavity.

The heated box was an issue because initially a small space heater was implemented to simulate a hot day. The heater had an internal thermostat, which turned off if it reached a certain temperature. The result was an oscillating temperature vs. time curve. Item three of Appendix A has a graph of this phenomenon. The range in

temperature is on the order of 10°C. It would be hard to record accurate steady state results if the constant outside temperature oscillates with in 10°C. Somehow the heater had to be modified such that it would not turn off and on randomly. The heater was rewired to two transformers, which acted as an external thermostat. Figure 11b shows an elementary circuit of the heater. One transformer was calibrated to a high design temperature of 102 °F and the other was calibrated to a low design temperature of 98 °F. One transformer was set at a low voltage and the other at a higher voltage. The heater would shut off if it exceeded the temperature (set by the high voltage transformer) on the upper bound, and the heater would turn on if the temperature (set by the lower voltage transformer)

Figure 11b Elementary circuit of modified heater

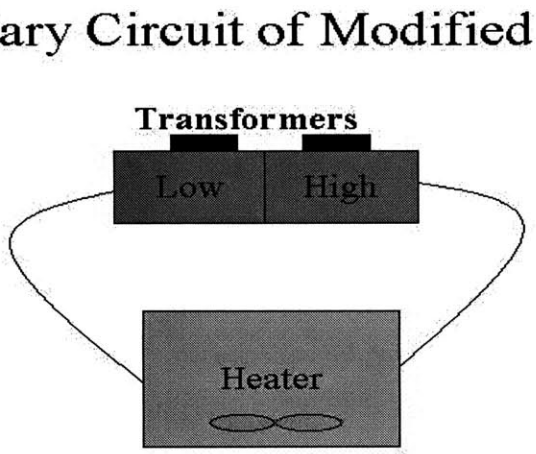

dropped below the lower bound. The modification drastically changed the temperature profile of the heated box. The oscillations became very small (on the order of .1°C). The uniformity of the heated box is illustrated previously in item 2 of Appendix A.

The second issue with respect to the heated box was directly related to the heater modification. The temperature profile was greatly improved, however, more changes were necessary to ensure that the air was properly mixed. One of the reasons for the oscillating temperature was because of the movement of air. The air that was hot tended

to remain near the top and push the cooler air down. It was difficult to get an even airflow through the box. The box fan was added to increase the motion of air, but it was not enough. A baffle or division was introduced three inches away from the exterior window. The baffle separated the thermocouples from the direct path of the heat source. The thermocouples were measuring the temperature of the circulating air that blew across the exterior window rather than the stagnant air. The combination of the baffle and box fan was the solution to make the heated box a uniform heat source. The illustration of figures 6c and 6d in chapter 2 shows the locations of the baffle and fan in the heated box.

When the sun lamp was used for a heat source the baffle was removed because it shaded the exterior window. The temperatures remained uniform because the temperature measured from the heat of the lamp was constant. The sun lamp sat outside the box because it was very powerful. White reflectors were attached to the lamp, and the rear of heated box. The lamp and box were well insulated with thick sheet plastic. Very little heat was lost to the system's environment. Modifying the heat source and implementing a baffle and fan solved the minor issue of temperature uniformity of the heated box. Figures 6e and 6f of chapter two illustrate the lamp and heated box configuration with out the plastic sheet coverall.

The method of measuring the heat flux from the sun lamp to the system was achieved by measuring the change temperature over time. One of the blinds was painted black so that is absorbed all of the heat and the temperature was measured vs. time. The

Figure 11c temperature vs. time of Blind

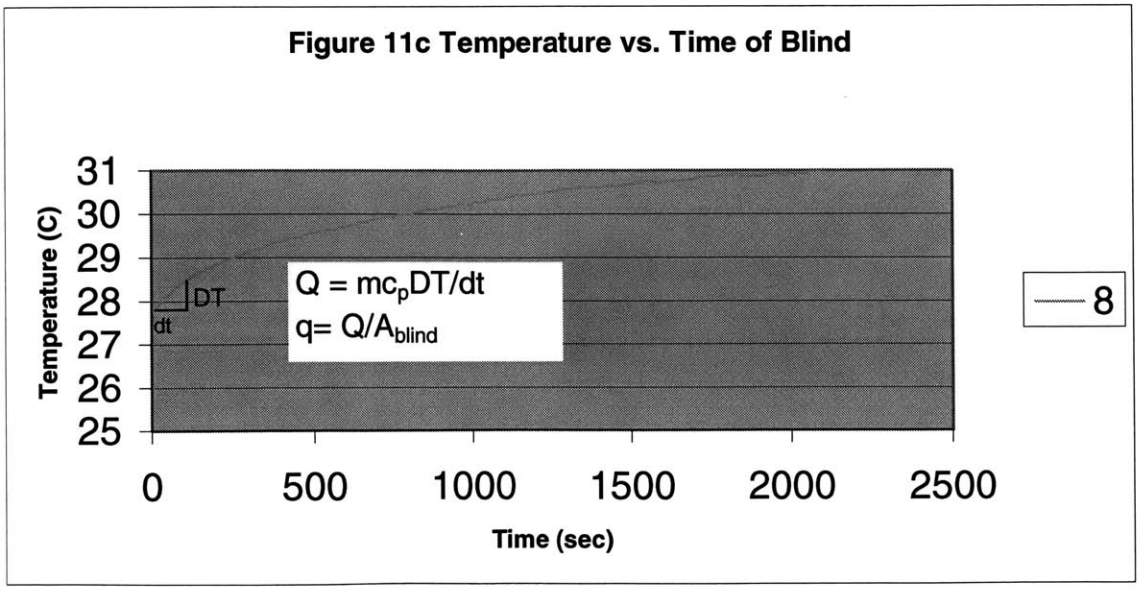

initial temperature rate was used to calculate the heat flux. Figure 11c is this time history of the temperature of the blind. The number 8 refers to the thermocouple number and the first equation calculates the heat transfer in Watts. The m is the mass of the blind; the c_p is the specific heat at constant pressure of aluminum and Dt/dt is the slope of the curve at the position labeled in figure 11c. The second equation is the heat flux measured in W/m^2. The area of the blind divides into the heat transfer to get this value. The estimated heat flux from the lamp was calculated to be 30 W/m^2.

The velocity was varying with the increase in interior cavity length. The air velocity in the exterior and interior cavity was measured at different interior cavity lengths to get a more accurate velocity profile. The mathematical model takes one input for the air velocity, however the user can decide the rate at which air goes through the interior and exterior cavity. Initially, all of the air was distributed evenly between the two cavities in the mathematical model. This was not an accurate description of the actual experiment mock up. The exterior cavity (the cavity closest to the exterior window which is fixed in size) did not receive much air. When the interior cavity dimension was increased the exterior did not change. Item 5 in appendix A describes the velocity level in the exterior cavity for varying interior cavity dimensions. Note that when the interior cavity increases the velocity on the exterior side significantly drops. This phenomenon will be discussed further in the results section. Item 6 of appendix A illustrates the velocity profile in the interior cavity. The low on the graphs refer to the fan speed setting.

3.4 Summary of Experiments

The spreadsheet located in Appendix B as item 1 lists all of the experiments that were run for the duration of the research. The fan column refers to the voltage setting on the duct fan variac. The blind column refers to the position of the blinds. The heat column is the temperature of the heated box, 100 °F, all temperature are taken in degrees Celsius so the equivalent would be about 38°C. ECL is the exterior cavity length and ICL is the interior cavity length. The last column is left for the type of heat source.

3.5 Summary

The preliminary experiments helped to eliminate any future issues, which would result in useless data. For instance, the start of steady state was determined by running for two hours, and after the first hour the system was equilibrated. A few adjustments to the apparatus that was not obvious in the initial construction were implemented. The Heated Box configuration was altered when the heat source changed from heater to sun lamp, as well as the additional velocity measurements to ensure that the correct values were inputted into the mathematical model. It was necessary to calibrate the fans so that the rate of air in the cavity was known. The trial runs reduced the amount of experimental error by eliminating inconsistencies in the experimental data so that it can be compared to the mathematical model. Chapter four discusses the mathematical model in greater detail, the results of the experiments and compares it to the model and Permasteelisa data.

Chapter Four: Results

4.1 Mathematical Model

Daniel Arons took on the challenge of modeling the thermal responses of the double skin façade window systems. His model was created using Microsoft Excel which can handle sophisticated iterative calculations. To get an idea of the enormity of the file, his model contains 17 worksheets full of material properties for air, glass, and the blind material along with convective, conductive and radiative calculations. The configuration of the system is almost identical to the experiment setup; the difference between the two is a double glazed exterior window. The air cavity and an interior piece of glass are in both models. In addition, a blind is located in the middle of the air cavity. The air is assumed to enter from the inside and exits at the top (inside ventilation). Figure 12 illustrates the Mathematical model. The pale purple arrows represent the airflow and the other components are labeled. The purpose of the program is to virtually assemble a specific double skin façade by inputting the physical parameters of the window. The model will calculate the energy balances and output temperature profiles and energy flow graphs, which will determine the efficiency of the DSF window system. The model can be used to minimize energy consumption and compare different façade designs. The mathematical model is a simplified numerical model intended to predict the energy performance of multiple types of double skin facades [Arons, 2000].

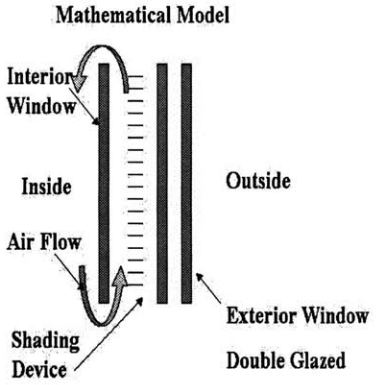

Figure 12. Mathematical Model

4.2 Mathematical Model Assumptions

Quite a few assumptions were made to create the mathematical model. The model was created to predict the long-term energy performance so the transient thermal

responses were not necessary. That is the reason why the modeling did not get more complicated than two-dimensional heat transfer. Moreover, the edge effects were neglected because the thickness of the windows was much smaller than length (thin plate assumption).

Heat Transfer Modes

The model calculates heat transfer in two dimensions; however, each direction has a different form of heat transfer. In the horizontal direction there is one dimensional conduction and radiation heat transfer. Conversely, in the vertical direction convective heat transfer and vertical airflow is utilized. Figure 13 illustrates the heat transfer directions.

The horizontal direction has one dimensional solar radiation and conduction happening simultaneously. The solar radiation is calculated from the reflected and absorbed or transmitted solar energy at the blinds. The radiation is determined in part by the solar altitude, which corresponds to the angle at which the sun hits the exterior window, the blind angle (whether the blind is open or closed) and the blind geometry. The material properties of the blind are the input to these calculations. Because the solar radiation comes in at an angle, the program must convert the radiation to a value in the direction normal or perpendicular to the window. The Excel spreadsheet takes that into account when computing the solar energy values. The program allows the user to input a value for the incident solar radiation in heat flux (W/m^2). Infrared radiation is also calculated based on the surface temperatures and geometries of the window.

The other mode of horizontal heat transfer is conduction. There are three possible areas of conduction, which are the glass, the blind and the air. The conduction through the glass is determined by the glass material properties, which are located in appendix C. The conduction through the air is inputted as a constant and used in calculating the convective heat transfer coefficient in the vertical direction. Air is a good insulator because it poorly transfers the energy horizontally from the outside to the inside. The moving air in the cavity transfers the energy before it reaches the interior window. The material properties of air are also located in appendix C in graph and chart form. The conductivity of the blinds is ignored because of its small impact to the overall energy balance and the temperature distribution.

Finally, the third form of heat transfer is convection in the horizontal direction the two locations of the convection are between the air and window and air and blind. Since the air is flowing through the cavity parallel to the windows the energy is transferred in the same manner. The inside room and outside convective heat transfer coefficients, which greatly effect the primary output, temperature, are inputted by the user or default values are set. The physical dimensions and surface temperatures determine the convective heat transfer for the exterior window. The shading device separates the air cavity and the program assumes that the interior and exterior cavity do not share the same air, and that the air temperature is constant at any given height. The convective heat transfer coefficients in the cavity are determined by correlations for forced convection flow in a long channel with smooth walls [Arons, 2000].

Chart 1. Summary of Heat Transfer

Location	Convection	Conduction	Radiation
Outside			X
Exterior Window	X	X	X
Exterior Cavity	X		X
Blind		X (ignored)	X
Interior Cavity	X		X
Interior Window	X	X	X
Inside			X

Figure 13. Detailed Heat Transfer Model

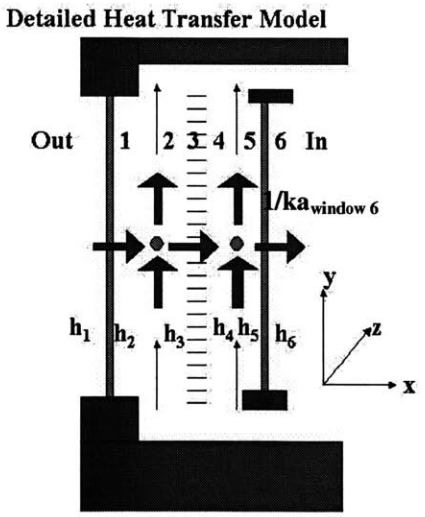

A more detailed heat transfer model of the program is drawn in figure 13. The red arrows represent the flow of energy. The black arrows are the flow of air. Again, the model is two-dimensional with a combined heat transfer in the vertical and horizontal direction. The numbers will

be discussed in greater detail with the temperature profiles. The small $h_{1\text{-}6}$ represents the convective heat transfer coefficients. The h_1 and h_6 are picked given the inside and outside weather conditions the other four h's are calculated from the material properties of air and surface temperatures. The $1/ka_{glass}$ corresponds to the thermal resistance or conduction energy through interior window.

Heat Transfer Equations

The formulas that describe the three different modes of heat transfer are

Equation (1)

$$q_{rad} = h_{rad}\,(T_2 - T_1),$$

Equation (2)

$$q_{conv} = h_{conv}\,(T_2 - T_1),$$

Equation (3)

$$q_{cond} = \frac{k\,(T_2 - T_1)}{l}.$$

Equations (1) and (3) represent the heat transfer in the horizontal position. Q_{rad} and q_{cond} are the symbols for heat flux (W/m^2) for radiation and conduction respectively. T_2 and T_1 are the temperatures measured in degrees Celsius. The thermal conductivity (W/m^2K) is a material property given by *k*, and *l* is the thickness in meters of the conduction length. The h_{rad} is determined from surface temperatures and emissivity of the object. Equation (2) is an expression for the convection in the horizontal direction. The q_{conv} corresponds to the heat flux (W/m^2), and the h_{conv} are the $h_{1\text{-}6}$ in the figure 13. Depending on the location in the system, the convective coefficient changes. The modeling process is done using an electrical analog where the temperature represents the current, the heat transfer coefficients are the resistances, and the heat flux is the voltage.

Convective Heat Transfer Coefficients

There are four different possibilities for the convective heat transfer (h_{conv}) coefficients. The h_{conv} values are heavily dependant on the geometry of the object. The options are flow over a flat plate, flow over a cylinder, flow in a cavity, and Hens' model. The hconv are expressed in formulas (4)-(7) respectively.

Equation (4)

$$h_{\substack{flat\\plate}} = \left(k/l_{glass}\right).644\left(vk/\upsilon\right)^{1/2}\,\mathrm{Pr}^{1/3}$$

Equation (5)

$$h_{cylinder} = \frac{.3 + \left(\left(.62\,vl_{blind}/\upsilon\right)^{1/2}\right)\mathrm{Pr}^{1/3}}{\left(1 + \left(.4/\mathrm{Pr}^{2/3}\right)\right)^{1/4}}$$

Equation (6)

$$h_{cavity} = \frac{kNu_{dh}}{D_h}$$

Equation (7)

$$h_{hens} = 5.8 + 4v$$

The thermal conductivity of the air is represented once again by k; the v is the velocity of air. Pr and Nu_{dh} are dimensionless numbers, which are determined by material properties. L_{glass} is the length of the blind and D_h is the hydraulic diameter (similar to a characteristic length). The kinematic viscosity of the air is υ. Equations (4) and (5) are complex compared to the latter two.

Hens' model for h_{conv} was formulated from actual experimentation, which states that there is a linear relationship between the air velocity and h_{conv}. Hens formulated this relationship by plotting the relationship between the overall heat coefficient (U-value) and the airflow rate [Hens, Saelens, 1999]. He noticed that the U value increased with the increase in air velocity. Since, the U value is inversely proportional to the thermal resistance, it increased with the air velocity. Taking the experimental data of the U value and converting it to h_{conv} and comparing it vs. air velocity, created a linear relationship between the air velocity and the h_{conv}.

Originally, h_2 and h_5 (located on figure 13) were represented mathematically by the flow over the flat plate, h_3 and h_4 were expressed with Hens' model, and h_1 and h_6 were determined by the interior and exterior weather conditions.

4.3 Experiment Assumptions

Adapting the mathematical model to the experiment set up was challenging because the input parameters were not so obvious. The h_{conv} was changed to more accurately describe the apparatus. The flow of the velocity was altered as well as the solar altitude. The velocity measurements were taken in both cavities of the blind and the velocities inputted in the model were changed accordingly. The solar altitude was determined to be almost 0^o because of the lamp configuration (see figure 6e); the heat transferred to the window does not come in at an angle. The emissivity of the blinds and

windows were measured and minor changes were made to this property for both the blinds and window. The result was a better representation of the experiment set up with the mathematical model.

The h_{conv} for the interior and exterior cavity was set as Hens' model, however the simple relation was not describing the heat transfer well. A more in depth relation was needed. The h_{conv} between air in the interior and exterior cavity and the blinds was set to flow over a cylinder when the blind was in the open position and set to flow over a flat plate when the blinds were closed. The exterior and interior window remained with the flow over the flat plate relationship. The h_{conv} values for the inside and outside were not altered because they were approximately the correct values.

The model assumes that the air velocity inputted in the model is the same for both the interior and exterior cavity. In the experiment this is only true for when the length of both cavities are equal. When the interior cavity increases in length the value of the air velocity also increases. The increase in air velocity affects the h_{conv}, which is directly related to the temperature. There is a multiplication factor, *M factor*, which controls the velocity of the air through each cavity. The multiplication factor was determined by measuring the air in both cavities for different interior cavity lengths at a height of .6 meters from the bottom of the system. Chart 2 lists the velocities measured for different voltages in each cavity. The M factor, which is a ratio of the air velocity in the exterior to the air velocity of the interior cavity is computed and was inputted into the mathematical model.

Chart 2. Calculation of M factor

		Interior Cavity			**Exterior Cavity**	
Voltage	ICL = 4.5"	ICL = 9"	ICL = 13.5"	ECL = 4.5"	ECL = 4.5"	ECL = 4.5"
Low 40	0.108 m/s	0.207 m/s	0.163 m/s	0.108 m/s	0.036 m/s	0.001 m/s
Low 60	0.257 m/s	0.315 m/s	0.310 m/s	0.257 m/s	0.036 m/s	0.016 m/s
Low 80	0.405 m/s	0.444 m/s	0.452 m/s	0.405 m/s	0.036 m/s	0.049 m/s

M Factor ICL = 4.5"	**M Factor ICL = 9"**	**M Factor ICL = 13.5"**
1	0.1735	0.0046
1	0.1141	0.0515
1	0.0810	0.1085

The solar altitude or the angle at which the sun hits the window was also altered. A default value of 30^{o} from the vertical was used in the mathematical model. The experiment is run indoors and the lamp used to simulate sunlight is set level with the windows. The light does not come in at an angle like the sun, but shines directly on the windows. The solar altitude was changed to roughly zero, so that it emulates the experiment set up.

A few tests were run to check the reflectivity of the blinds and the emissivity of the windows. The heat flux was measured using a light meter on both sides of the exterior window to check if the emissivity value inputted as default was accurate. The default value was on the same order of magnitude as the measured emissivity. Similar test was performed for the reflectivity of the blinds. The flux was measured using a light meter in front of the blind facing the light source and measured facing the blind. The ratio of flux coming off the blind over the flux going towards the blind was calculated. The value was within 2 percent the default value. The properties inputted into the mathematical model reflect the materials that were used to construct apparatus.

The assumptions that were made to adapt the mathematical model to the experiment setup improved the results tremendously. Many of the default values that the model uses such as: the solar altitude, the type of h_{conv}, the window and blind properties, and the air cavity velocity are for typical cases. Moreover, it is important to understand what critical parameters have to be changed to ensure that the model is accurate. The next section discusses the key parameters in the model and describes the step-by-step process of creating a DSF window system scenario.

4.4 Initial Conditions

The mathematical model can be altered to pattern any type of window configuration. The airflow cavity may be increased or minimized depending on the situation. The dimensions of the interior and exterior window may be changed as well as the blind orientation and spacing. The properties of the blinds and window in terms of reflectivity, absorptivity, emissivity, and transparency may also be manipulated to capture the exact double skin façade setup.

Appendix D has a typical input page of the mathematical model for the double skin façade. The critical input parameters are bolded in green numbers. Since SI units are used all of the dimensions that were mentioned in the chapter two were converted to meters. The key parameters are located in the geometry, design temperatures, incident radiation, heat transfer coefficients, blind properties, and air properties sections.

Geometry

This section of the input page refers to the physical dimensions of the window, such as height. The length of the window in the horizontal direction is not needed because it is assumed that the heat transfer is happening in the vertical direction and on the horizontal plane the temperatures are constant. The convection in the vertical direction dictates the temperature at any given height and because of steady state assumptions the temperature is the same for any horizontal position at that height.

There are three inputs for spacing of the windows. D_2 and D_1 refer to the exterior and interior cavity length respectively. The interior window can move so the value for D_2 changes depending on the interior window position. D_o is used for a particular scenario known as double-glazing. Double-glazed windows are two windows set about a centimeter apart; the double windows replace the exterior window of a DSF window system. There is an airtight seal around the windows, and is sometimes filled with a gas. For the purpose of this research D_o is very small, which essentially forms one exterior window because only two widows were used in the experimental setup. In Appendix D there is an option for window or glass three properties, which refers to the double glazed window. Figure 13a is a drawing that shows the cavity lengths.

The division number refers to how many sections in the vertical direction that the system is separated. For each segment a temperature profile is created in the horizontal direction through the system. For instance, 20 divisions are inputted so the program divides the height by 20

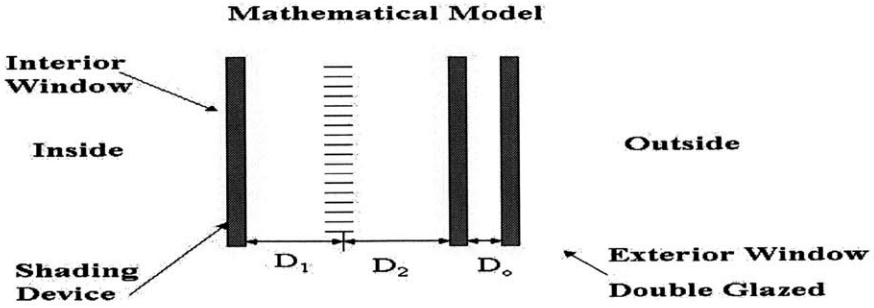

Figure 13a Cavity Length Dimensions

and for that length the temperature from outside to the exterior window to the cavity, etc… is calculated. The output will be discussed in greater detail in section 4.6.

Design Temperatures

The inside and outside temperatures must be set so that there are boundary conditions. The temperature chosen for the outside temperature, which the temperature in the heated box set was 100 °F (a hot day) which converts to 37.8 °C. The temperature was reached using both the modified heater and sun lamp. The lab's ambient temperature determined the room temperature, which was approximately 25 °C or 77 °F. The air inlet temperature was determined by the room temperature since the system is an inside ventilated configuration. The air inlet temperature refers to the air entering the cavity below the windows. It is pulled directly from the room so its temperature is 25 °C.

Incident Radiation

The incident radiation refers to the heat flux that the sun is emitting on the window. The default value of 1000 W/m^2 is used. This value is extremely high for the light used to simulate the sun. Through measuring heat flux with a light meter and rate of temperature vs. time curves described in chapter three, a more realistic value of 30.2 W/m^2 is utilized, which gives more accurate temperature trends.

Heat Transfer Coefficients

The heat transfer coefficients for the inside and outside were determined from the design temperatures in environment conditions. The value for h_1 is rather large (23 W/m^2K) because the air on the outside is constantly circulating at speeds on the order of 5 m/s. The air on the outside is under forced convection. The value for h_6 is smaller (8 W/m^2K) because the air is under natural ventilation.

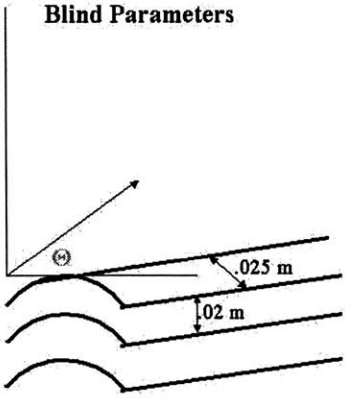

Figure 14. Blind input parameters

Blind Properties

The three parameters needed for the blinds are the blind length, blind spacing and blind position. The blind length

refers to the conduction length, which for this case is .025 m. The spacing is the vertical spacing between each blind, which is .02 m. The blind angle, Θ (theta), refers to the angle from the horizontal, which the blind is positioned. The blind is opened when the angle is 0^o, and closed when the angle is 90^o. The value of zero is never used because the program uses the value in many locations in the spreadsheet and if the zero ends up in a denominator then no useful results would be calculated. An angle of 2^o was inputted instead. The material properties of the blind were not altered because the material used was the same. Figure 14 illustrates the three parameters. It is imperative that user understand the geometric values because inputting in a wrong number may result in negative numbers or unrealistic data.

Air Properties

There are two important parameters in the air properties input area. The mass flow rate, which easily converts to velocity and the h_{conv}, are located in this group. The h_{conv} is determined by the geometry and is one of the four convective coefficient scenarios discussed in the section, Mathematical Model Assumptions. For this particular example, the h_{conv} calculated to be 5.18 W/m^2K on both the inlet and outlet (inside and outside cavity). If the interior cavity velocity increased the h would increase. The same is true for the mass flow rate. The interior cavity dimensions determines the mass flow rate on the inside cavity. For the example in Appendix D, the mass flow rate is .01 kg/s.

The hey parameters which create a mathematical model are: the physical dimensions of the windows and their spacing, the design temperatures of the air inside and outside the DSF window system, the incident radiation which the heating element emits, the heat transfer coefficients inside the room and outside, the blind dimensions and position, and the mass flow rate and h_{conv} of the air in the cavity. Once the user inputs these values into the program, a variety of graphs and charts are created which will be discussed in the next section.

4.5 Output of Model

The mathematical model analyzes many aspects of the thermal performance of the Double Skin Façade Window System. The model illustrates the effects of the air velocity, solar altitude, and the blind position. The mathematical model has many capabilities,

however the focus is primarily on the temperature distributions through out the model. The data collected will be compared to the temperature distributions, which the model calculated for various initial conditions.

One of the key areas of the model is the summary page. It is similar to the input section, because it stores all of the initial condition data in one area. Some of the input parameters are not in obvious locations, however the summary page facilitates looking up parameters. If the user is running more than one scenario, the summary page is perfect for keeping track of which case is being analyzed.

Graphs and Charts

The bulk of the output of the mathematical model is easily read through graphs and charts. Appendix E has the charts and graphs that will be explained in this section. The graphs and charts which will be discussed are: Temperature Distribution vs. Height, Temperature vs. Partition Number, Heat Transfer Coefficients vs. Different Horizontal Stations, Temperature vs. Horizontal Position at Different Vertical Heights, Solar Heat Gain Coefficient (SHGC) vs. Air Flow Rate, Heat Transfer Coefficient (h_{conv}) vs. Air Velocity, and Solar Altitude vs. Solar Heat Gain Coefficient.

Since the focus of the research is temperature measurement, the Temperature Distribution vs. Vertical height chart is necessary for evaluating the accuracy of the model. Item 1 of Appendix E, Temperature Distribution vs. Height, is a sample chart, which the model calculates for every scenario. The first row of the chart lists the horizontal position in the double skin facade window system. Below each location there is a number, which corresponds in the horizontal position. The numbers will represent the horizontal position in the comparison graphs in the next section. The first column is the vertical height where zero represents the bottom of the system. The number of vertical partitions is 20 and the height of the window is 1.21 m so it calculates the temperature every .06 meters.

The second item of Appendix E is the Temperature vs. Partition Number graph. This graph takes the first eleven vertical sections (i.e. 0 corresponds to vertical height of 0 m, and 1 corresponds to a vertical height of .06 m, etc…) of the graph and plots it versus temperature. Each curve represents a horizontal location, so for example, 5 refers

to the temperatures on the interior window on the cavity side. The graph shows that the temperatures vary very little with height for the first eleven vertical sections.

Item 3, Heat Transfer coefficients at different Horizontal Stations compares the h_{conv} and h_{rad} to horizontal locations throughout the model. The lighter blue bars are the convective coefficients and the darker bars are the radiative coefficients. Note that the h_1 is much higher because of the high velocities of the air due to fan in the heated box. The radiation and the convection coefficients do not follow the same trends though out the system. Neglecting h_1, the radiation coefficients are higher at the exterior window and the lower near the room. The Convective coefficients are the exact opposite. They are higher near the room and lower near the exterior. This generalization is logical because the sun, which generates the h_{rad}, is outside, and the cavity where the h_{conv} is most prominent is on the inside.

The fourth item of Appendix E is the graph, Temperature vs. Horizontal Position at Different Vertical Heights. This graph is an inverse of item 2, where each curve represents the horizontal position. The difference between the graphs is that each curve represents a vertical height in item 4, where series 1 is at the bottom of the window and it increases in increments of .06 m. From looking at the graph the largest change in temperature occurs in the air cavity and blinds.

Item 5, Solar Heat Gain Coefficient (SHGC) vs. Air Flow Rate graph describes the effect of altering the air velocity to the calculated SHGC. The solar heat gain coefficient takes into account the contribution of the solar energy to the system. It is determined by the h_{rad} coefficient and the geometry of the system (i.e. the angle at which the sun hits the DSF window system). It is obvious that there is very little change in SHGC due to the air velocity, because of the almost constant curve.

The sixth item of Appendix E is the graph Heat Transfer Coefficient (h_{conv}) vs. Air Velocity. The relationship between the two parameters is almost directly proportional by a factor of about 2.3. The increase in velocity corresponds to an increase in h_{conv}, which in turn reduces the thermal resistance. The temperature difference from the top of the system to the bottom should be greater for higher h_{conv} because of the smaller thermal resistance. The smaller the thermal resistance, the larger the temperature changes because they are indirectly proportional.

Item 7, Solar Altitude vs. Solar Heat Gain Coefficient, is a graph, which compares the SHGC vs. the angle at with the sun hits the DSF window systems. Each curve represents a different position of the blinds where open is 0^{o} and 90^{o} is closed. The largest SHGC logically corresponds to the open blinds position, because the maximum amount of light can enter at that point. The maximum SHGC is at a solar altitude of zero, when the sunrays are perpendicular to the DSF system. At any other angle only the energy in the direction perpendicular to the system can be used, so the SHGC drops off. At about a solar angle of 50 there is very little difference between the different blind positions. Figure 14a illustrates the correct representation of the solar angle and blind position.

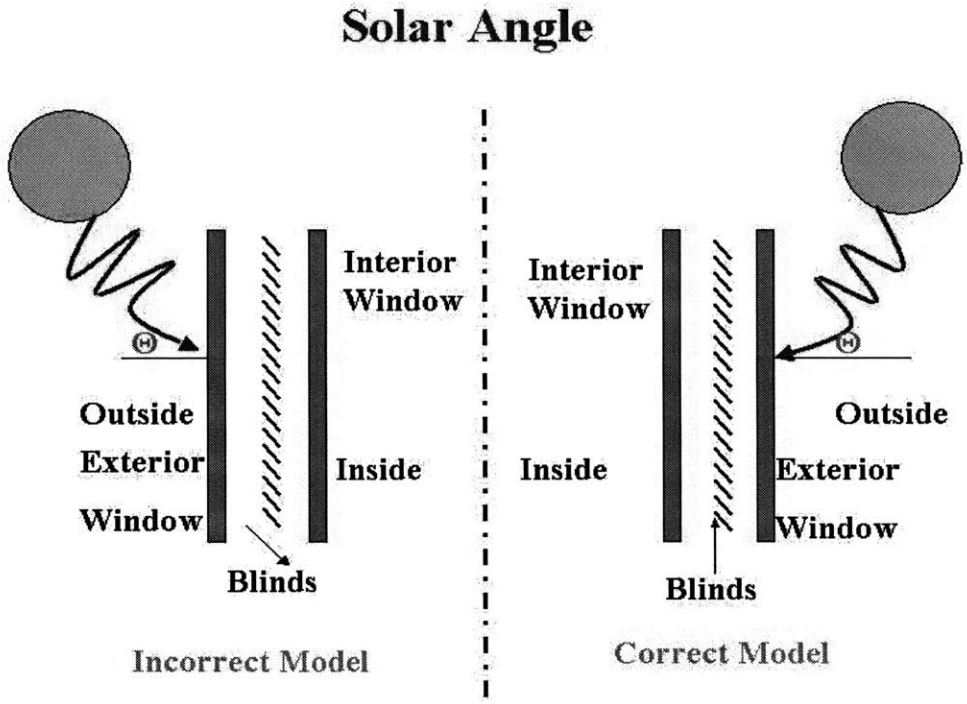

Figure 14a Solar Angle

4.6 Analyzing Data

Now that the double skin facade system and the mathematical model have been defined, the results can be compared. A few comments on the format of the comparisons are necessary to facilitate in the explanation of the graphs, such as dividing the system into sections. The types of graphs, which the data is expressed, are then discussed, and are followed by the temperature trends of the model and data. The accuracy of the model is determined. Various sets of data are compared, looking at how interior cavity length and blind position may or may not affect the temperature trends. Finally, the possible reasons for the error will be discussed.

Format of Comparisons

The data is compared to the model by vertical height and horizontal position. The plots of the temperature vs. vertical height at a given horizontal location are straightforward. However, when comparing the temperature to the horizontal location, the graph becomes more complicated. The interior window is movable so it is harder to define the window because it is not fixed. Each component of the DSF was given a number, which represents a horizontal position. Figure 15 illustrates a typical curve comparing the model to data at different horizontal positions (H Position). Note the

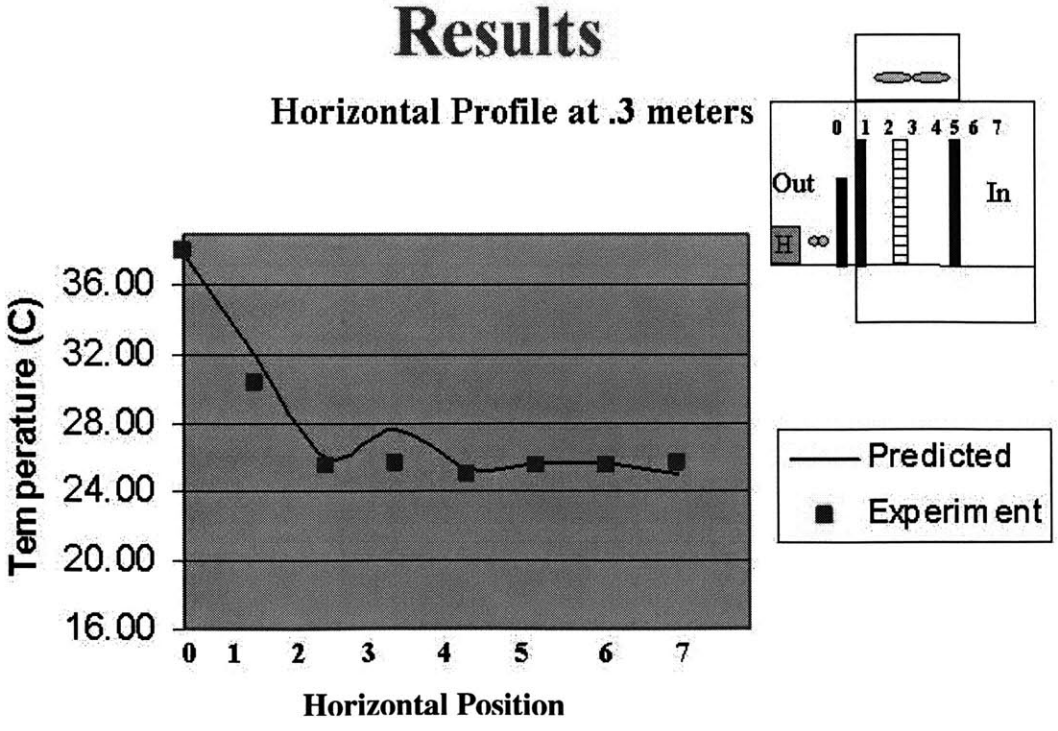

Figure 15. Sample Temperature vs. H Position Graph

schematic of the experiment setup in the top right corner, which helps visualize the horizontal position . The temperature of the heated box corresponds to the out location. Traversing the window system, the exterior window is the number one position, the exterior cavity is position two, position number three is the shading device, the interior cavity is position four, the two sides of the interior window are position five and six respectively, and finally the inside of the room is appropriately represented by the in location.

Types of Graphs

The experimental data was expressed in three different ways. The first type of graph was temperature vs. time graph. For each horizontal position there is time history vs. temperature for every set of data. This graph is a verification of the steady state of the system and also can be used to explain any inconsistencies from data sets of the same scenario.

For example, if on a particular data set the exterior window temperature is lower at the top than the bottom, but every other temperature profile shows that the temperature is increasing from bottom to top, the time history graph is key to finding the reason this has happened. The time history vs. temperature may show that the temperature trends were consistent with the system (i.e. increasing height and increasing temperature) but at some time the values dropped drastically near the top of the window it could explain the inconsistencies. The thermocouples may have become loose and may have started to read the air temperature instead of the window temperature. Figure 16 through 18 are sample temperature versus time graphs at various locations.

The numbers in the legend represent the thermocouple position and a detailed description of the thermocouple positions is located in chapter three. The title of the graphs describes where the thermocouples are placed. Note that in figures 17 and 18 there is a slight dip in the temperature in the first 1000 seconds (roughly 17minutes). This is in response to the decrease in temperature in the heated box in figure 16. The DSF window is sensitive to slight temperature changes. Another observation of the time history graphs, the temperature of the air cavity seems to be the most erratic out of all three plots.

Initial Conditions Group D

- Blinds Closed
- Interior Cavity Length = 9"
- Air Cavity Velocity = .1 m/s
- Heat source, Sun Lamp

Figure 16 Time history of Temperature in Heated Box, Group D

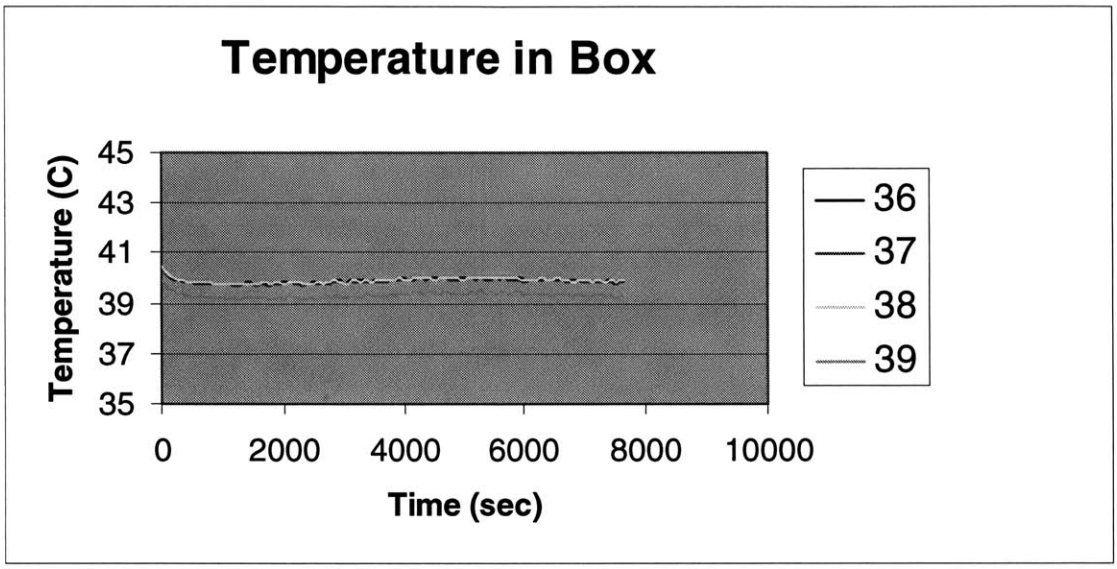

Figure 17 Time History of the temperature of the Blinds

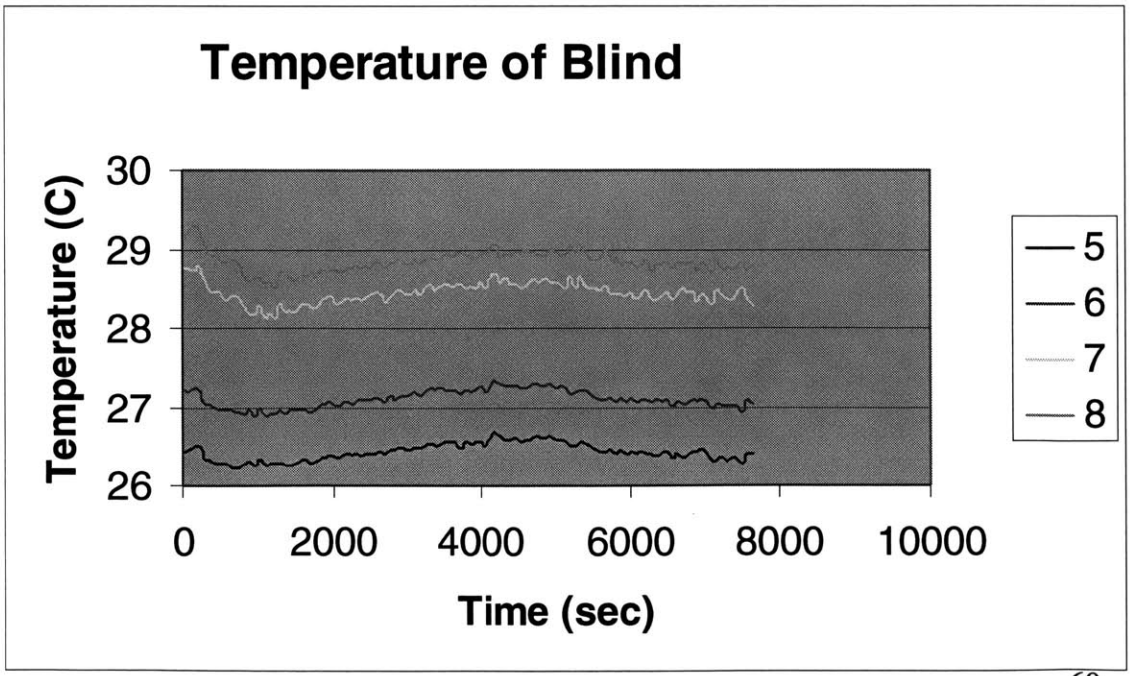

Figure 18 Time History of temperature in Cavity, Group D

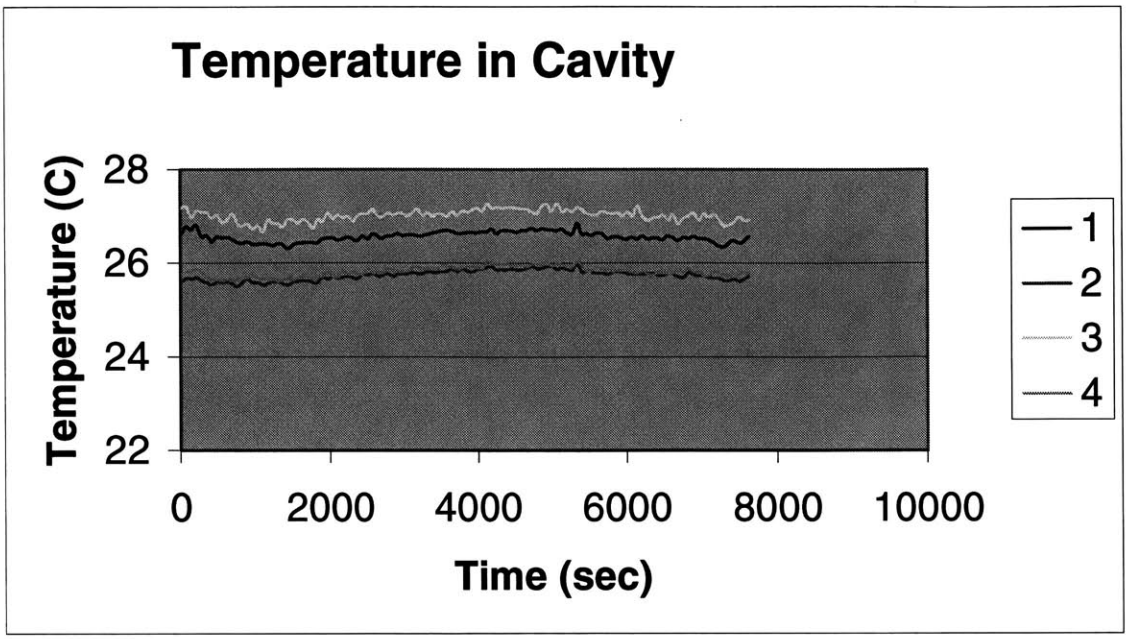

The second type of graph is a temperature versus vertical height graph. The temperature is plotted against vertical height for each horizontal section. The zero position is at the bottom of the window. The next four figures (19a to 19d) are a series of chart also from group D, which illustrate the temperature vs. vertical height.

Initial Conditions Group D

- Blinds Closed
- Interior Cavity Length = 9"
- Air Cavity Velocity = .1 m/s
- Heat source, Sun Lamp

Figures 19 a – d Vertical Distance vs. Temperature, Group D

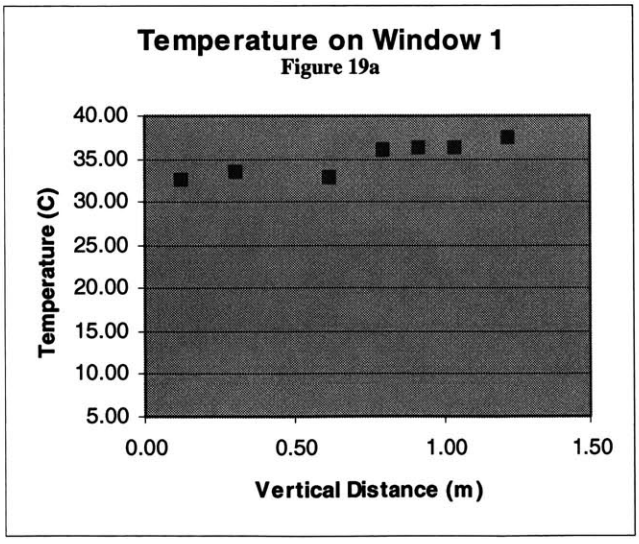

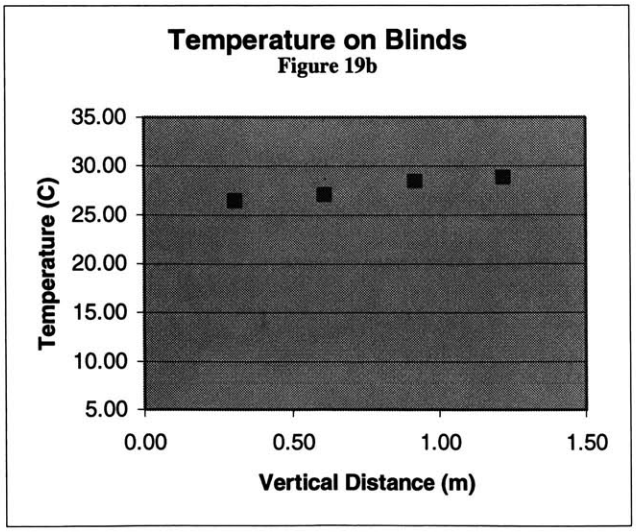

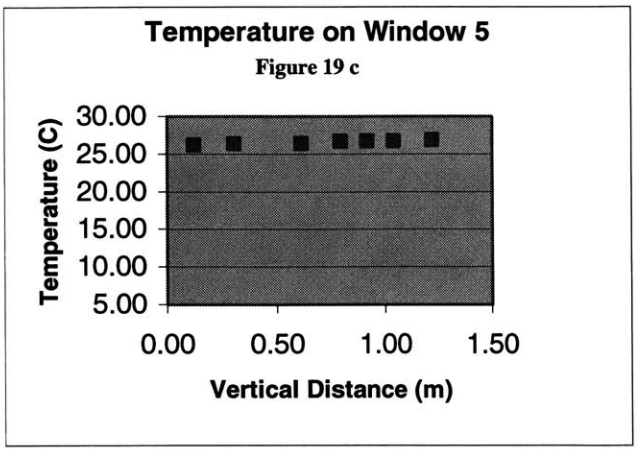

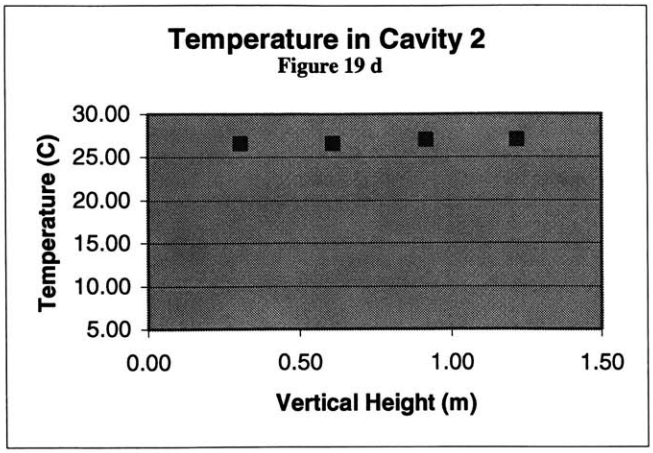

The experimental data does not have a signisficant temperature change in cavity two. The air is moving through the cavity relatively fast; there is not much time for the air to warm up as it goes through the cavity. The most variation in temperature is on window 1 or the exterior window. The temperature is increasing with the increase in height for the four graphs.

The last type of graph is a temperature vs. horizontal position. The horizontal temperature profile was plotted at every .3 meters of elevation, where the reference point is the bottom of the double skin façade window system. The next four figures (20a –d) are the horizontal temperature profiles for different heights.

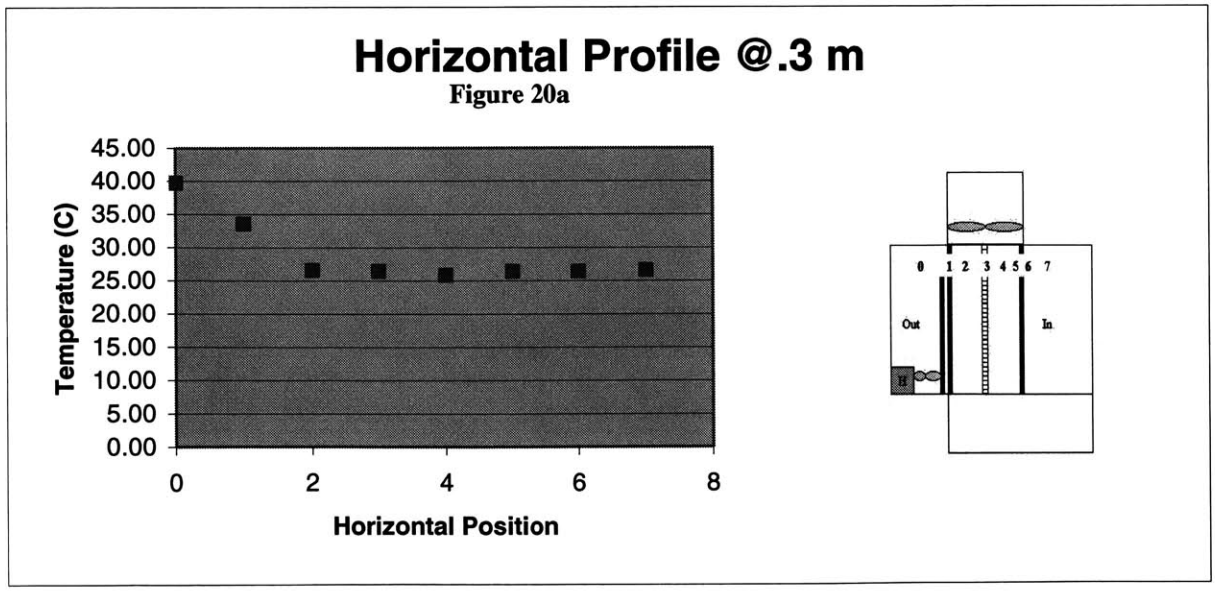

Figure 20a-d Horizontal Temperature Profiles for Varying Heights, group D

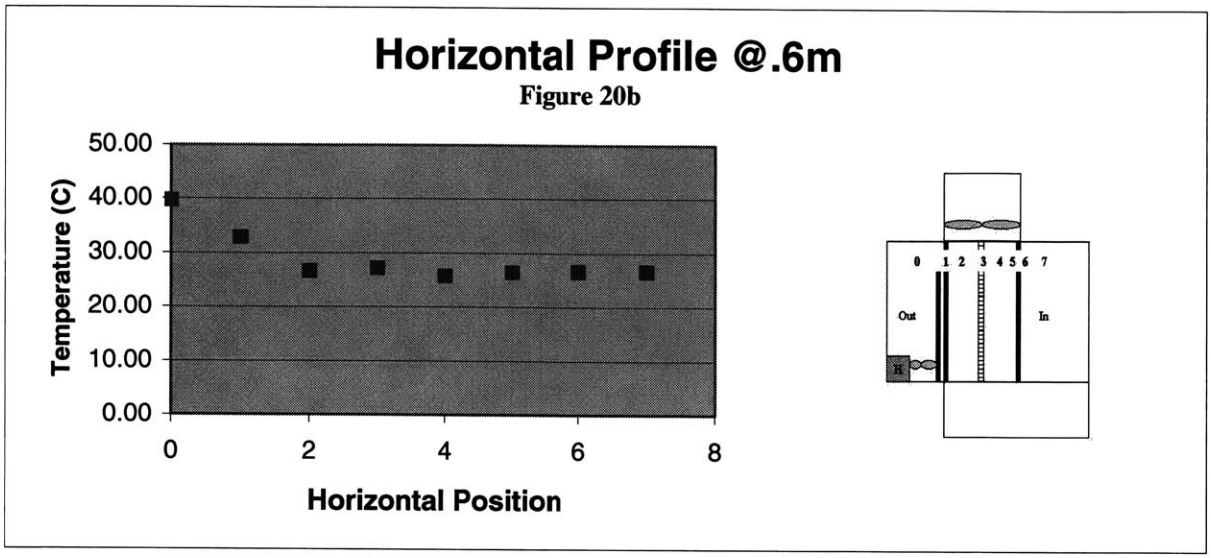

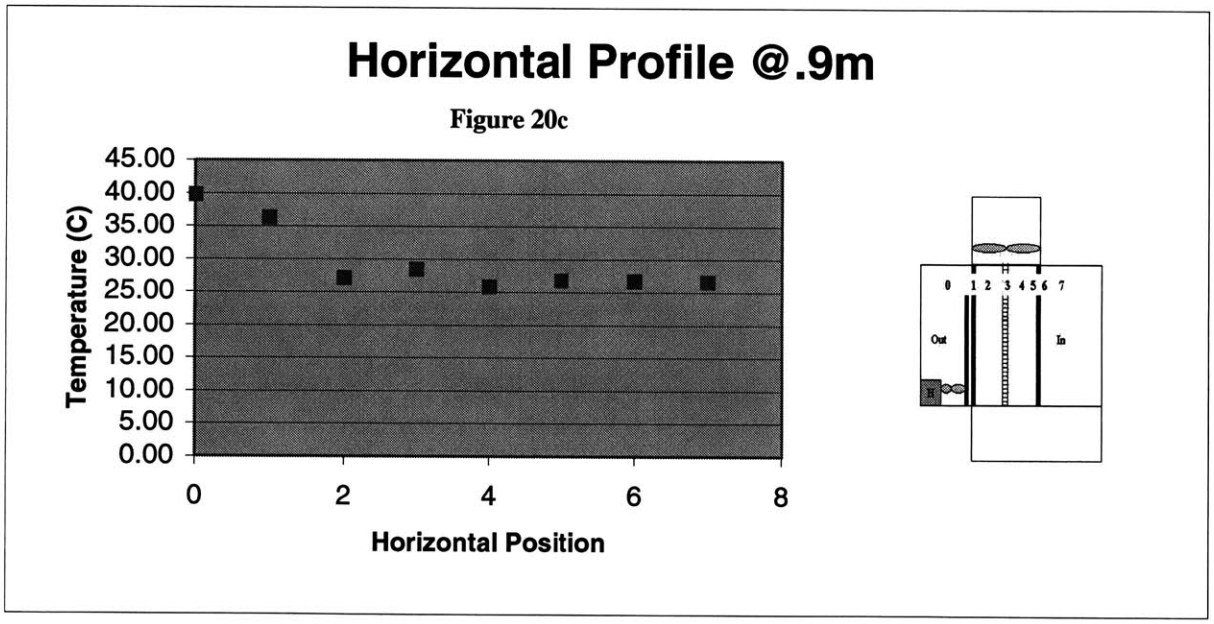

The temperature drops off significantly from position 0 (heated box) to position 2 (exterior cavity). At position four (interior cavity) the temperature does not change more than one to two degrees. At position four the heat source is much further away and the system is closer to the room temperature, which is roughly 25° C.

Figure 20d

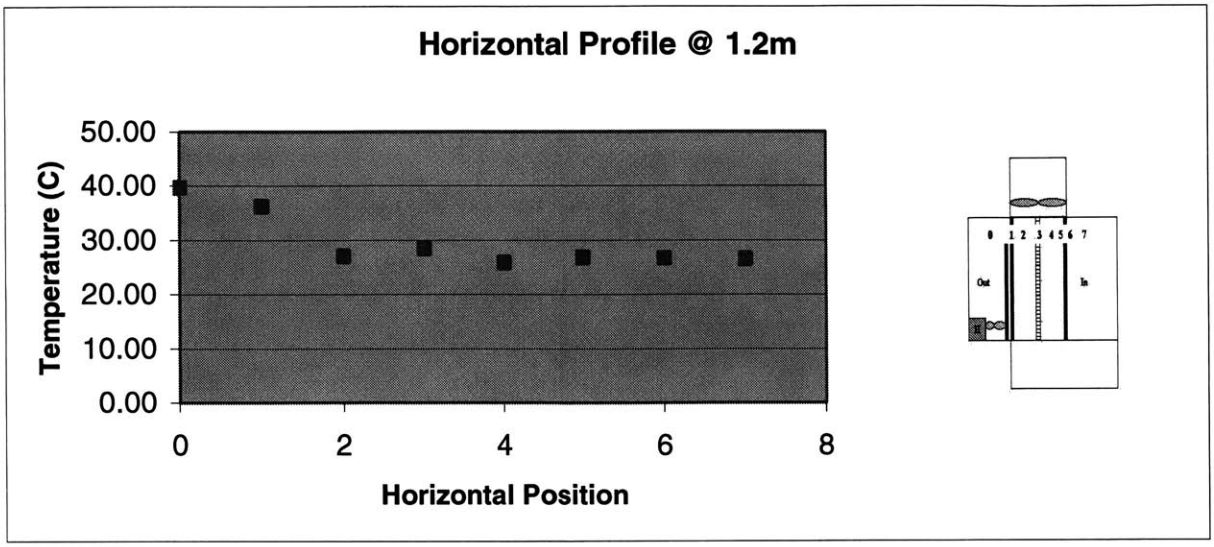

Temperature Trends of Model and Experimental Data

Figure 21 plots the temperature curves of the model for a typical DSF case. Each series represents a different vertical height. Series one corresponds to the bottom of the system and for each series the vertical height increases by .06 m. The horizontal position refers to the location in the system. The numbers represent the components of the system, however, there is a slight change from the experimental data. The

Figure 21 The Model's Temperature Profile and Initial Conditions, group A

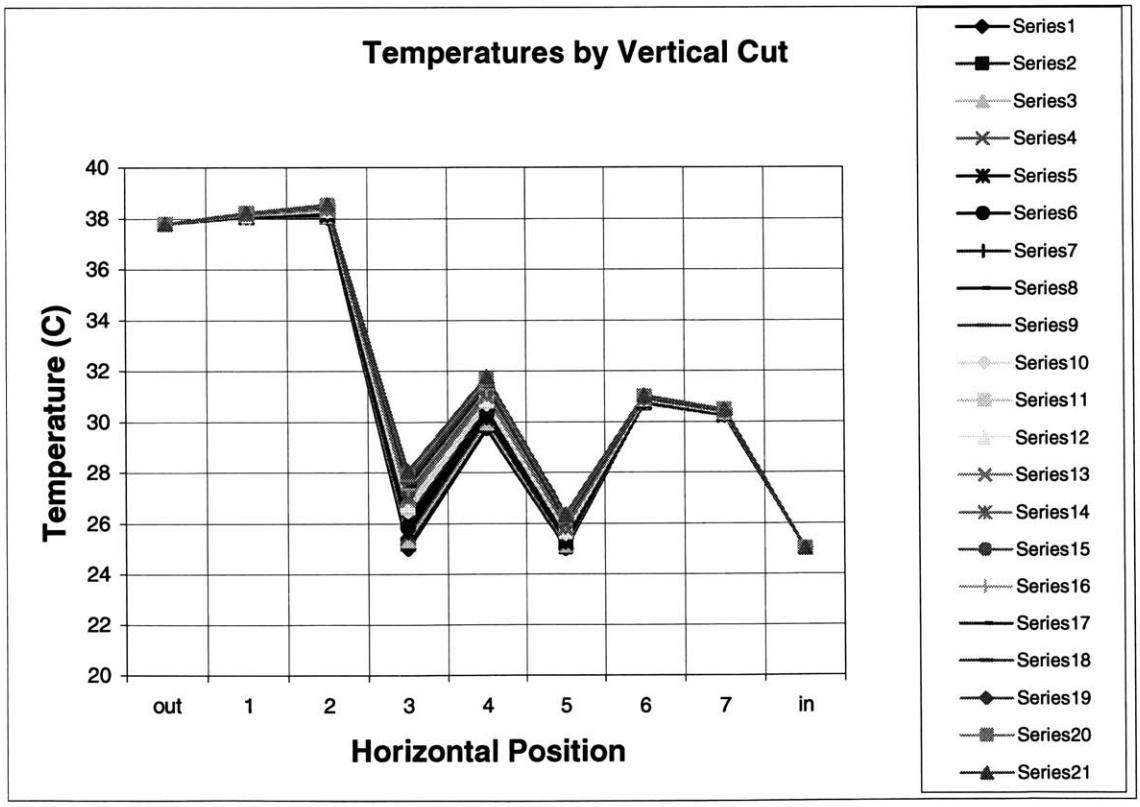

mathematical model calculates the temperature of the outside face of the exterior window and the experiment does not measure it. The two data points at locations 1 and 2 correspond to the exterior window and locations 3 and 5 become the cavities, location 4 the blinds, and positions 6 and 7 are the interior window. However, when the experimental data is compared to the model the extra point is left out. The initial conditions of the model come from group A.

Initial Conditions Group A
- Blinds Open
- Interior Cavity Length = 4.5"
- Air Cavity Velocity = .1 m/s
- Heat source, Sun Lamp

The graph is a little difficult to read but the darker lines have lower temperatures and they represent the temperature profiles near the bottom of the system. The light orange and yellow lines, which are higher in temperature, represent the temperature profiles at the top of the DSF system. The temperature is increasing with the increase in vertical height. The direction of heat transfer in the vertical direction is from the bottom to the top, which explains why the temperature increases with an increase in height. The blind temperature, which is represented by location four, is significantly higher than the surrounding air cavity temperature locations two and three. The heat is transferred from the outside to the blinds by radiation, and since the air is moving and has a much lower thermal conductivity it is more difficult for it to maintain the same temperature as the blinds. There is very little temperature drop across the windows, which means the thermal resistance is low as well across the windows. Finally the temperature difference in the vertical direction is greatest in the exterior cavity. There is about a 3.5°C temperature difference, and the second largest temperature difference in the vertical direction is about 2.5 °C on the blinds.

Figure 22 is a sample of the temperature trends of the experimental data. There are two sets of data on the graph. One set corresponds to blinds open and the other corresponds to blinds closed. The height of .9 meters is referenced from the bottom of the system. The air cavity temperature is slightly higher with the blinds closed, because the blinds are absorbing more heat, which is transferred by convection to air. The fact that the blind temperature is higher with the blinds closed corroborates the air cavity temperature difference. The data will be compared in greater detail in the following sections.

Figure 22 Temperature trends of experimental data

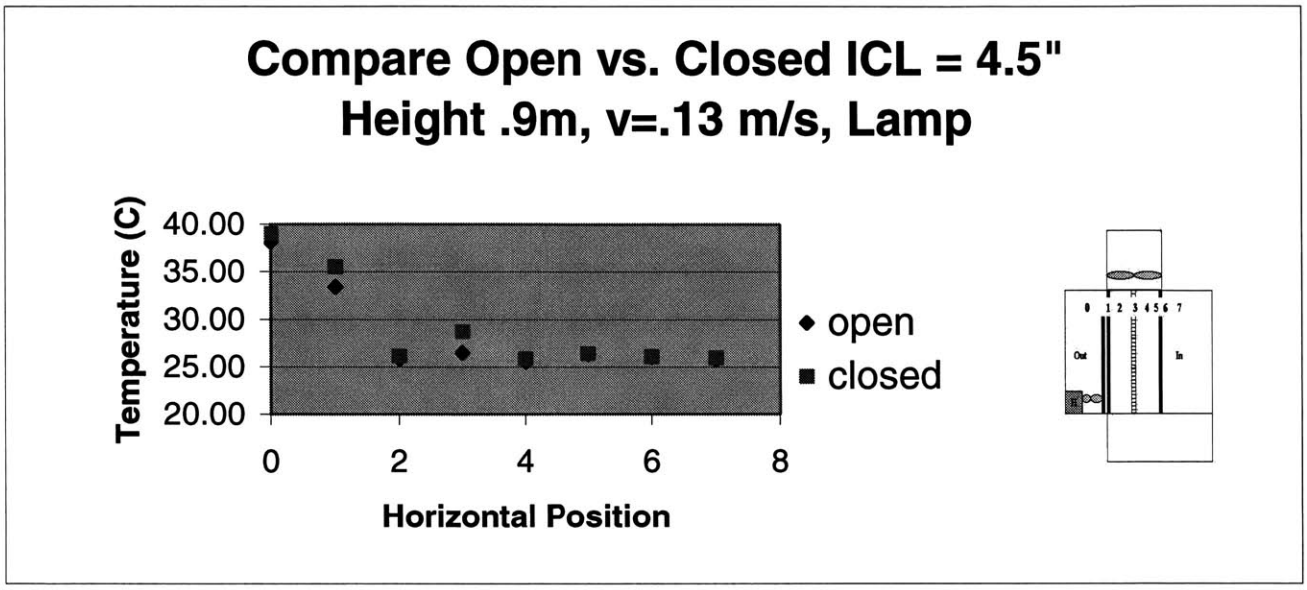

Accuracy of Model

Now that the types of graphs have been established, they can be evaluated against the model to determine accuracy of the mathematical model. Because the model was created for steady state results, the time history curves are not needed to calculate the accuracy. The data from the time history curves are averaged and the temperature averages over time are used to compare the mathematical model to the data.

Six groups (A-F) of experiments were run, which were defined by the blind position and interior cavity length. The light source used was the sun lamp, but a few of the scenarios the modified heater was used. Within each group there were variations of air cavity velocity and type of heat source. Group A had initial conditions of interior cavity length 4.5" and an open blind position. Group B had the same interior cavity length but the blind position was closed. For Group C, the interior cavity length was doubled to a value of 9", and the blind position was opened. Group D had the same interior cavity length, but the blind position was closed. Group E had a interior cavity length of 13.5 ", the blind position was opened. Finally, group F had the same interior cavity length, but with the closed blind position (See Chart 3 for Summery of Groups).

Figure 23a Comparison of Model and Experiment Temperature vs. Vertical Height for Group A

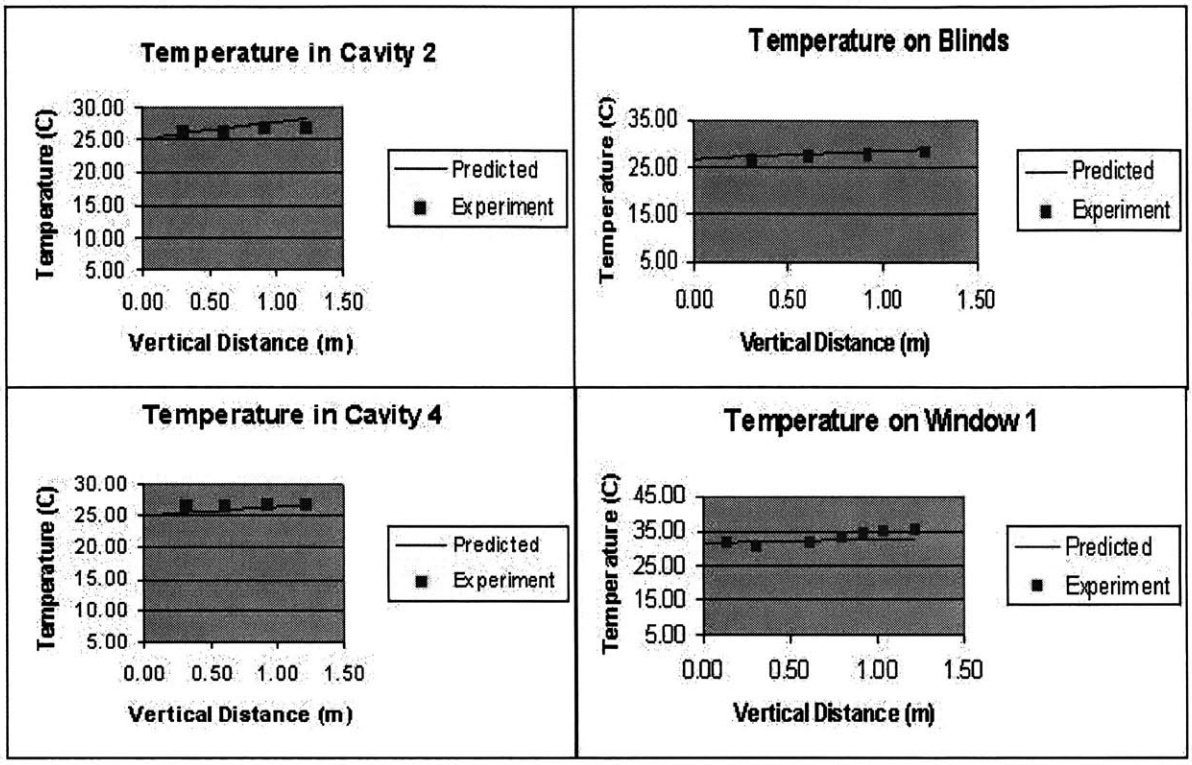

Chart 3. Description of Experiment Groups

	Group A	Group B	Group C	Group D	Group E	Group F
Blinds	Open	Closed	Open	Closed	Open	Closed
ICL	4.5 "	4.5"	9"	9"	13.5"	13.5"
Air Velocity	.1 m/s	.1 m/s	.1 m/s	.1 m/s	.1 m/s	.1 m/s
Heat	Heater	Heater	Sun Lamp	Sun Lamp	Sun Lamp	Sun Lamp

The model and experimental data were compared in two ways, the first was by temperature vs. height for each component, and the second was temperature vs. horizontal position. Figure 23a and b are the comparisons of group A, where the interior and exterior cavity length are equal (both are 4.5" from blinds). The blinds were open and the modified heater was used to heat the system. The experimental data is represented by

the pink squares and the blue curve is the model's output. The temperatures vs. vertical height graphs were made for each component (i.e. blinds, interior and exterior windows, both air cavities, and inside and outside) but the most interesting locations were in the air cavity so the blinds and air cavity temperature are featured. The figure 23b is a multiple graph. The individual graphs are temperature vs. horizontal location, but at different heights. The height of the graph is located to the left on the figure and it forms the second graph, which describes the entire system.

Initial Conditions Group A

- Blinds Open
- Interior Cavity Length = 4.5"
- Air Cavity Velocity = .1 m/s
- Heat source, Heater

Taking the difference between the model and data and dividing it by the temperature range from outside to inside defined the error of the system. The equation is,

Equation (8)

$$error = \left(\frac{\left| T_{predicte} - T_{data} \right|}{T_{outside} - T_{inside}} \right) * 100 .$$

Figure 23b Comparison of Model and Experimental Data Temperature vs. Horizontal Position for Group A

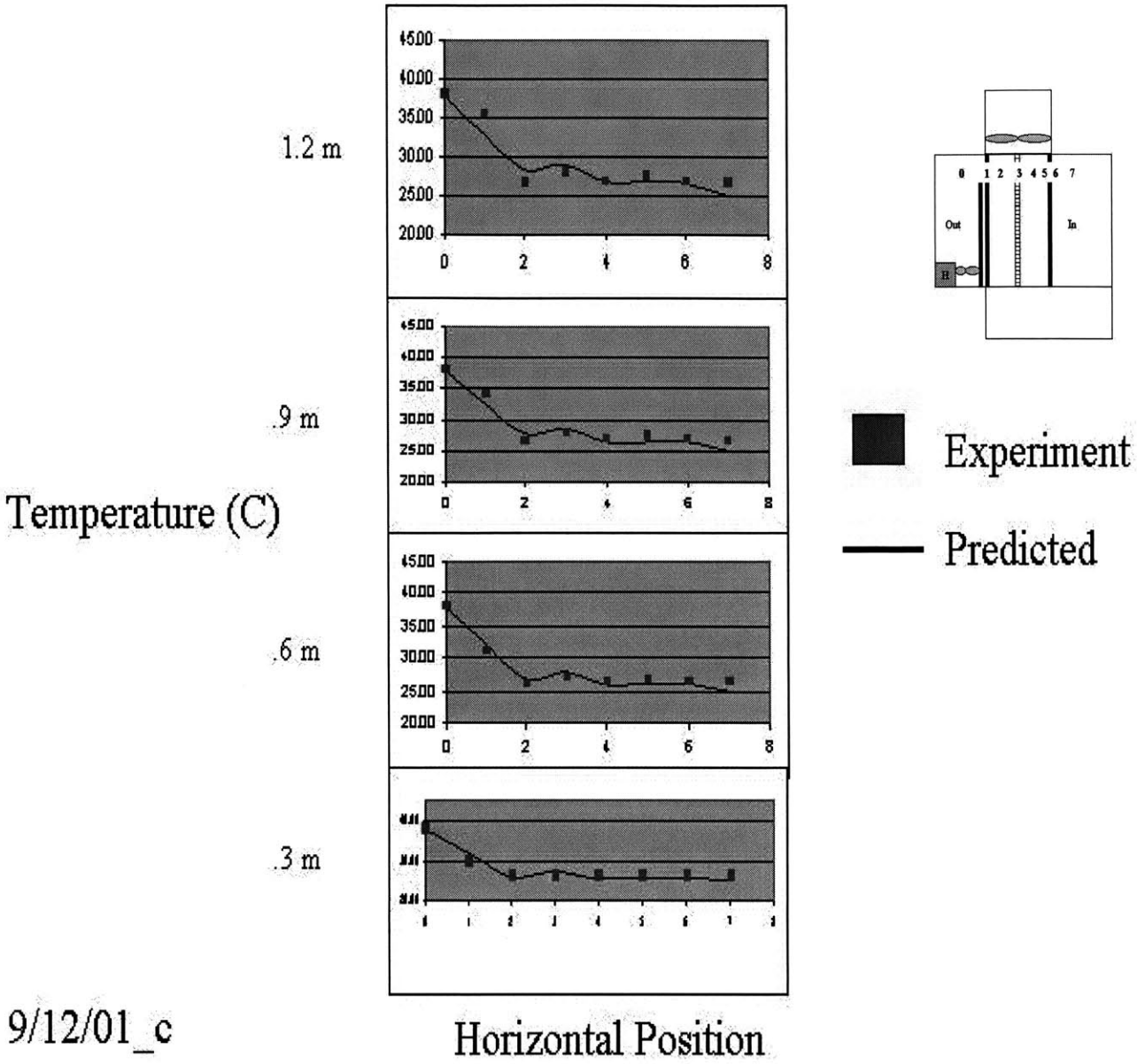

There is very good agreement between the model and the data for the blinds and both cavities, where cavity 2 is the exterior cavity and cavity 4 is the interior cavity. The experimental data for window 1 starts of close to the model but eventually bypasses the model. Figure 23b shows the overall temperature trend of the model and data. At the lower heights the model and data are in better agreement than near the top of the system. The convective coefficient, which directly affects the temperature, is constant for each height segment. Although the model uses the same value of the convection coefficient, on the plain surfaces it should decrease with height. For this particular case the error of the model was 2.07% of the data. This was the best agreement for this scenario.

Figure 24a and b illustrate the comparison of the experimental data and model for group B where the interior and exterior cavity length are the same (both are 4.5"

Figure 24a Comparison of Model and Experiment Temperature vs. Vertical Height for group B

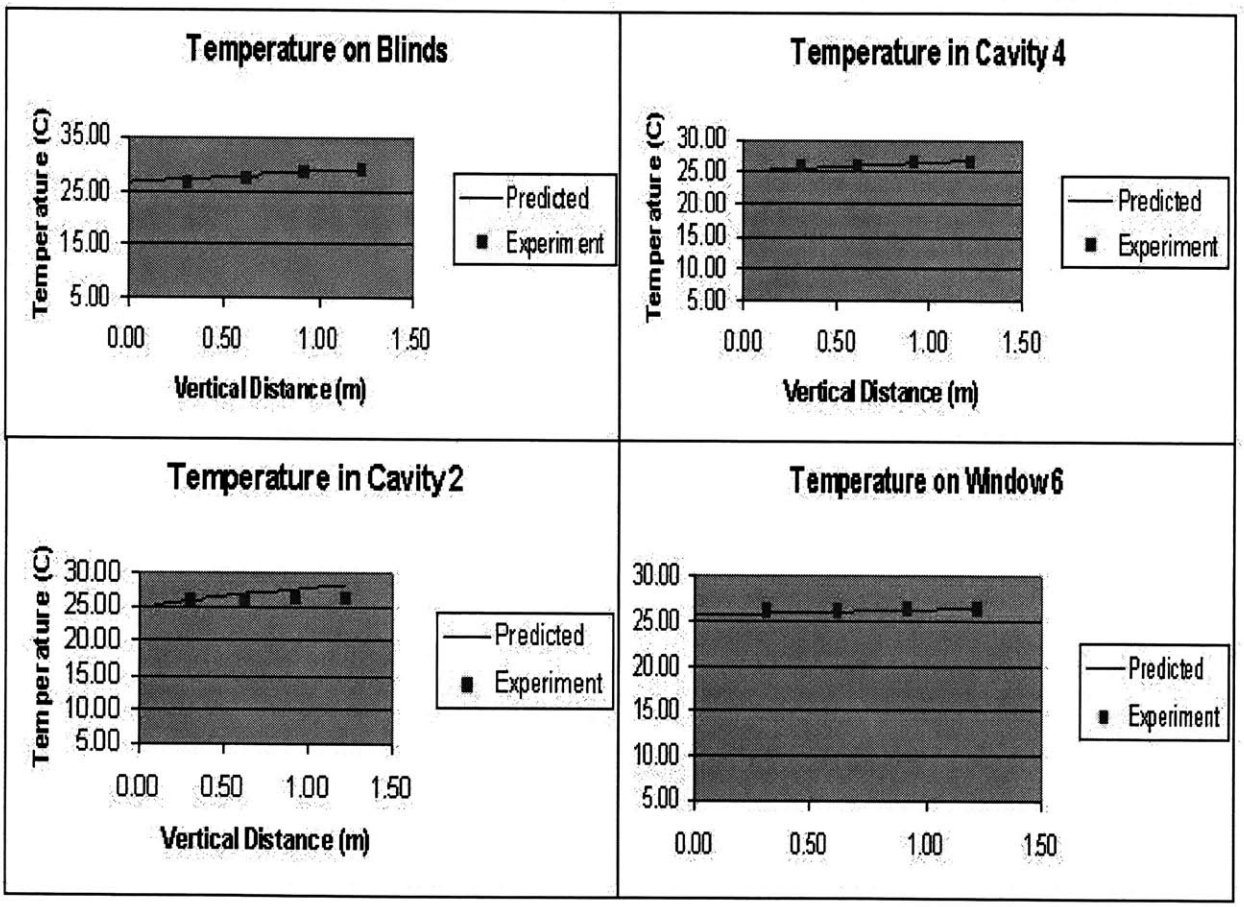

from blinds), but the blinds are closed. The modified heater was used again to heat the system.

Initial Conditions Group B

- Blinds Closed
- Interior Cavity Length = 4.5"
- Air Cavity Velocity = .1 m/s
- Heat source, Heater

In Figure 24a the temperature of the air cavity 2 is slightly lower in the experimental data than the predicted as the height increases. The other DSF components have excellent agreement between the predicted and the experiment. The same trend of the data deviating from the model near the top of the double skin facade system is observed from looking at figure 24b. For this particular case the error was 1.68%. It was slightly lower than the error of group A.

Figure 24b Comparison of Model and Experimental Data Temperature vs. Horizontal Position for group B

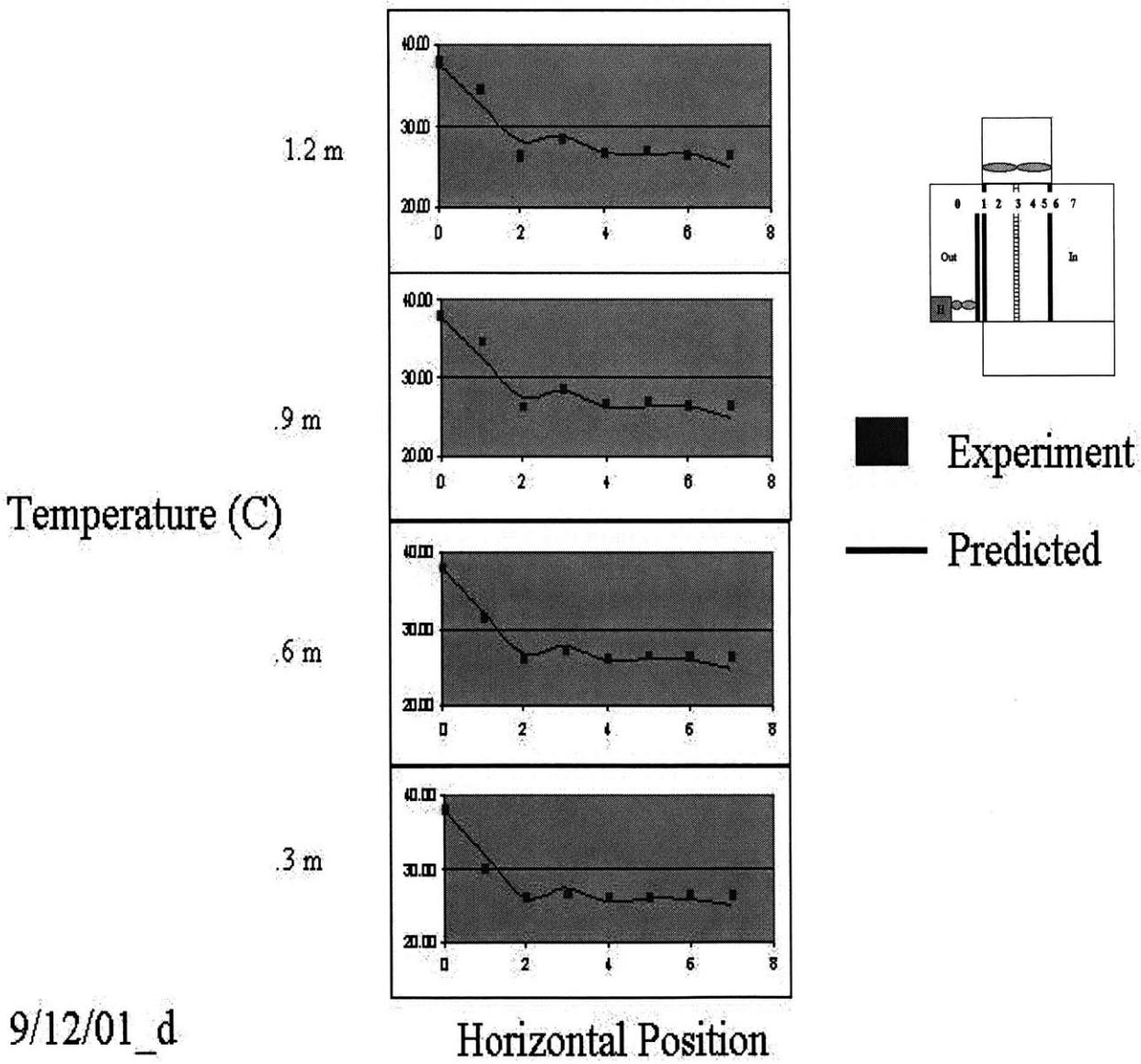

The data and model evaluation of group C, where the interior cavity length is 9" and the exterior cavity length is 4.5, is expressed by figures 25a and b. The blinds were open for this case and the sun lamp was used to heat the system. The agreement of the model and data are not as good as the agreement in the first two cases. There is a significant difference in the model and data for the blind temperature vs. height.

Figure 25a Comparison of Model and Experiment Temperature vs. Vertical Height for group C

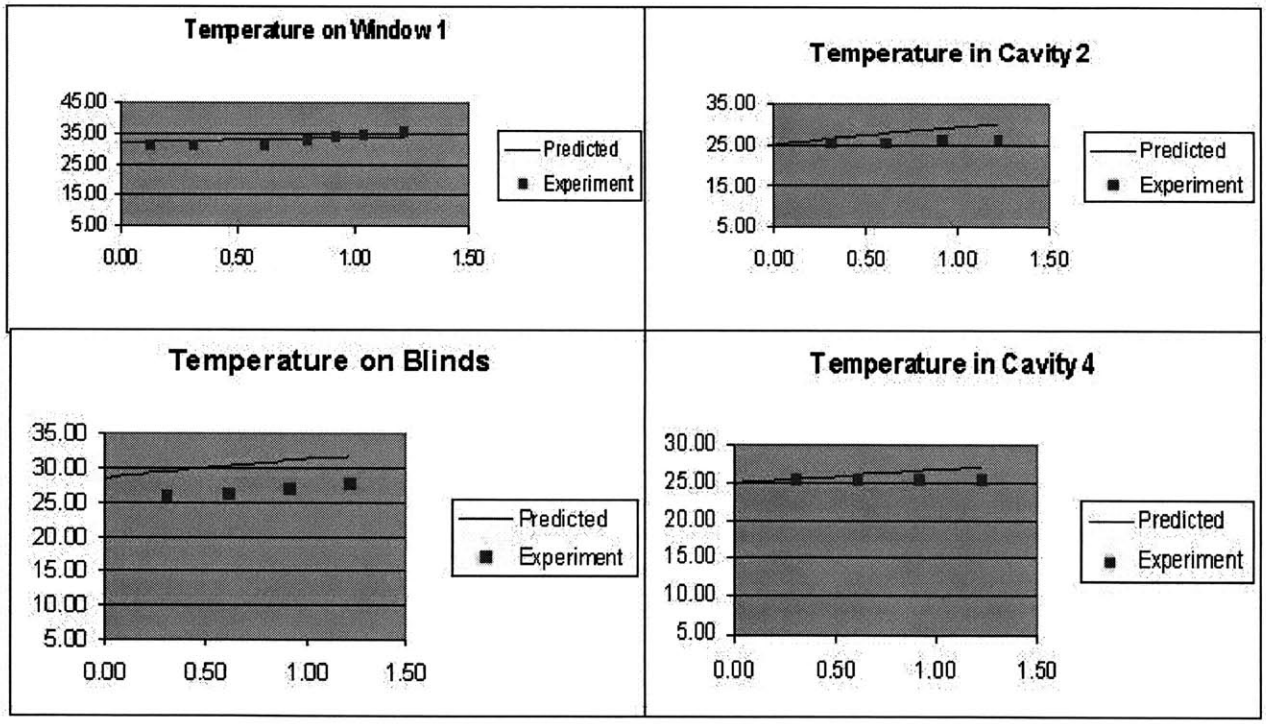

Initial Conditions Group C

- Blinds Open
- Interior Cavity Length = 9"
- Air Cavity Velocity = .1 m/s
- Heat source, Sun Lamp

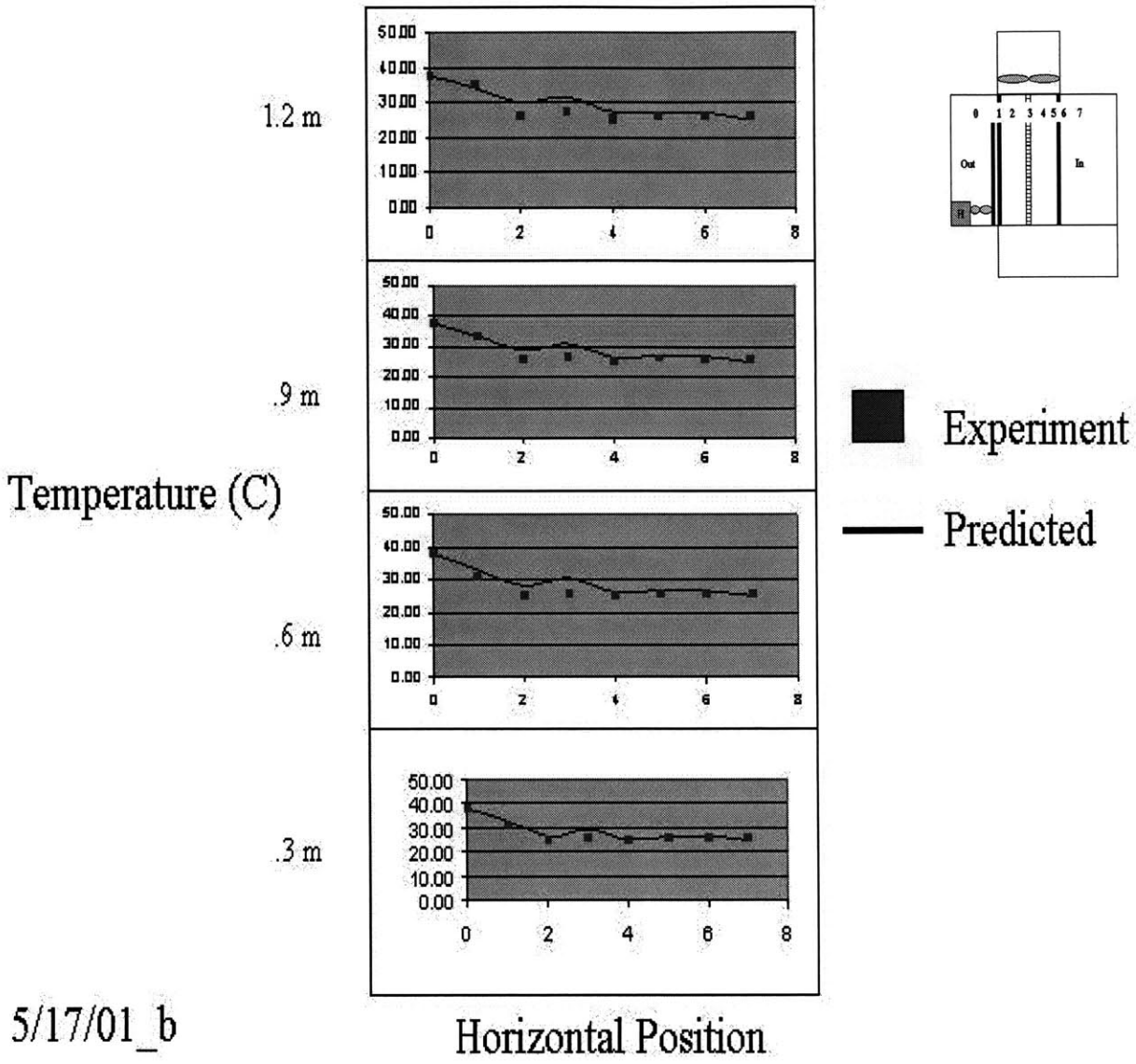

Figure 25b Comparison of Model and Data Temperature vs. Horizontal Position for group C

Looking at the horizontal profile of group C, the blind temperature is large contributor to the error probably due to an erroneous value for the heat transfer coefficient. The temperature difference of the model and data in air cavity 2 was the second largest component of the error. Even though, there are deviations between the model and data, the overall temperature trends are similar. For this particular case the error of the model was 3.18% of the data.

Group D has the same cavity dimensions as group C (ECL = 4.5", ICL = 9"), but the blinds are closed for this case. The sun lamp was used to heat the system. Figures 26a and b are the experimental data and model comparisons for group D. Notice the significant temperature difference in window 1,

Figure 26a Comparison of Model and Experiment Temperature vs. Vertical Height for group D

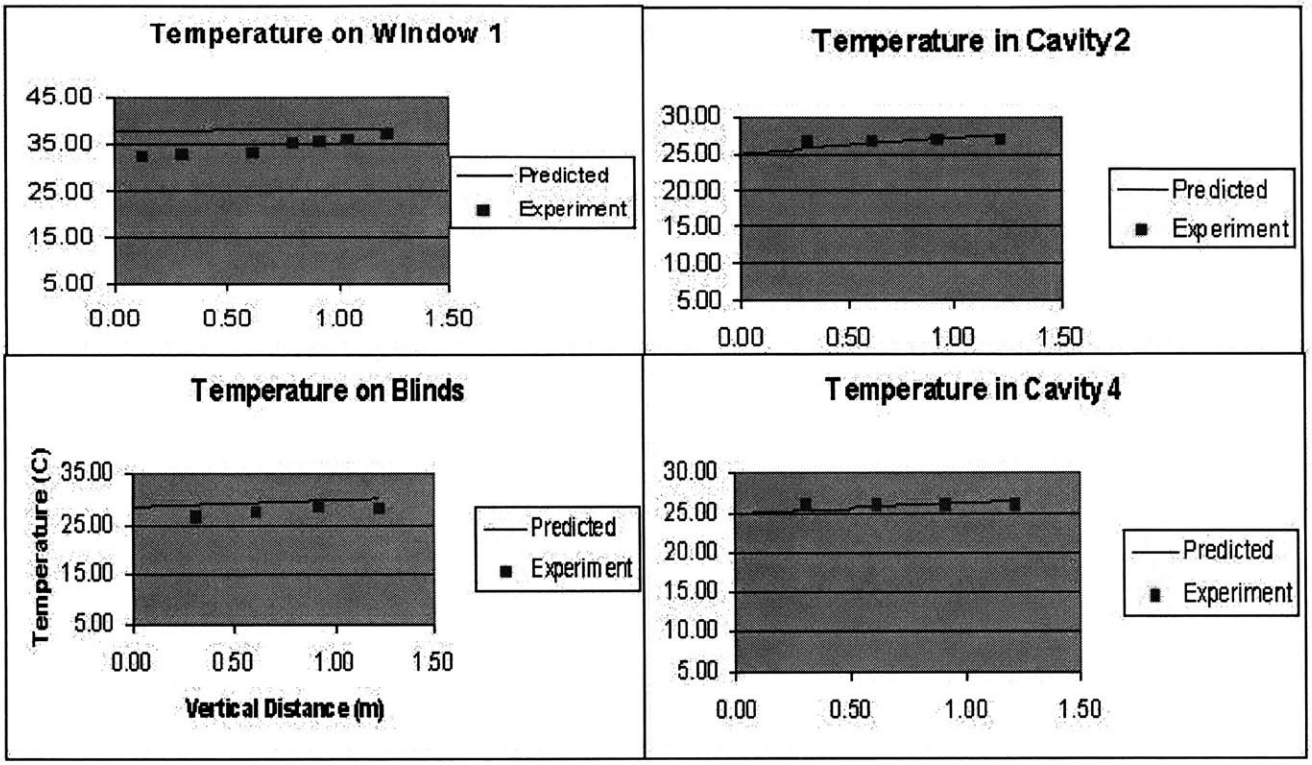

which decreases with the increase in vertical height. The other components have a pretty good agreement between the model and data. The difference in temperature of window 1 between the model and data is also expressed in figure 26b. The second data point represents window 1 and it is well below the blue curve. The data point does get closer to the curve at the top of the system, because the experimental temperature increases. The accuracy of the model for this particular case is 96.9%. Note that as the interior cavity increases the accuracy of the model decreases. The reasons for this will be discussed at the end of the section.

Initial Conditions Group D

- Blinds Closed
- Interior Cavity Length = 9"
- Air Cavity Velocity = .1 m/s
- Heat source, Sun Lamp

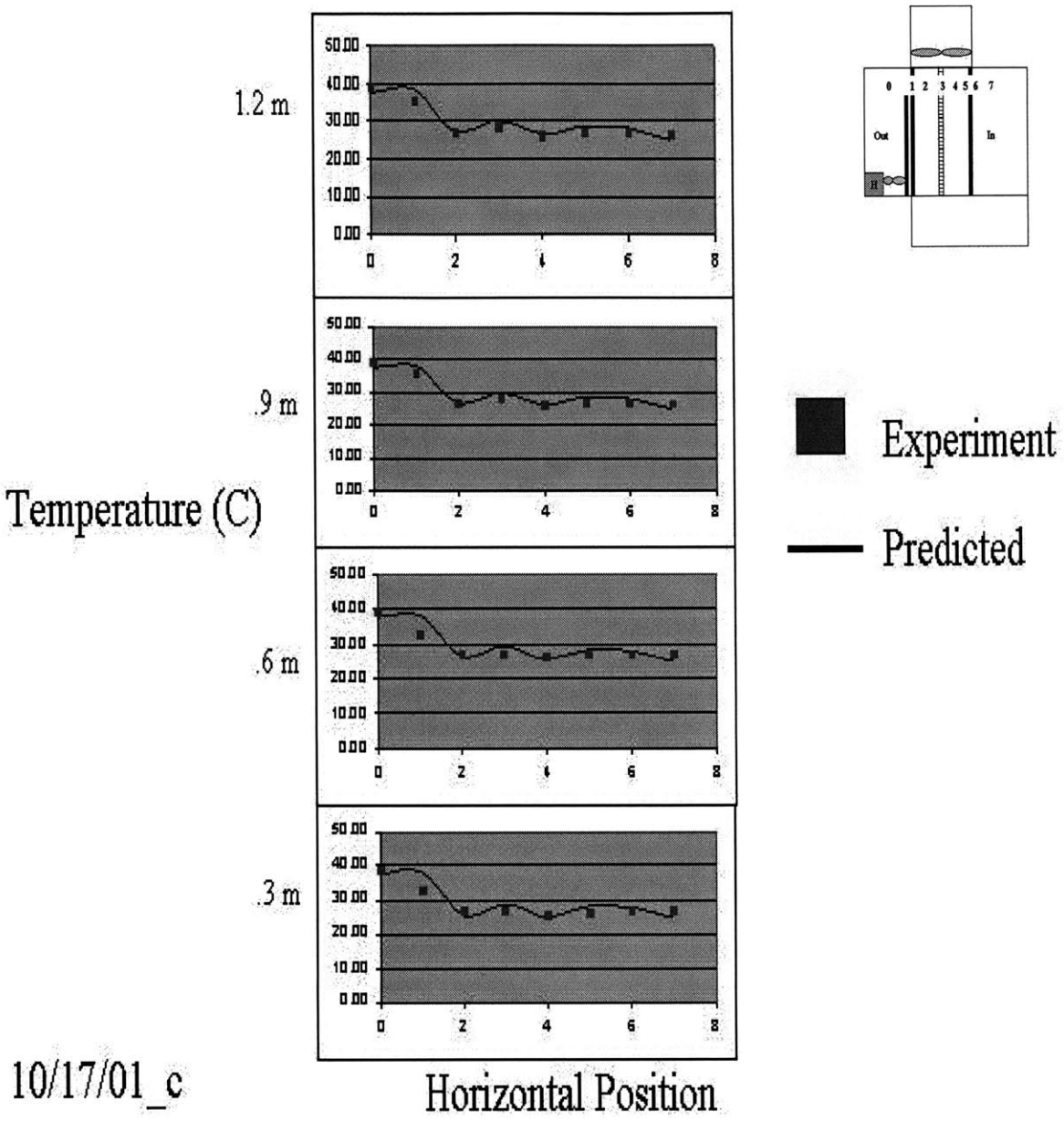

Figure 26b Comparison of Model and Data Temperature vs. Horizontal Position for group D

Group E, which has the initial conditions of the ICL of 13.5" and ECL of 4.5", is evaluated next. The blinds were open for this case and the sun lamp was used to heat the system. Figures 27a and b express the comparison between the model and data.

There are significant discrepancies between the model and the experiment for window 1 and blind temperatures. Surprisingly, the cavity temperatures in the model and experiment are very close. In figure 27b, it is apparent that there is poor agreement between the model and data at both the interior and exterior windows and the blinds (locations 1,3,5,and 6 on the graphs). The accuracy of the model for this case is 95.4 %.

Figure 27a Comparison of Model and Experimental Data vs. Vertical Height for Group E

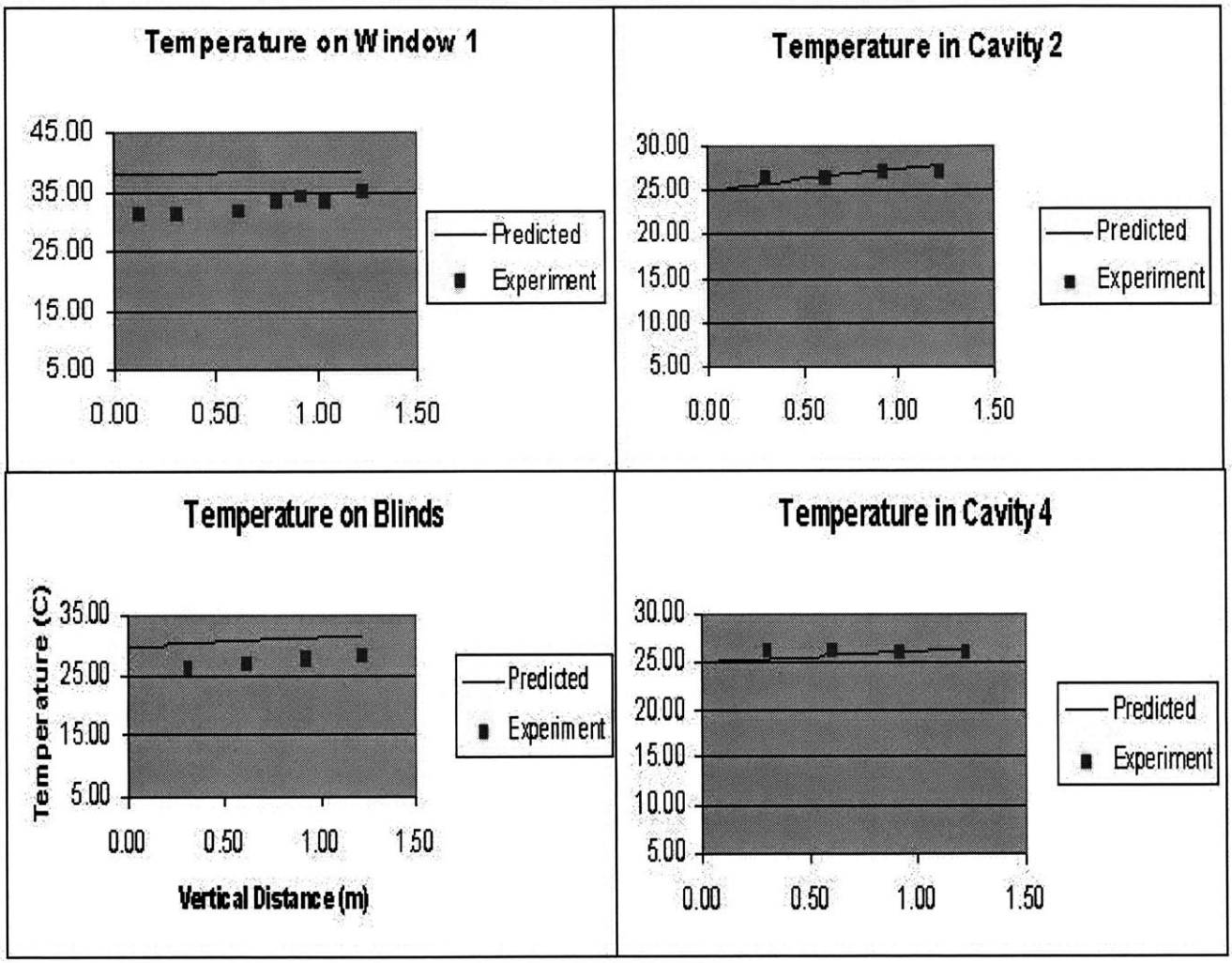

Initial Conditions Group E

- Blinds Open
- Interior Cavity Length = 13.5"
- Air Cavity Velocity = .1 m/s
- Heat source, Sun Lamp

Figure 27b Comparison of Model and Experiment Temperature vs. Vertical Height for group E

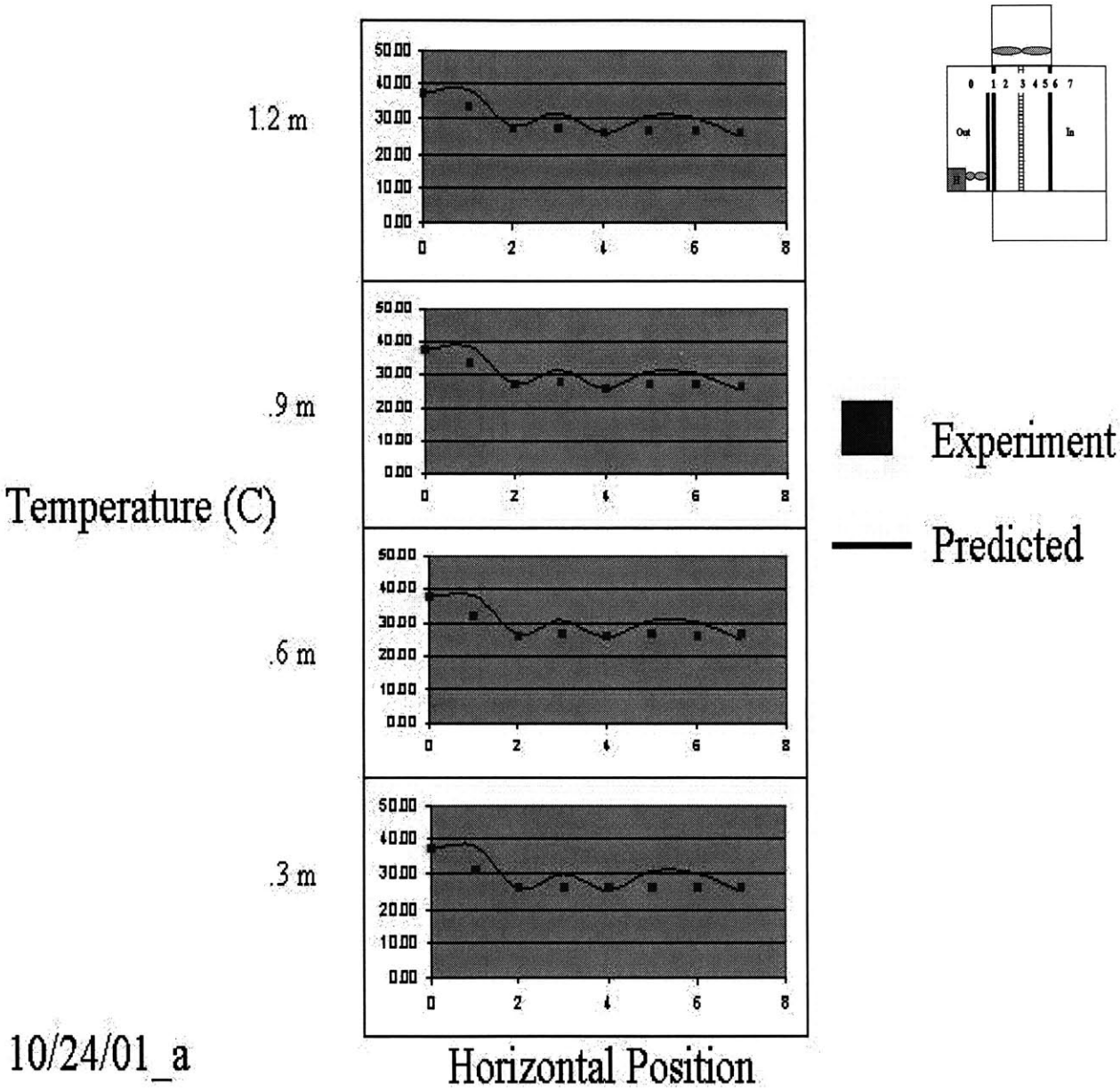

Finally group F represents the scenario similar to group E but the blinds are closed. The modified heater was used to heat the system. Figures 28a and b are the comparisons between the model and the data.

Figure 28a Comparison of Model and Experiment Temperature vs. Vertical Height for group F

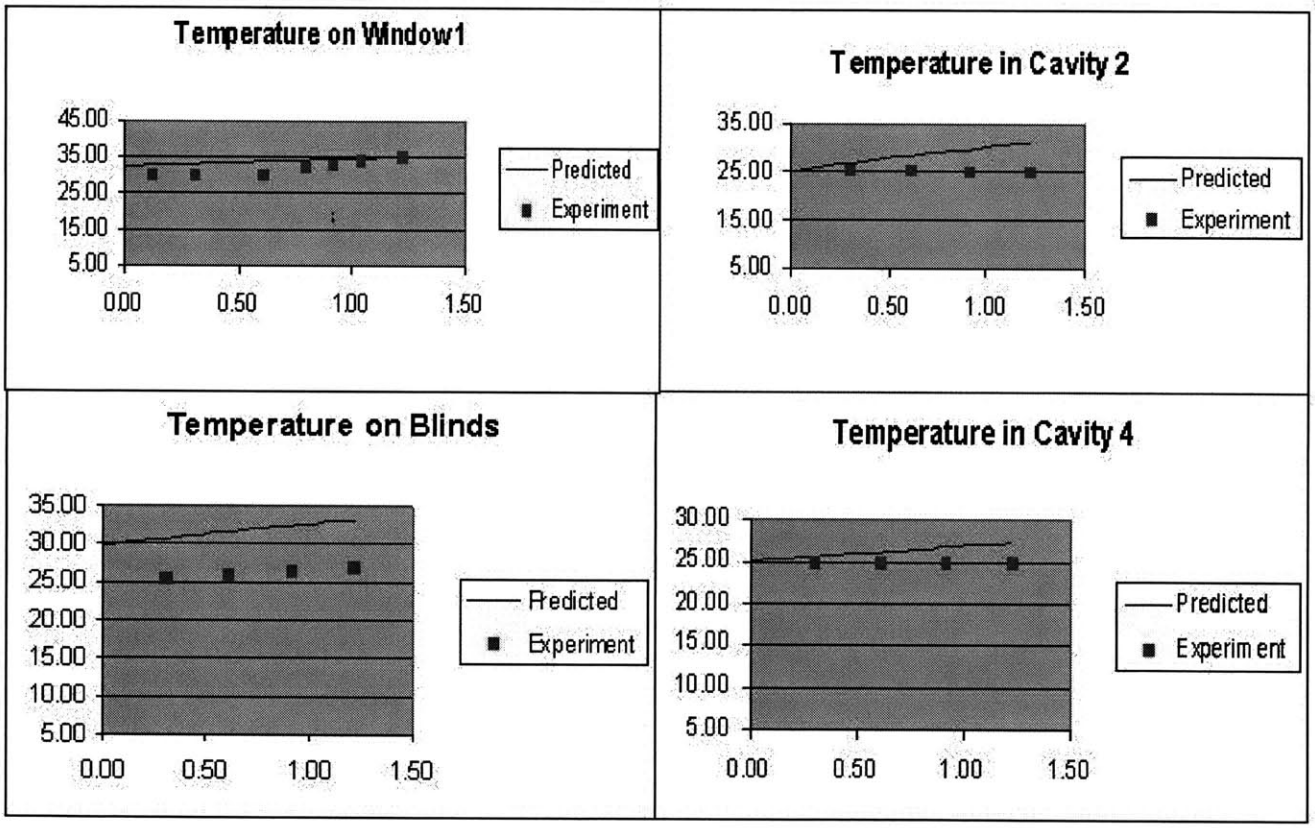

Initial Conditions Group F

- Blinds Closed
- Interior Cavity Length = 13.5"
- Air Cavity Velocity = .1 m/s
- Heat source, Sun Lamp

Figure 28b Comparison of Model and Data Temperature vs. Horizontal Position for group F

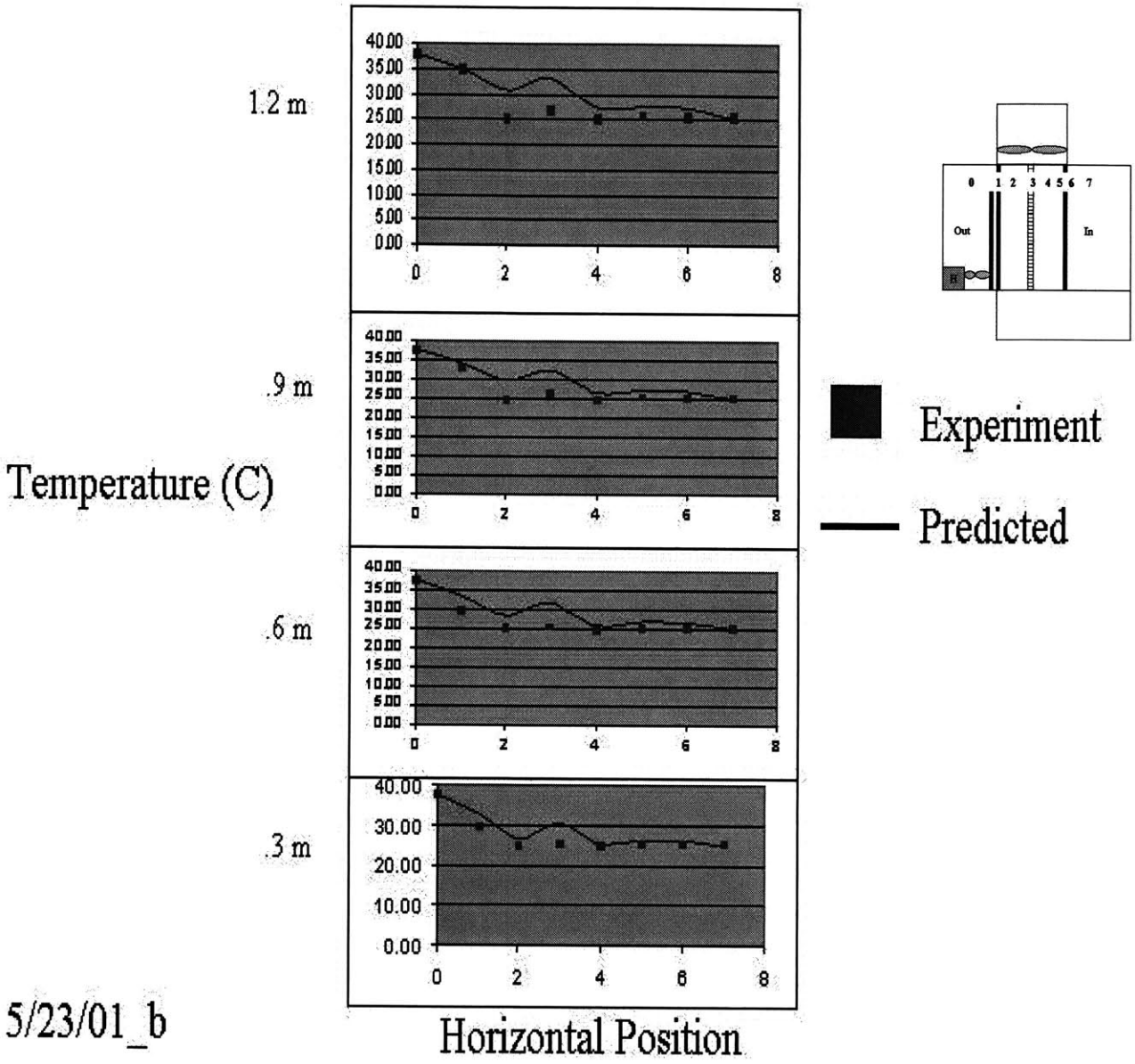

There is very little agreement between the model and data for both cavities and the blinds. The data follows the model well on Window 1. There is about a 6° temperature difference between the model and data on the blinds. The temperature difference between the model and data is further illustrated in figure 28b. The best agreement is at the bottom of the system and it gets progressively worse as the height increases. Figure 28b corroborates figure 28a because the blind and air cavity have the

largest error (locations 2 - 4). The accuracy of this model is 95.3%. Appendix F has more comparisons of the model and data of groups A-F.

The accuracy of the model for the previous groups was for particular cases. The overall accuracy for each of the groups was slightly higher than the individual cases because it averages many experiment/model comparisons. Chart 4 lists the error of each group, but separates them by the type of heat source.

Chart 4 Summation of Model Error

Heat Source	Group A Blind Open	Group B Blind Closed	Group C Blind Open	Group D Blind Closed	Group E Blind Open	Group F Blind Closed
ICL (in)	4.5	4.5	9	9	13.5	13.5
Heater	2.04%	1.68%	2.75%	2.83%	4.60%	4.04%
Sun Lamp	2.07%	1.99%	3.18%	3.06%	4.68%	4.73%

The comparisons of the model and data using the sun lamp to heat the system resulted in less error in all of the groups. The model was also more accurate with the blinds closed vs. blinds open for the same interior cavity length. As mentioned earlier the model becomes less accurate with the increase in cavity width. The reasons for these discrepancies will be discussed at the end of the section.

Comparing Different Scenarios

The model has been verified by comparing it to the data, however it would be interesting to compare the different groups of data. The reason for range in error could be because of the uncertainty of the data acquisition system, which will be determined at the end of the chapter. The next series of figures (29 – 31) illustrates the similarities and differences between the different data sets. The model results are also included so the variations of the different models can be compared as well.

Figure 29a Comparing Data Sets, middle of System

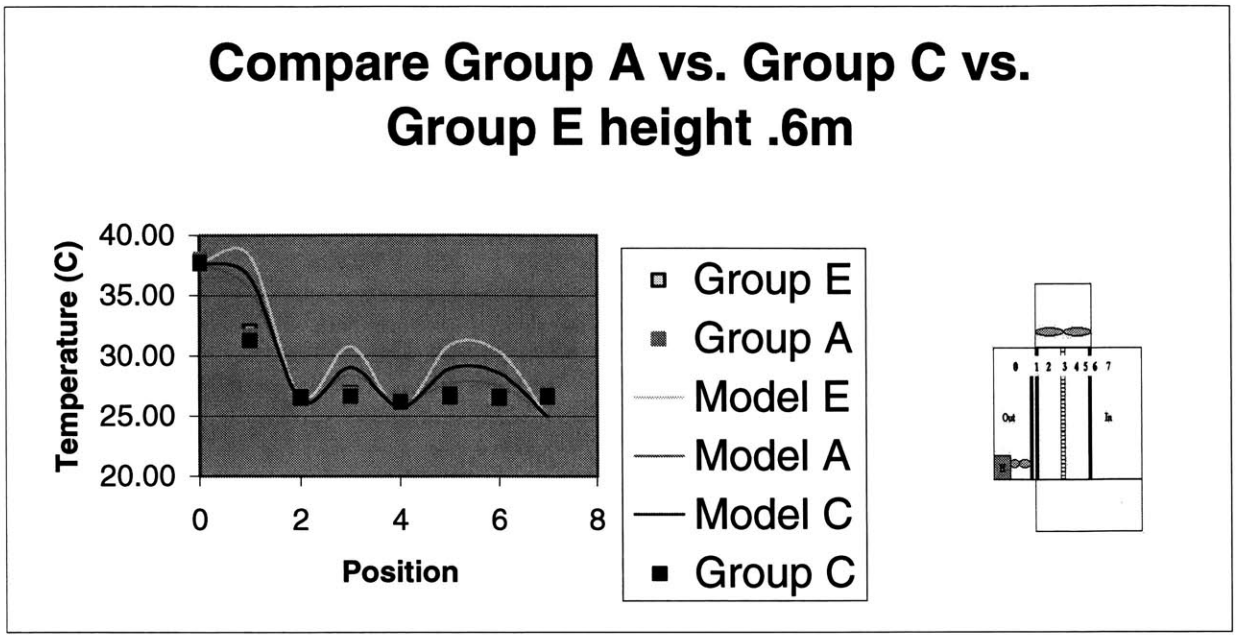

Initial Conditions Group A
- Blinds Open
- Interior Cavity Length = 4.5"
- Air Cavity Velocity = .1 m/s
- Heat source, Sun Lamp

Initial Conditions Group C
- Blinds Open
- Interior Cavity Length = 9"
- Air Cavity Velocity = .1 m/s
- Heat source, Heater

Initial Conditions Group E
- Blinds Open
- Interior Cavity Length = 13.5"
- Air Cavity Velocity = .1 m/s
- Heat source, Heater

Figure 29b Comparing Data Sets, top of System

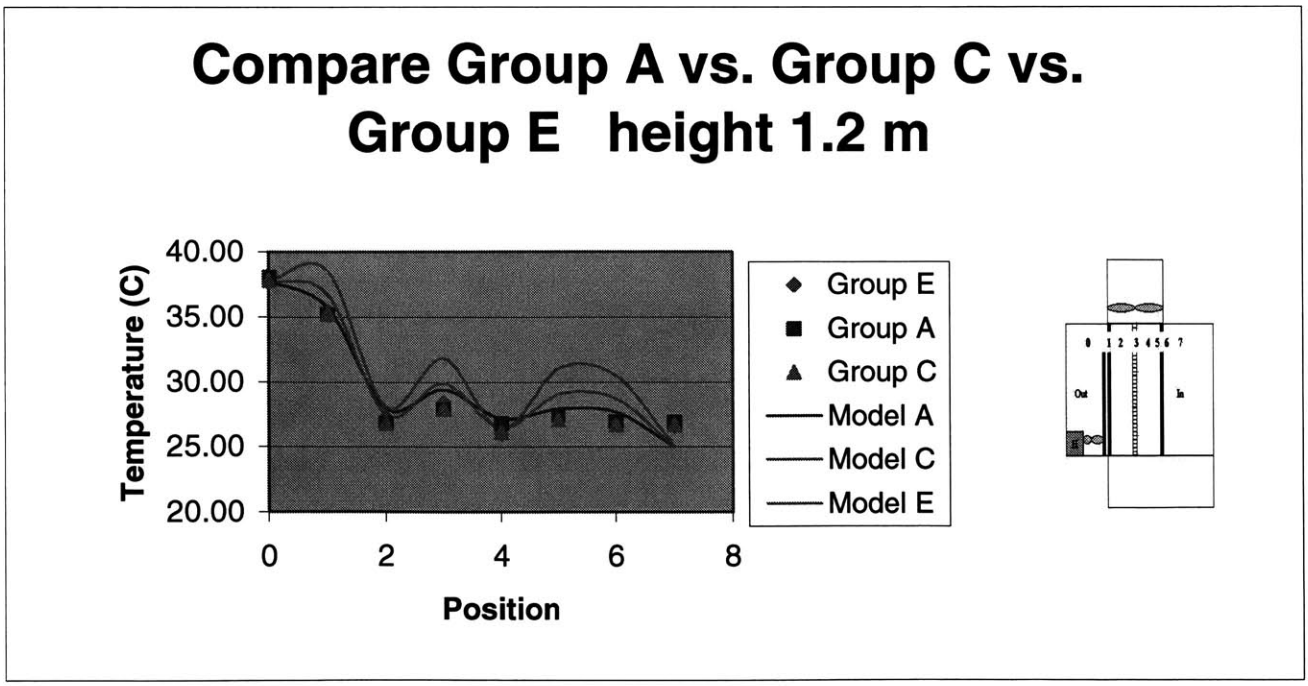

The first set of figures, 29a and b, which compares the scenarios open blinds at different interior cavity lengths reveals interesting information. Model A (represents the mathematical model for narrow spacing) and group A (represents the data sets) agree very well, and the results are a closer match at the top rather than the middle of the system. In general, the experiment data points are very close together, however, the model is predicting significant differences as the cavity width increases (on the order of 5^{o}). This observation correlates with the error results; the model is less accurate as the cavity width increases. One possible reason is that there is error in the heat transfer coefficient for very low velocities or the velocities are much higher then what was measured in the narrower cavity.

For figures 29c and d, which compares the scenarios of closed blinds at different interior cavity lengths shows slightly different results. There is a couple of degrees Celsius distinction from group F data and the other two groups. Group F, where the interior cavity is the greatest, has significantly lower temperatures than the groups B and D. Again the agreement between the models and data sets improves at the top of the system. There is better agreement between models B and D to groups B and D compared to the agreement between models A and C to groups A and C. Simply, the model is more accurate for the scenarios where the blinds are closed. When the blinds are closed the air cannot move from the exterior to the interior cavity. The movement of air through the blinds (when they are open) adds more complexity, which the mathematical model is not capable of handling, so the model could generate more error. The effect of the air velocity will be examined more closely at the end of the chapter. The disagreement between the model and data was also observed in the previous section because less error was calculated for groups B, D, and F (see chart 4). The model still predicts a significant temperature change as the interior cavity length increases.

Figure 29c Comparing Data Sets, middle of system

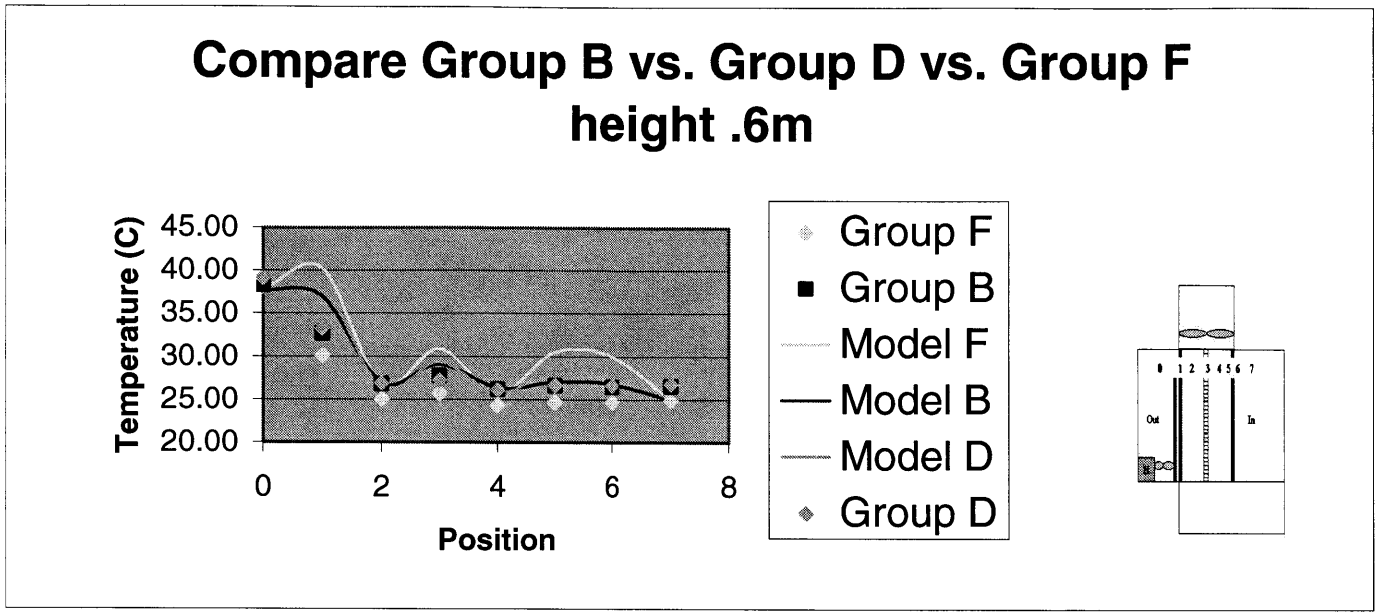

Initial Conditions Group B
- Blinds Closed
- Interior Cavity Length = 4.5"
- Air Cavity Velocity = .1 m/s
- Heat source, Sun Lamp

Initial Conditions Group D
- Blinds Closed
- Interior Cavity Length = 9"
- Air Cavity Velocity = .1 m/s
- Heat source, Sun Lamp

Initial Conditions Group F
- Blinds Closed
- Interior Cavity Length = 13.5"
- Air Cavity Velocity = .1 m/s
- Heat source, Sun Lamp

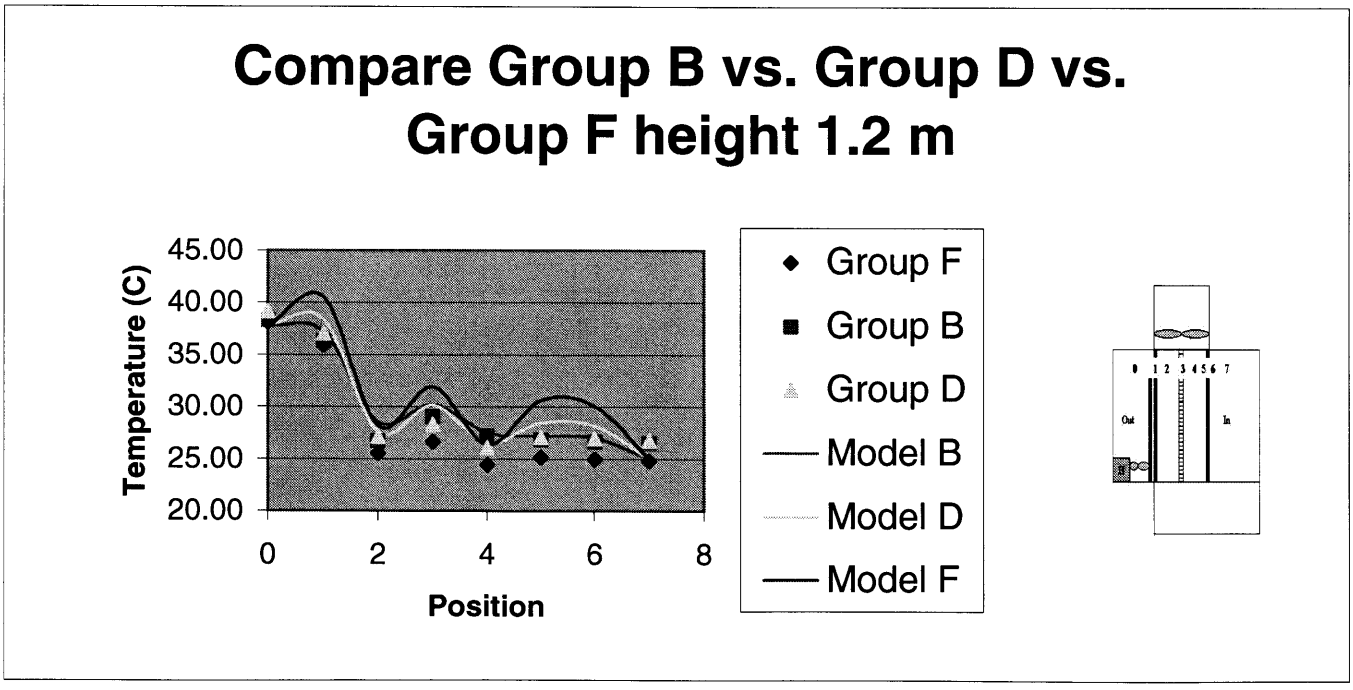

Figure 29d Comparing Data Sets, top of system

Figure 30a Comparing Data Sets, middle of system

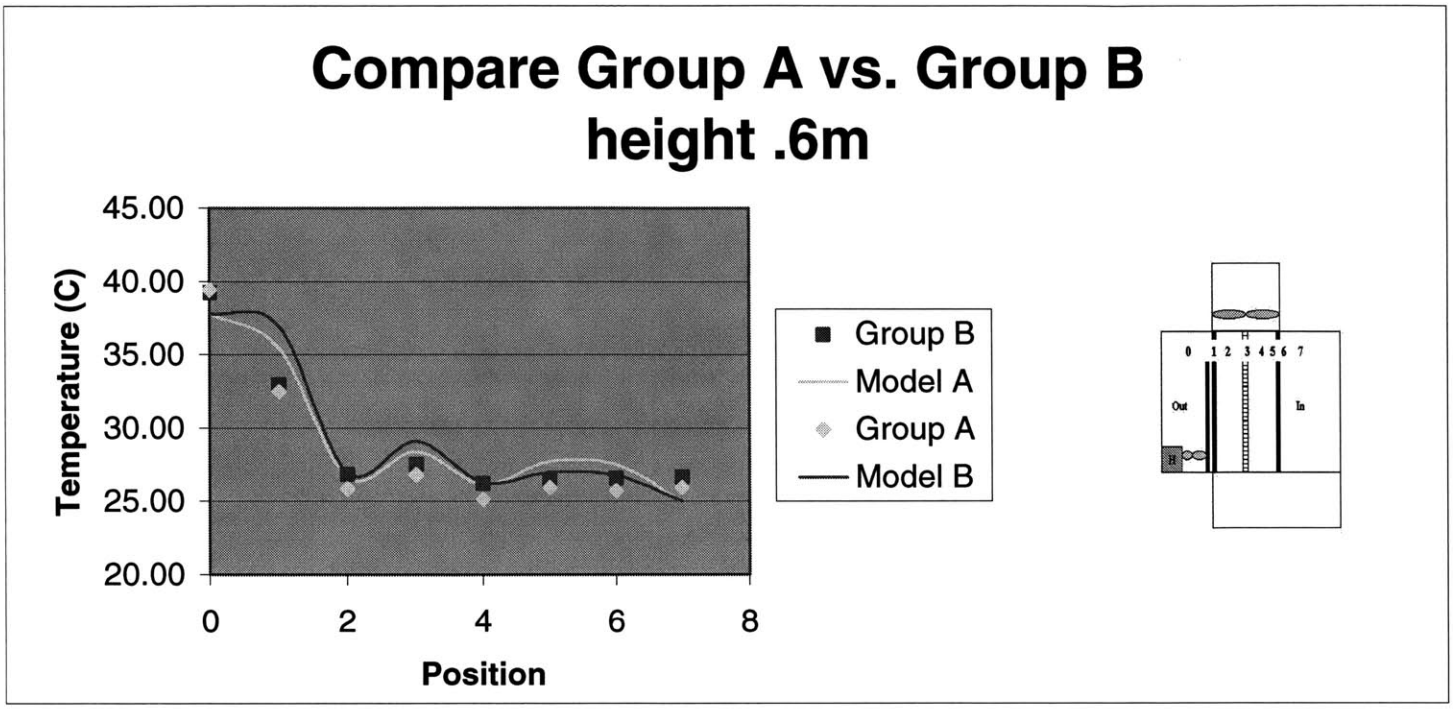

Initial Conditions Group A
- Blinds Open
- Interior Cavity Length = 4.5"
- Air Cavity Velocity = .1 m/s
- Heat source, Sun Lamp

Initial Conditions Group B
- Blinds Closed
- Interior Cavity Length = 4.5"
- Air Cavity Velocity = .1 m/s
- Heat source, Sun Lamp

Figure 30b Comparing Data Sets, top of system

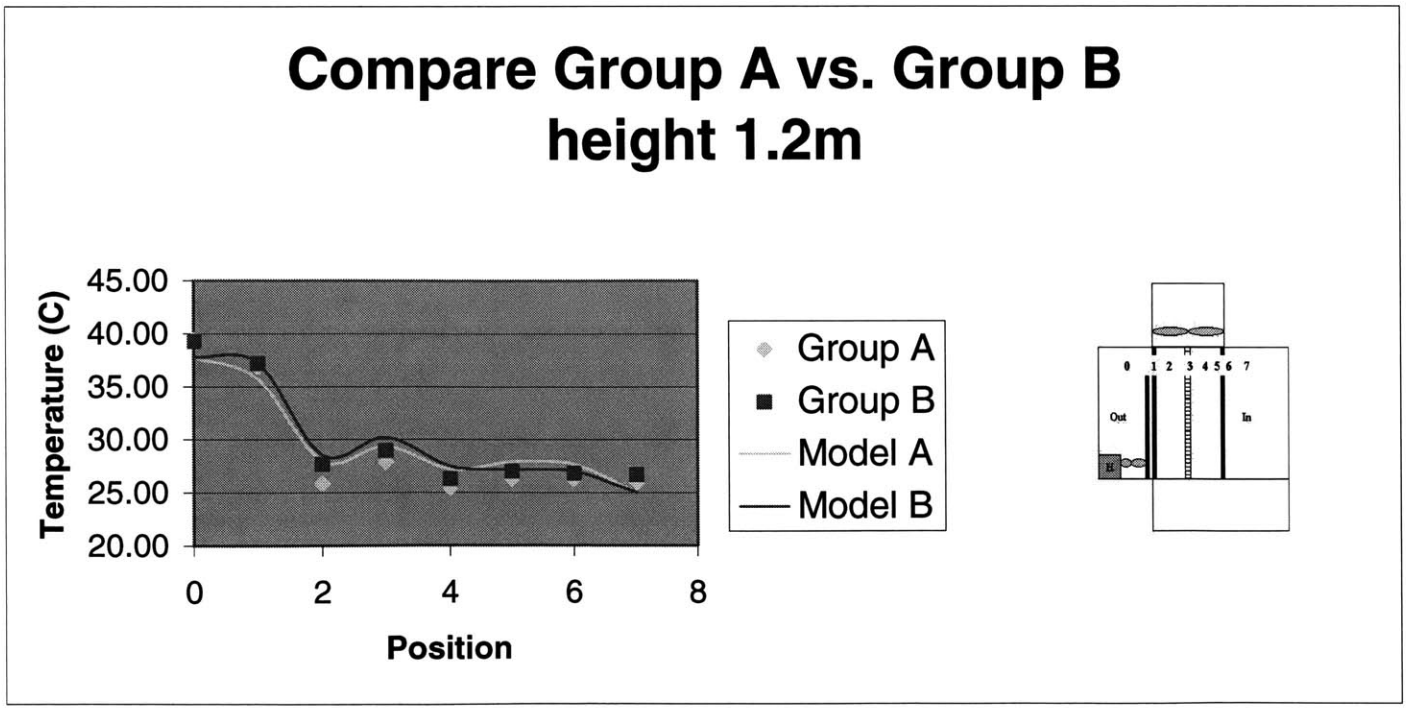

Figures 30a and b compare the blinds open vs. closed with an interior cavity length of 4.5". The temperature measurements for group B (blinds closed) are about a 1°C higher. The two models have very little differences. Model B predicted a slightly higher temperature at the exterior window than model A, but ended up with a lower temperature at the interior window than model A. The reason why this happens is that the closed blinds prevent some of the energy from reaching the interior window, which is why model B has lower temperatures on the interior window. The data does not follow the same trend, because group B data points are consistently higher than group A. The accuracy of model B improves at the top of the double skin facade system, but model A predicts the temperature trends better at the middle of the system.

Figure 30c Uncertainty of data acquisition system

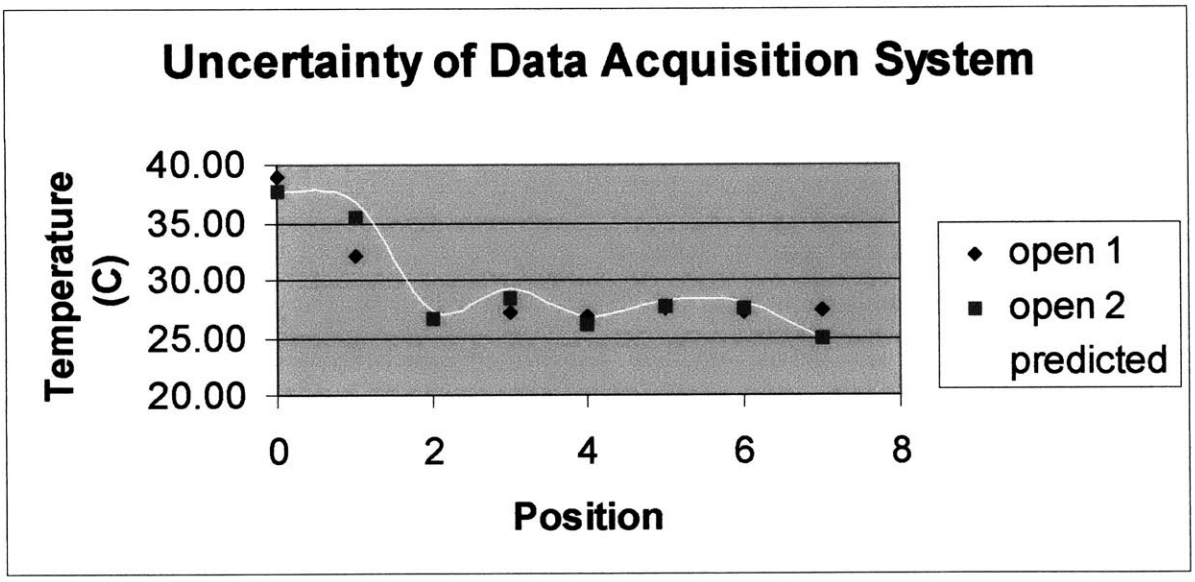

One of the reasons for the discrepancies between the model and data could be because the uncertainty of the data acquisition system. Figure 30c illustrates a comparison of the model versus the data for the same initial conditions, which were blinds open, ECL = ICL = 4.5", the lamp was used as the heat source, and the air velocity was about .1 m/s. There is obviously variation in the data for the same initial conditions, and this uncertainty is a significant part of the overall error between the model and data. The uncertainty contributes about 2% of the error. The specifications chart of the Keithley Instrument Data Acquisition System lists that the thermocouple readings are

with +/- 1°C, [Keithley, 2000]. The agreement of the model and data is with in the limits of the specifications.

Figures 30c and d compare the blinds closed vs. open for an interior cavity length of 9". There is almost no significant change in the model from blinds open to closed. There is about a 2° C to 3° C temperature difference between group C and D and group D (blinds closed) has higher temperatures. The model and data correlates much better with group D than group C. In general, there is less deviation of the data and from model at the top of the DSF system.

Figure 30c Comparing Data Sets, middle of system

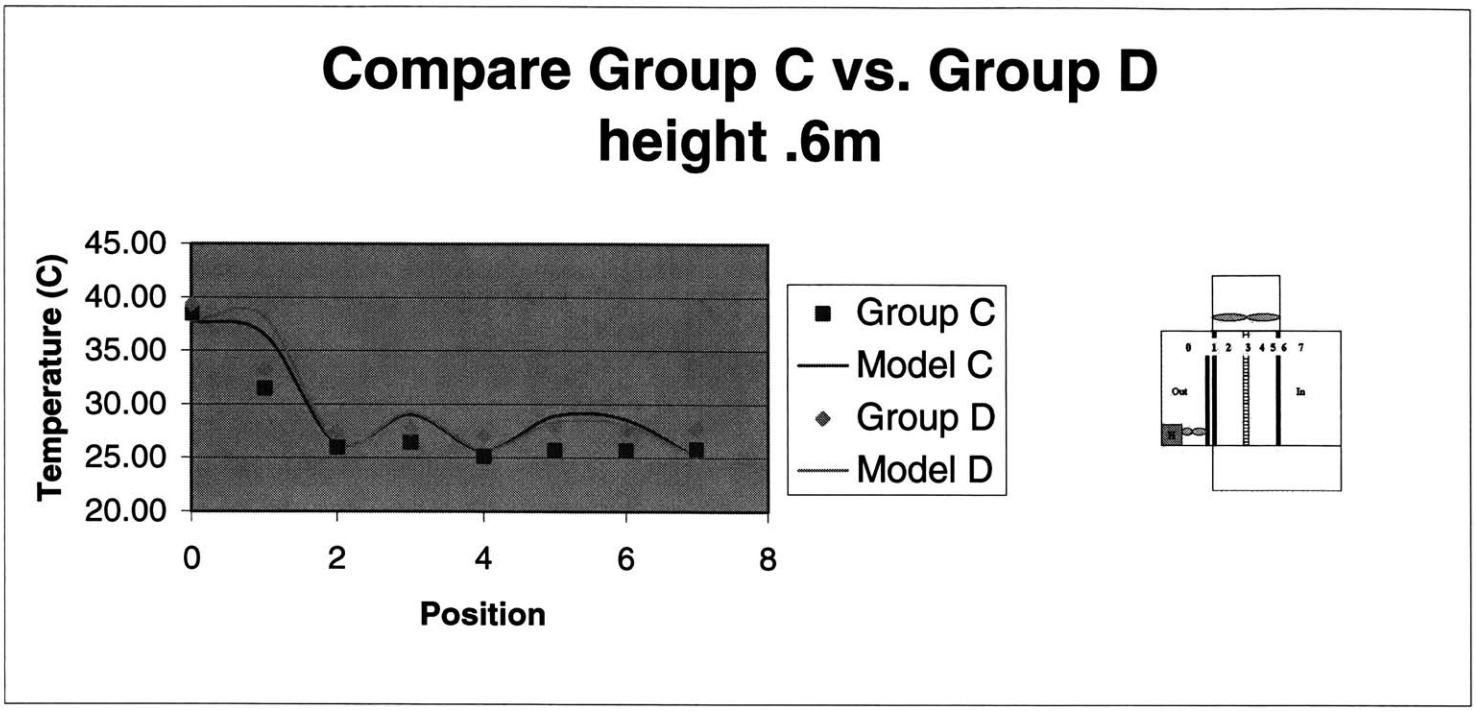

Initial Conditions Group C
- Blinds Open
- Interior Cavity Length = 9"
- Air Cavity Velocity = .1 m/s
- Heat source, Heater

Initial Conditions Group D
- Blinds Closed
- Interior Cavity Length = 9"
- Air Cavity Velocity = .1 m/s
- Heat source, Sun Lamp

Figure 30d Comparing Data Sets, top of system

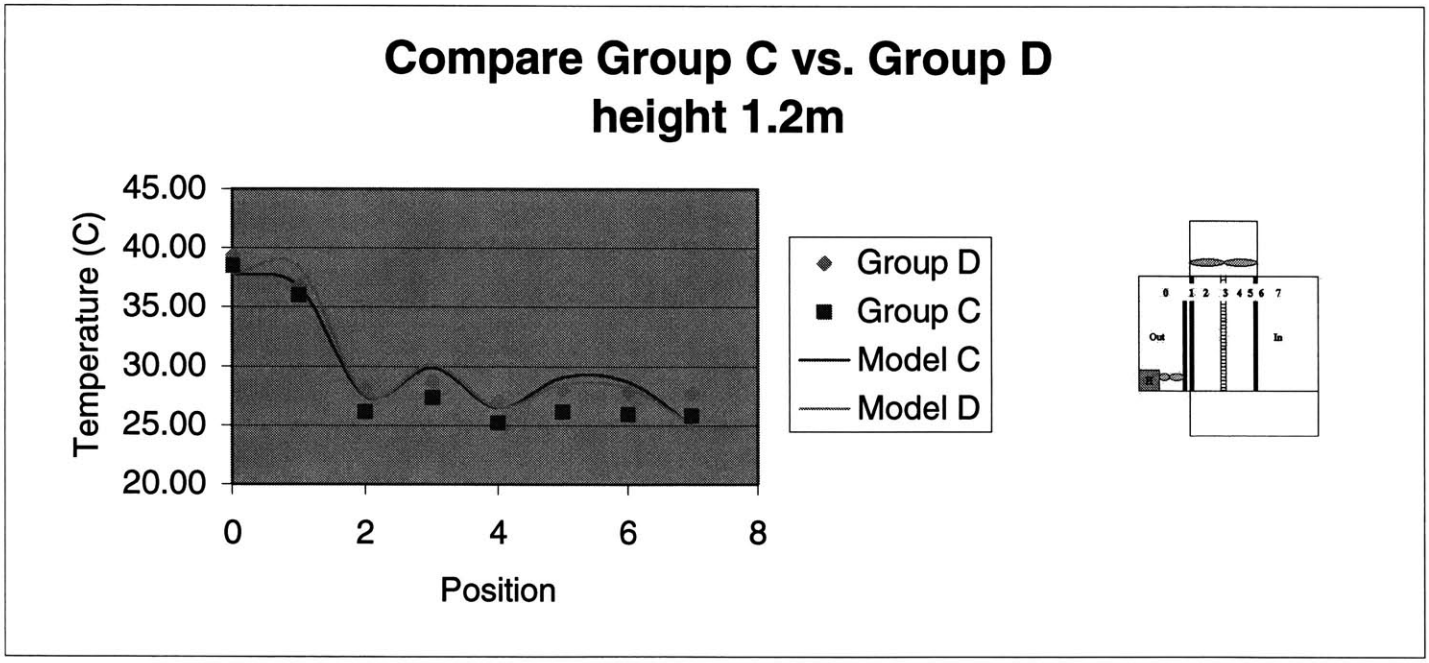

Figures 30e and f compare open blinds vs. closed for the last two groups where the interior cavity is 13.5 inches. These data sets are interesting because group F (blinds closed) starts off with higher temperatures in cavity 2 like the other data sets, but by cavity 4 the temperatures end up equal to those of group E. Perhaps, the cavity length is so large that the thermal effects of blinds do not influence the temperature of the interior cavity and the other horizontal locations, 5 –7. The accuracy improves somewhat with the increase in height.

The next series of figures 31a-f look only at the data sets for three of the groups and compares them by the type of heat source. The model did not differ significantly when it reflected the use of the sun lamp vs. heater so for all comparisons the sun lamp model was used. Referring to chart 3, where the error of the models was calculated, there was a little better agreement with the sun lamp. For group A (see figures 31a and b), the data points are almost identical, which makes sense because the difference in error of the models was on the order of .1%. For group C (see figure 31c and d) the temperature varies at the interior window and blinds. The temperature difference is more significant at the top of the system. For group E (see figure 31e and f) there is an apparent 1^{o} temperature difference for the two sets of data. The gap between the two sets of data shrinks at the top of the double skin facade system. Overall, the data sets do not significantly vary with the change in heat source, which suggests that the error lies primarily in the model.

Figure 30e Comparing Data Sets, middle of system

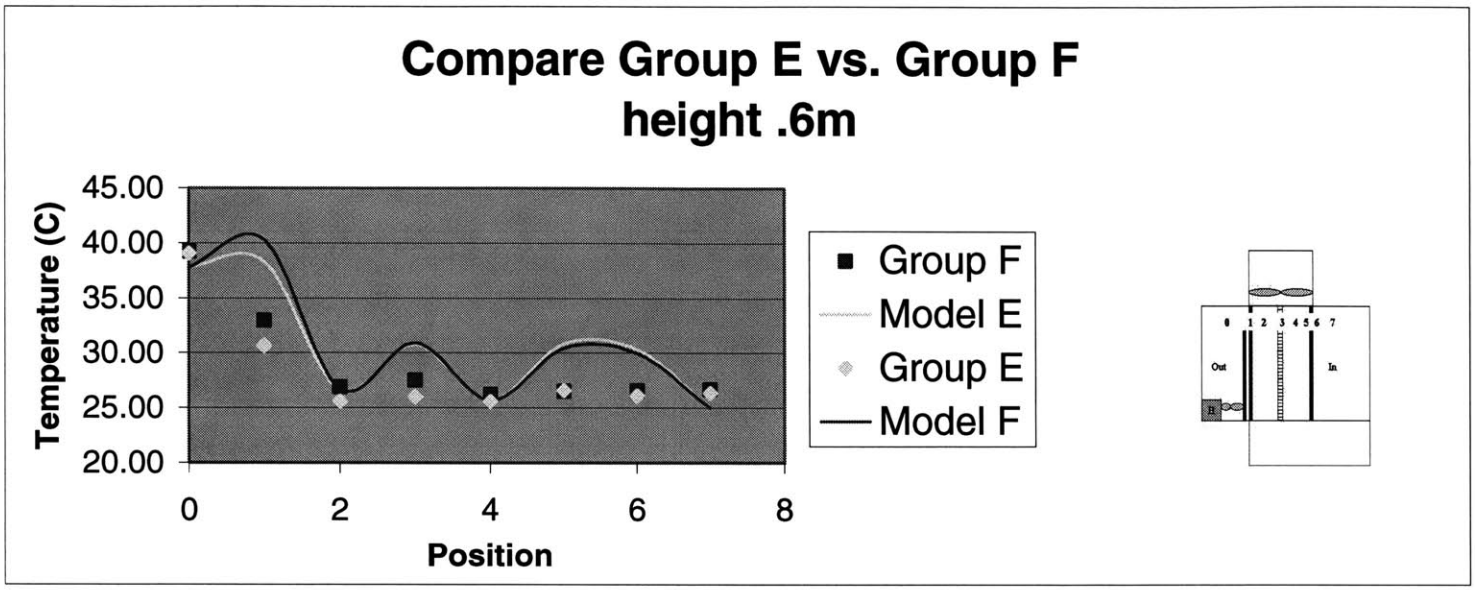

Initial Conditions Group E
- Blinds Open
- Interior Cavity Length = 13.5"
- Air Cavity Velocity = .1 m/s
- Heat source, Heater

Initial Conditions Group F
- Blinds Closed
- Interior Cavity Length = 13.5"
- Air Cavity Velocity = .1 m/s
- Heat source, Sun Lamp

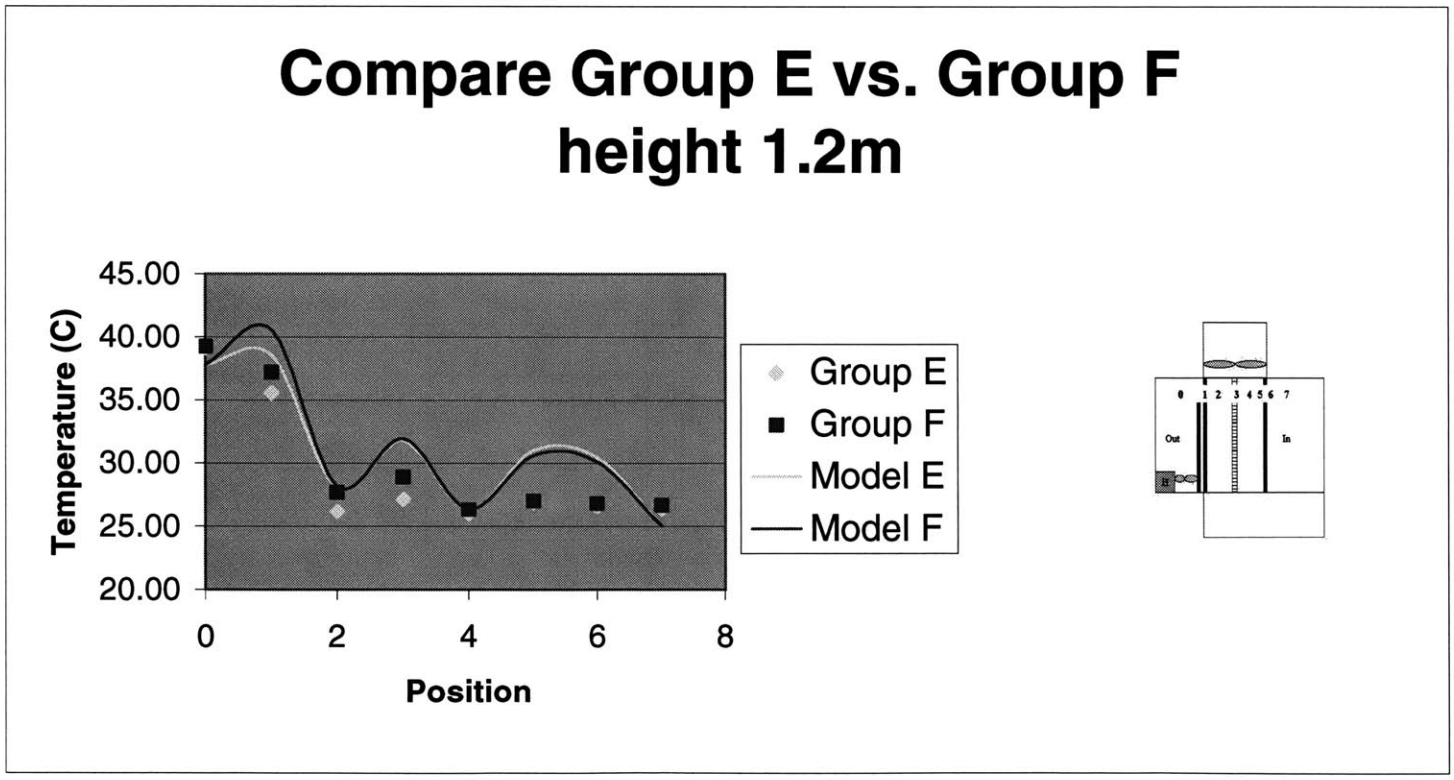

Figure 30f Comparing Data Sets, top of system

Figure 31a Comparing Data Sets, middle of system

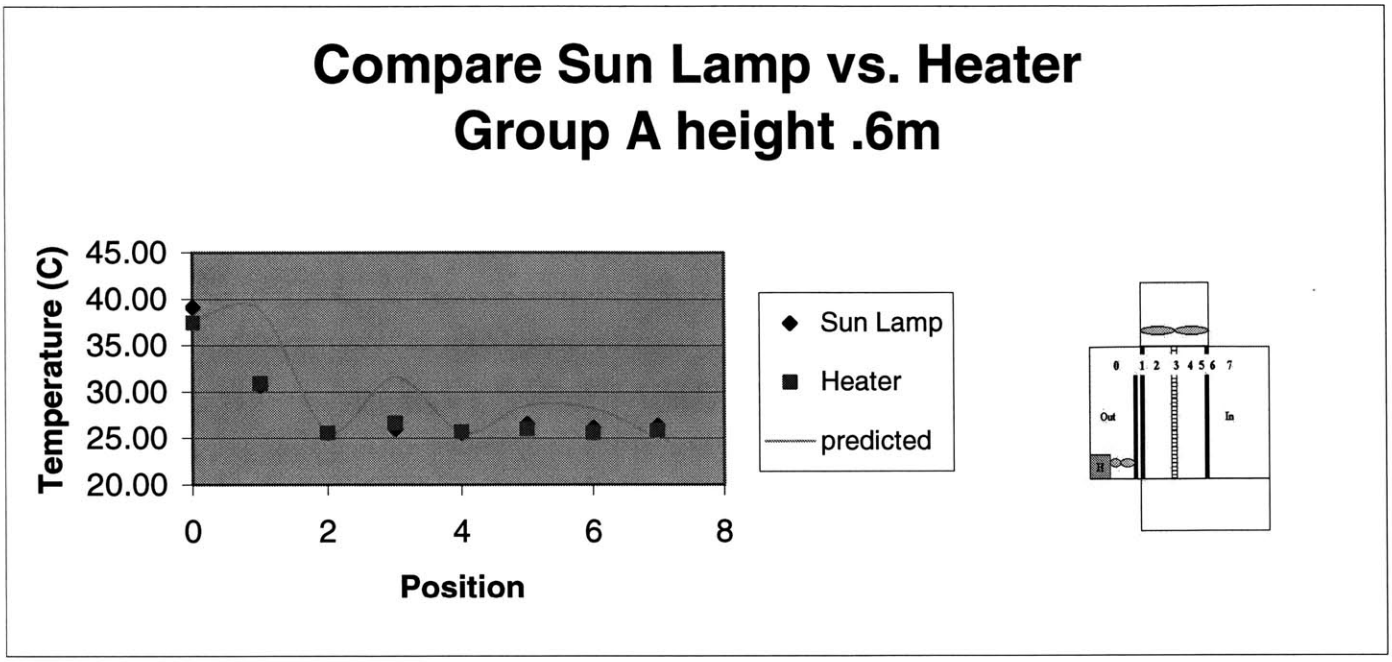

Initial Conditions Group A

- Blinds Open
- Interior Cavity Length = 4.5"
- Air Cavity Velocity = .1 m/s
- Heat source, Sun Lamp

Figure 31b Comparing Data Sets, top of system

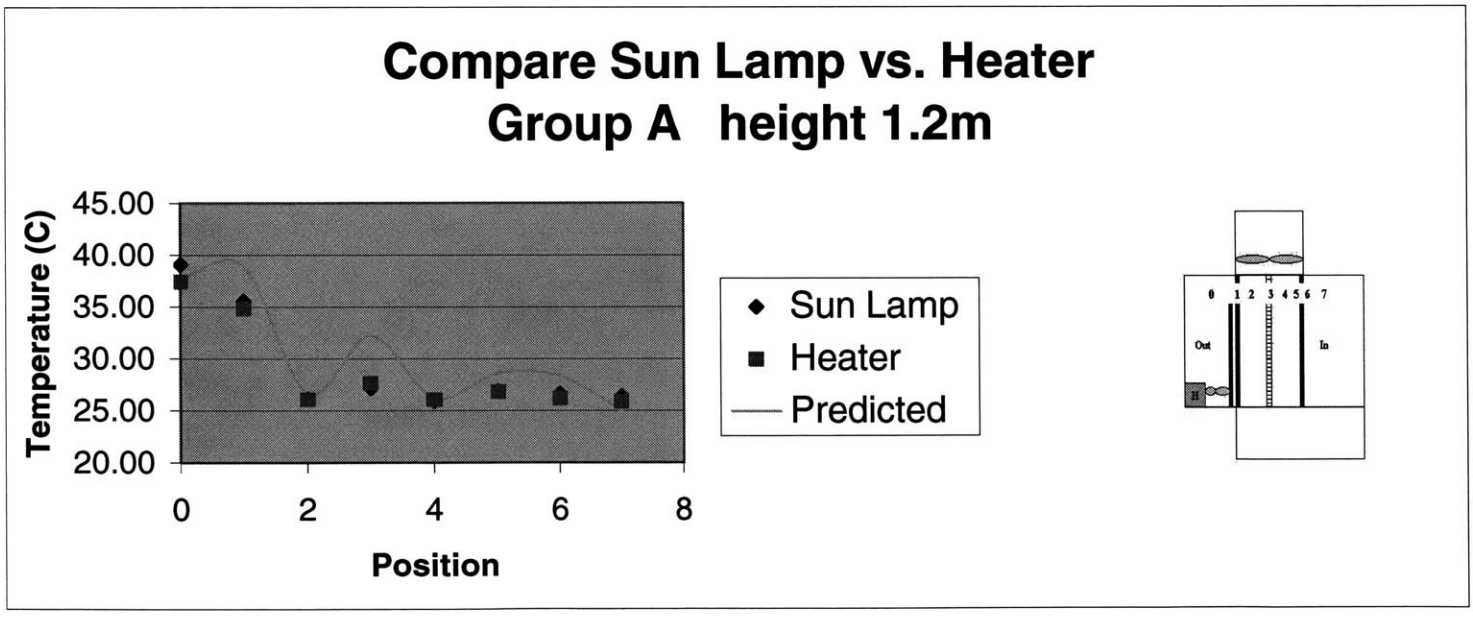

Figure 31c Comparing Data Sets, middle of system

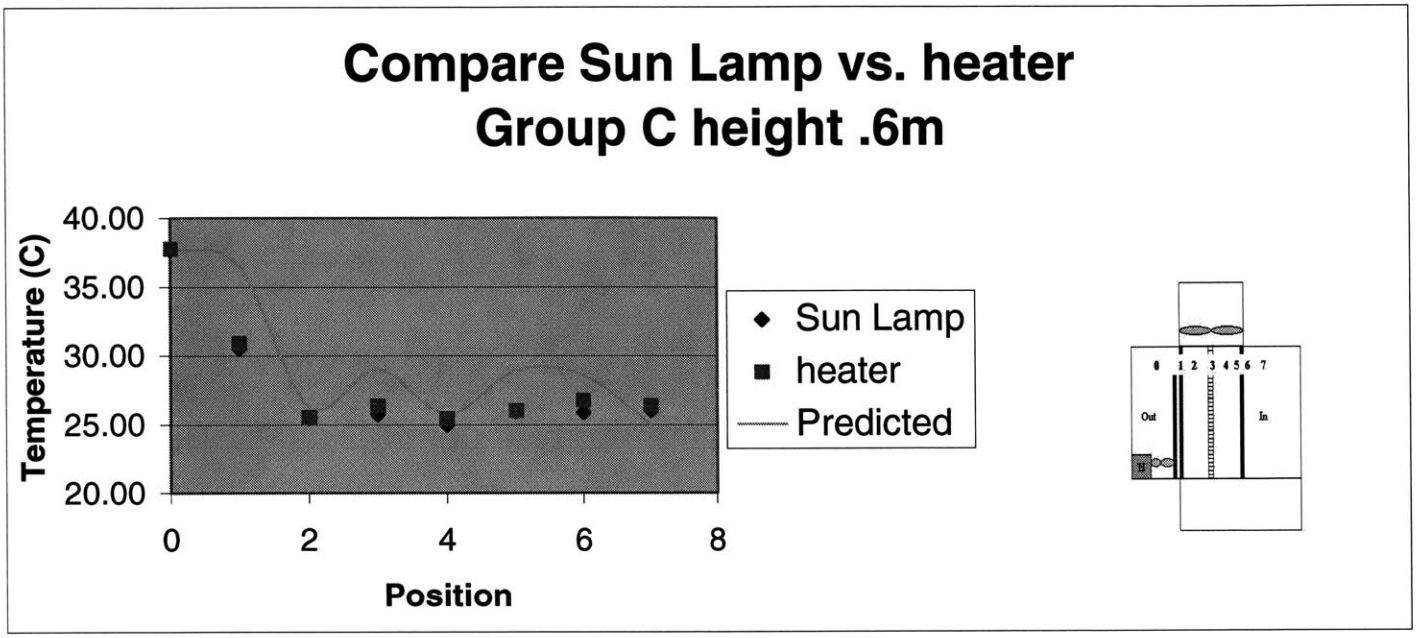

Initial Conditions Group C

- Blinds Open
- Interior Cavity Length = 9"
- Air Cavity Velocity = .1 m/s
- Heat source, Heater and Sun Lamp

Figure 31d Comparing Data Sets

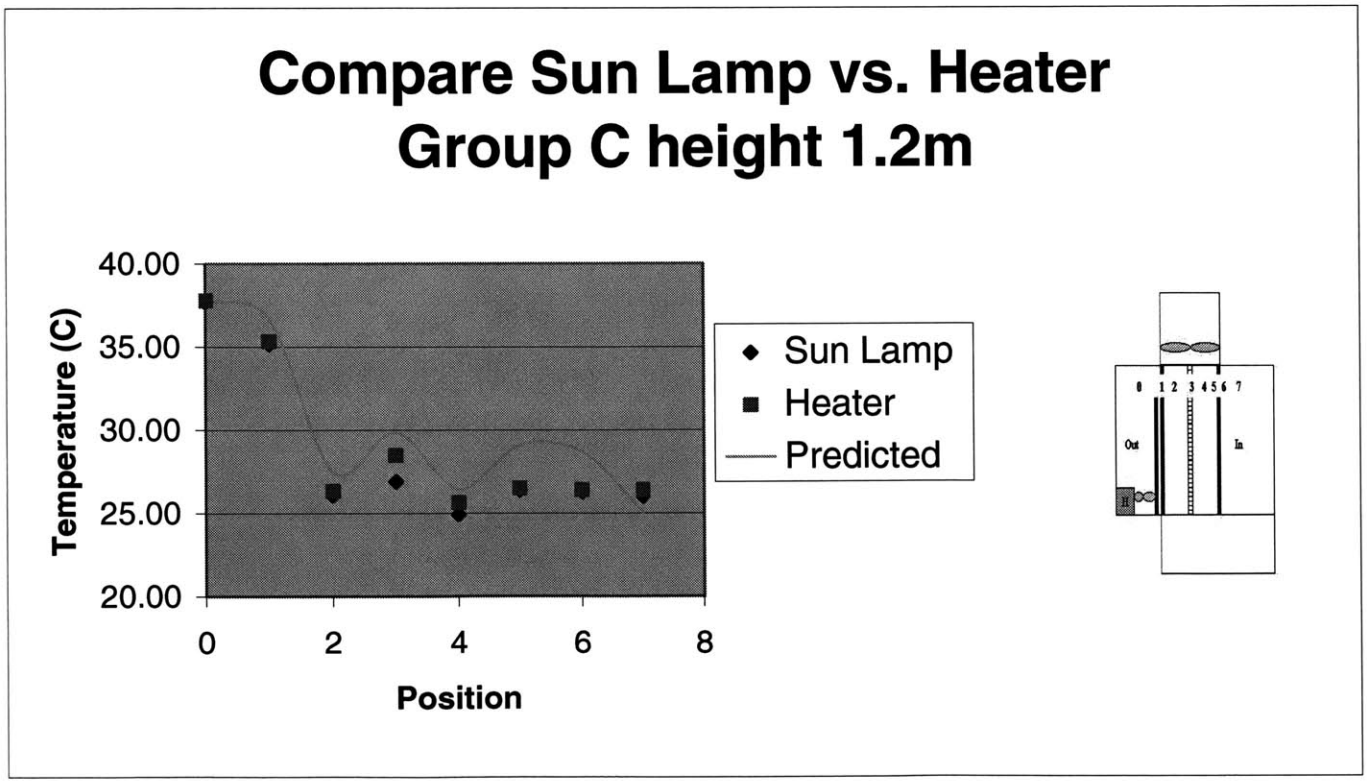

Figure 31e Comparing Data Sets, middle of system

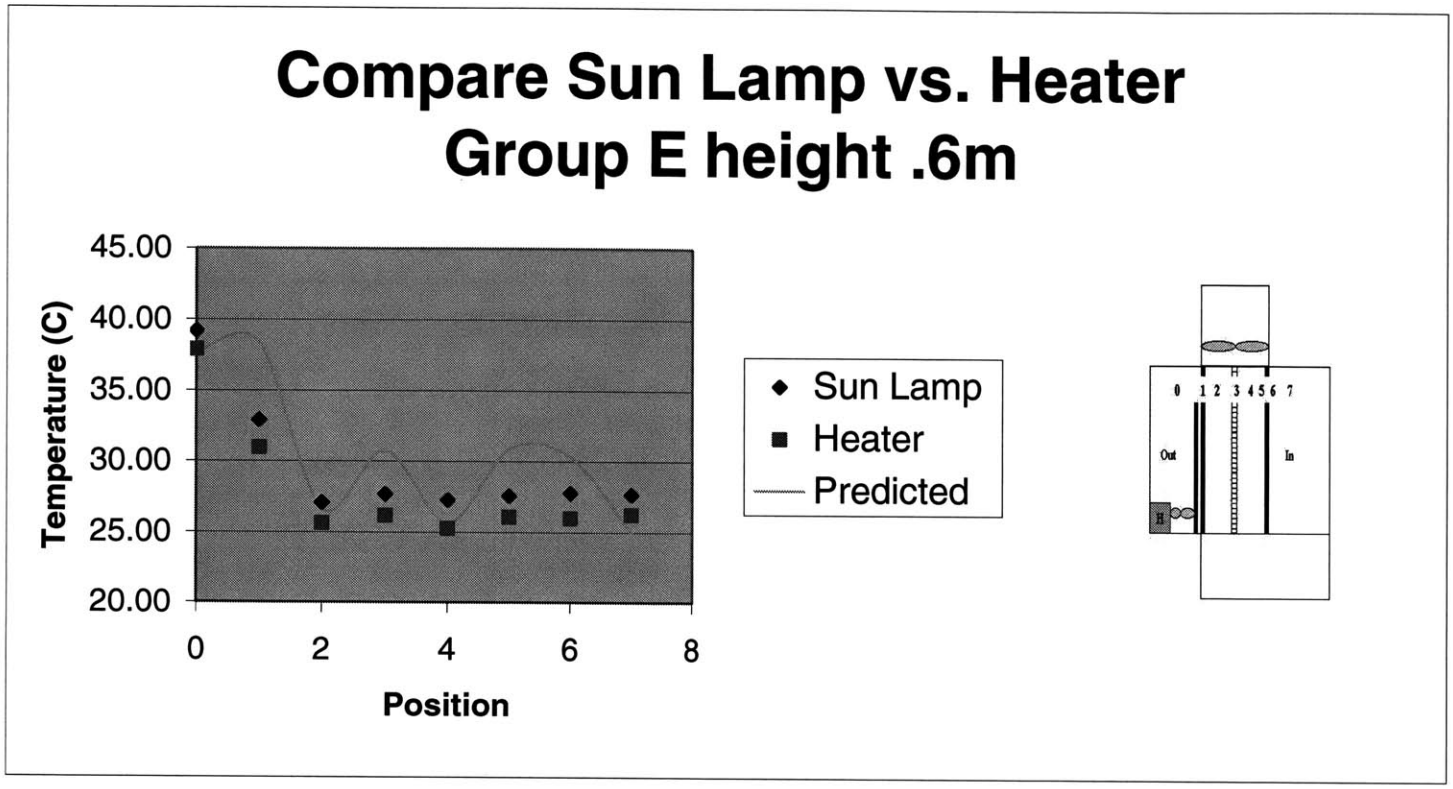

Initial Conditions Group E

- Blinds Open
- Interior Cavity Length = 13.5"
- Air Cavity Velocity = .1 m/s
- Heat source, Heater and Sun Lamp

Figure 31f Comparing Data Sets, top of system

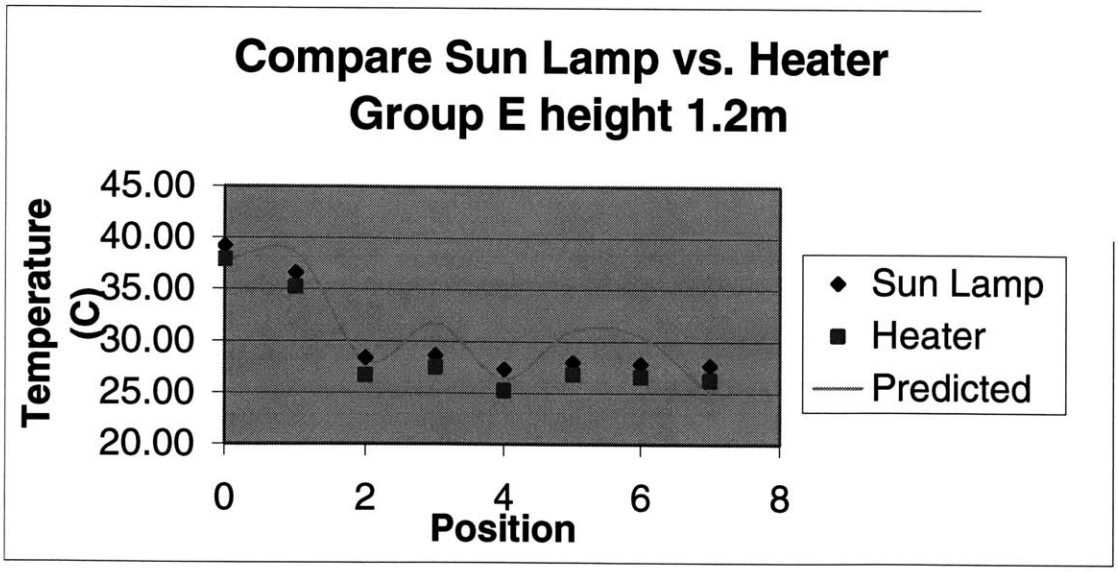

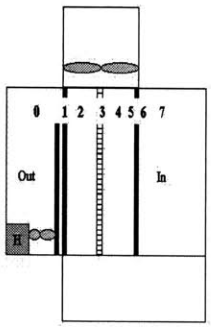

Reasons for Discrepancies

Now that the accuracy of the model is determined, the reasons why the model does not perfectly pattern the DSF experiment can be explored. The primary source of error was created when the interior cavity length increased. The model consistently predicted large increases of temperature in the interior and exterior windows and blinds as the cavity length increased. Another source of error was at the different heights of the system. In general, the correlation of the data and model improved with the increase in vertical location of the double skin façade system (see figures 29-31, the figures ending with an "a" are at .6 m, and the figures ending with a "b" are at 1.2 m). The convective coefficient, h_{conv}, for these locations control the predicted temperature.

The h_{conv} value is determined based on the material properties and the geometry of the system. This value is approximated from standard correlations; such has flow over cylinder and flow over a flat plate. One reason for discrepancies between the model and data is that the correlations implemented in the model do not entirely describe the system. For instance, the h_{conv} between the blinds and air was represented by flow over a cylinder. The geometry of the closed blinds are not exactly cylindrical, they over lap which creates a different geometry, which in turn does effect the h_{conv} value. Since the temperature is higher in the model for the windows and blinds, it is calculating a much higher h_{conv} than the experiment, because a higher h_{conv} yields a smaller thermal resistance. A smaller thermal resistance yields a larger the temperature difference. The affects of the h value were verified by increasing the value and monitoring the temperature trends.

A sensitivity test was performed on the h_{conv} to see for what range of heat transfer coefficients would the model yield unrealistic temperatures. Figures 35a and b illustrate the effects of increasing and decreasing $h_{conv.}$ The components, which were plotted, are the interior and exterior windows and the blinds because they were the source of the majority of the error. The h_{conv} was altered for all four components. The air cavity temperatures were not sensitive to the change in h_{conv} so those values were not plotted. The sensitivity tests reveal that the temperature does not change drastically for a large h value (on the order of 100) vs. a smaller h value (on the order of .01). The temperature varies on the order of 1°C to 2°C for the windows and roughly 9°C for the blinds, for the

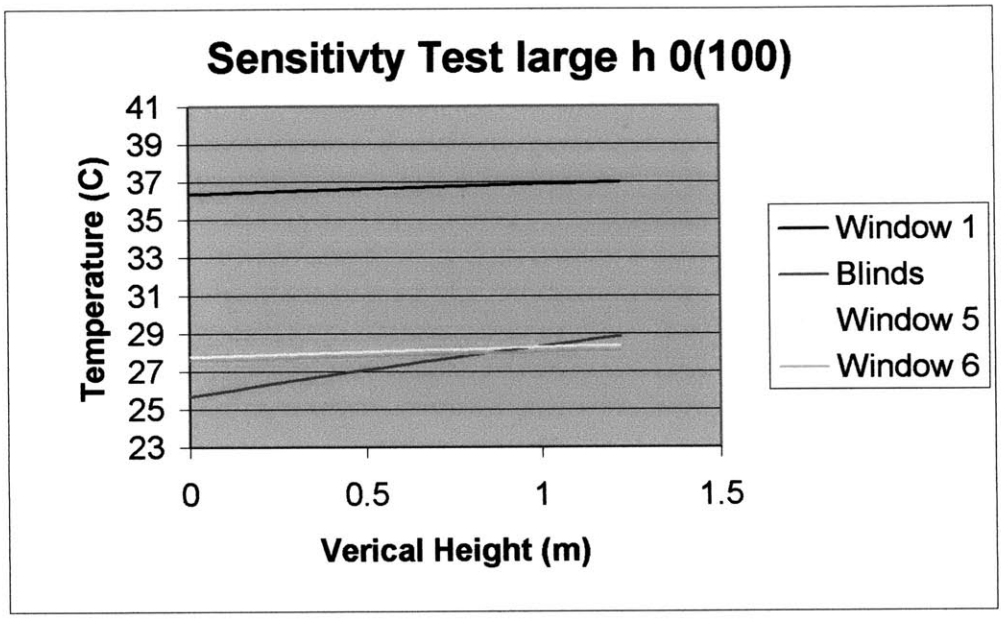

Figure 31h and i Sensitivity of h_{conv}

Initial Conditions Group A

- Blinds Open
- Interior Cavity Length = 4.5"
- Air Cavity Velocity = .1 m/s
- Heat source Sun Lamp

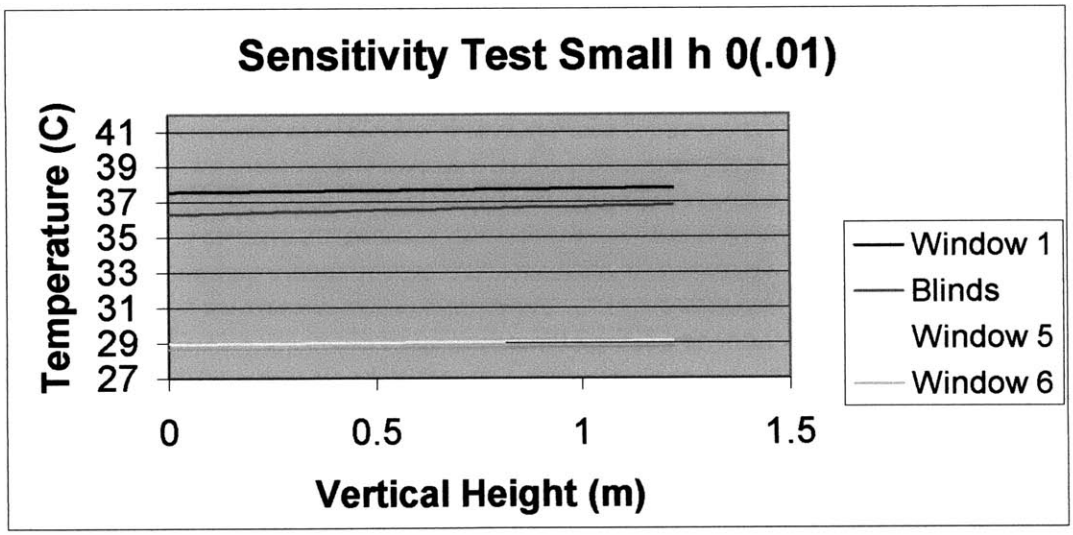

large h_{conv} range. So if the h_{conv} were off by a factor of two or three the temperature would not vary significantly.

The same argument applies to the external and internal windows. The error is amplified on the interior window because the h_{conv} may not approximate the window correctly in addition to heat transfer added from the thermal effects of the blind. The accuracy of the h_{conv} coefficient directly affects the overall accuracy of the system and

could be a reason why the discrepancies exist for the blinds and windows between the model and data.

The second phenomenon, improved agreement between the model and data at the top of the system, is also driven by the h_{conv}. The model calculates an average convective coefficient for each horizontal location, however the predicted h_{conv} does not vary with height. The experimental data illustrates (refer to figure 26a) a larger temperature difference from the top to the bottom of the window. It is not until the top of the window that the data meets the model, which would suggest that the h_{conv} should vary with the height to better emulate the data trends. Currently, the model does not vary the h_{conv} with height and some of the error can be eliminated if it were implemented. The two possible reasons for the discrepancies between the model and data are linked to the same factor the convective heat transfer coefficient. The h_{conv} should be higher at the lower elevations so that the temperature difference is larger, because a larger h yields a smaller thermal resistance, which in turn results in a larger temperature difference. More fundamentally, the h_{conv} should be higher in the entrance region because the thermal boundary layer is smaller.

Another factor, which contributes to the error, is the velocity profile. The velocity does not remain constant when the interior cavity width increases and when the blinds are open versus closed. When the blinds are open, there is a possibility that air will move across the blinds in the horizontal direction instead of over them in the vertical direction.

Figure 31j Temperature vs. vertical height, group A

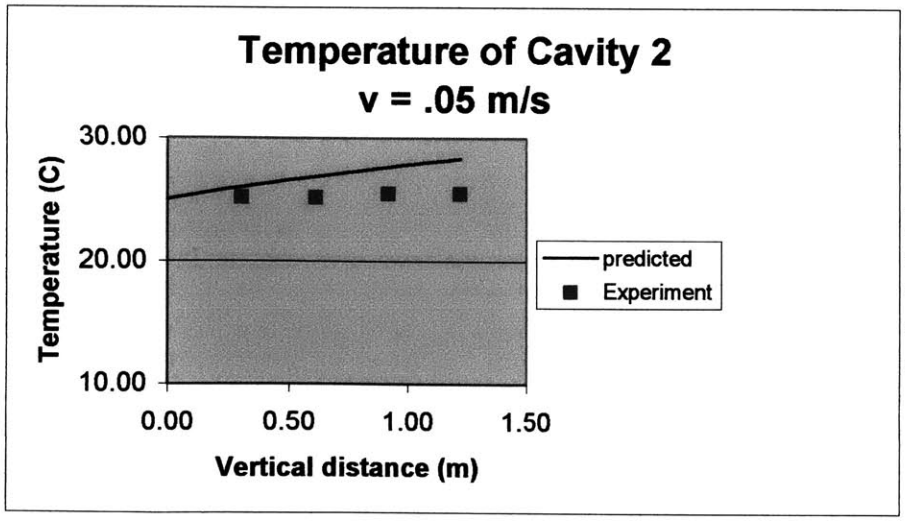

The movement of the air in the horizontal

Initial Conditions Group A
- Blinds Open
- Interior Cavity Length = 4.5"
- Air Cavity Velocity = .05 m/s
- Heat source, Heater

direction does affect the temperature profile and may account for some of the error. The mathematical model does not account for the secondary air movement.

In addition, the m factor, which controls the velocity of the air through the interior cavity and exterior cavity, may be slightly off. If the m factor is increased there is a smaller temperature difference from the top to the bottom of the system. The velocity is increased and the air has less time to warm up in the system, which affects the temperature on the blinds and windows. This holds true for the experiment set up as well. At the larger velocities, the temperature difference from the top to the bottom is smaller compared to the smaller air cavity velocity. The h_{conv} and the m factor are two parameters, which can greatly alter the accuracy of the model. These values were chosen to best represent the data.

Figure 31k Temperature vs. vertical height, group A

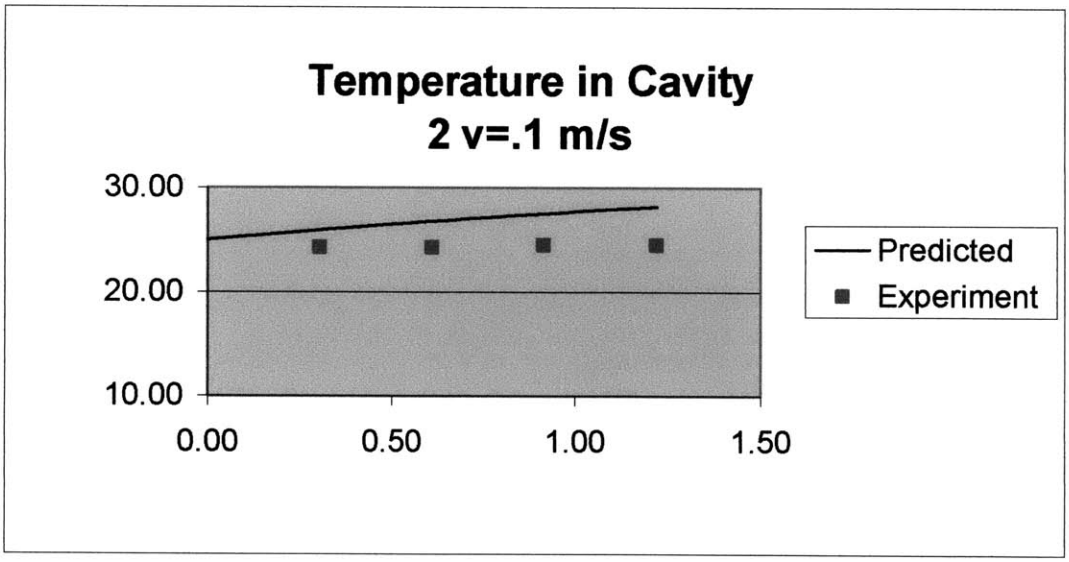

Initial Conditions Group A
- Blinds Open
- Interior Cavity Length = 4.5"
- Air Cavity Velocity = .1 m/s
- Heat source, Heater

Note that there is slight temperature increase of cavity 2, where the air velocity is lower (see figure 31j). In figure 31k the temperature difference is so small on the order of .2° C. If the m factor were larger in the model then it would predict a smaller

temperature difference and vice versa. The m factor is a possible source of error. Figure 31 l and m illustrate the effects of an increase in velocity, which is directly related to the m factor, to the components of the window system.

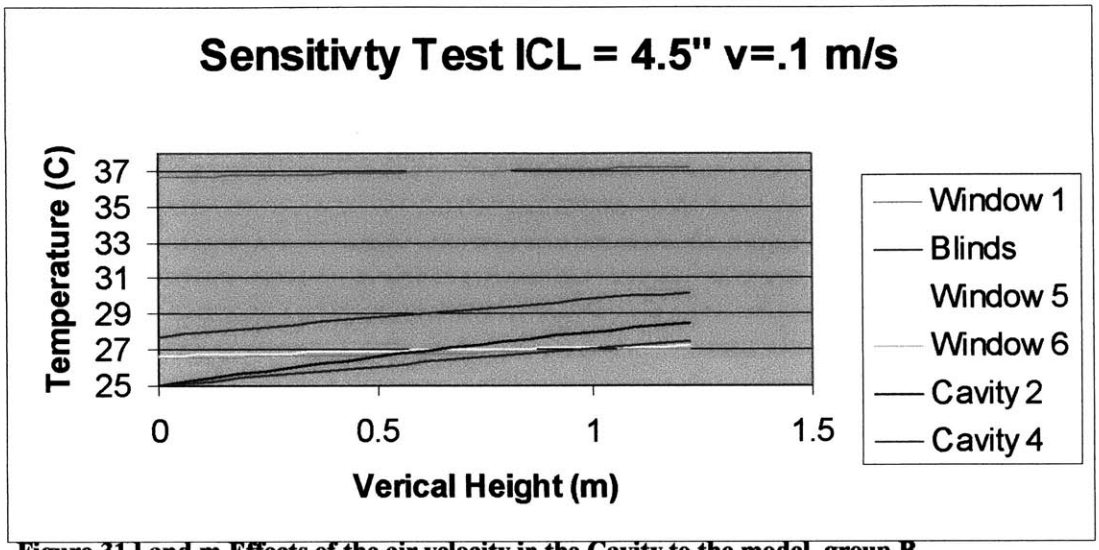

Figure 31 l and m Effects of the air velocity in the Cavity to the model, group B

Initial Conditions Group B
- Blinds Closed
- Interior Cavity Length = 4.5"
- Air Cavity Velocity = .1 m/s and 6.8 m/s
- Heat source, Sun Lamp

Increasing the velocity, which is comparable to increasing the m factor, increases the value of the initial temperature of the windows and blinds (temperature at bottom of the

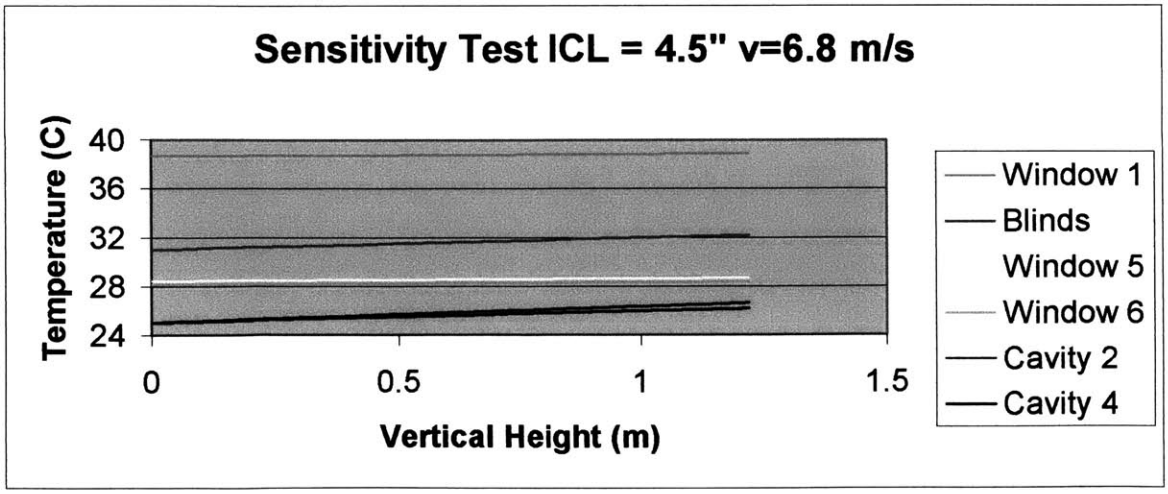

DSF system), but decreases the rate temperature change vs. height. The case with the smaller velocity has a lower initial temperature but a larger rate of temperature change vs. height. Observing figures 31 l and m, the increase in temperature vs. height is most apparent in the blinds and cavity. The window temperature does not increase much with height, which would suggest that the cause of error between model and data of the windows is due to an inaccurate value of the air velocity in the cavity. The air velocity influences the initial temperature of the interior and exterior window, so if the air velocity is too high in the model than a much higher temperature is predicted. The actual air velocity could be much lower than the measured value due to the method of measurement, which could account for the error of the m factor and the window temperatures.

4.7 Comparing results to Permasteelisa

The second part of the second objective is to compare the experiment results to Permasteelisa's (an Italian Manufacturer of double skin façade windows) data. The comparison was done to verify that experiment was giving reasonable temperature trends. Permasteelisa's research was done on a larger scale. The company built testing rooms where the double skin facades were implemented instead of a traditional façades. The type of glass and blinds are similar between the MIT experiment and the Permasteelisa full-scale model. Both DSF systems used interior ventilation, although Permasteelisa has a testing room where outside ventilation is used. Similar to the MIT experiment thermocouples are placed at varying heights and horizontal positions.

Figure 32 is a schematic of the thermocouple horizontal positions of the Permasteelisa setup. The thermocouples are represented by black dots, the blue rectangles represent the windows and the gray lines are the blinds. The data is collected continuously at many heights, and then it is averaged,

Figure 32 Horizontal locations of Thermocouples

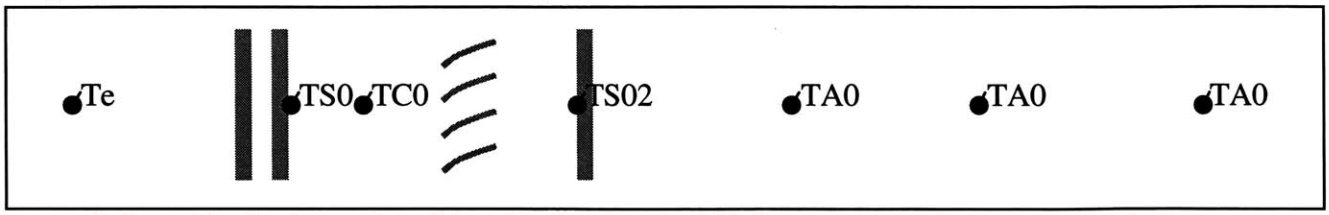

and plotted by horizontal position. Notice that the blind temperature is not measured. Another difference between the MIT setup and the Permasteelisa setup is that a double-glazed window is used as the exterior window. The double glazed window is completely sealed and the distance between the two windows is about 14 mm. The interior and exterior cavity widths are both fixed at .057m. The windows are about 8 cm closer together than the MIT set up. Despite all of the differences between the MIT experiment and the Permasteelisa experiment the data follow the same temperature trends.

Figure 33 Comparing MIT and Permasteelisa Data

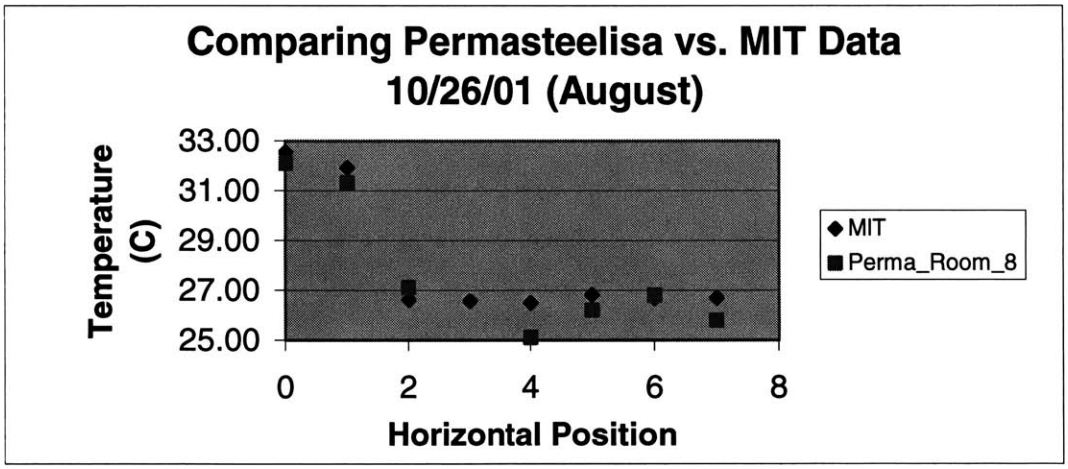

Figure 33 compares the MIT data to the Permasteelisa data. The blue diamonds are the MIT data points, and the pink squares are Permasteelisa data points. The Permasteelisa data was collected in August in late evening, so that the thermal effects of the sun could be minimized. It would be difficult to simulate the sun in a set up. The ambient room temperature of Permasteelisa's setup was 25.5° C and the outside temperature was about 32°C. There are only two points, which are not in good agreement, location 4 (interior cavity) and location 2 (exterior cavity). The blind temperature (location 3) was not plotted for Permasteelisa, because the value was not measured. Figure 34 compares the inside ventilated to outside ventilated Permasteelisa rooms.

Overall the temperature trends are similar between the sets of data. There are a few discrepancies, which could be caused by the different configuration. Location four, interior cavity length, has almost a 2° C temperature difference (see figure 33). The interior cavity length of the MIT setup is 11 cm and the Permasteelisa setup is almost half the distance. This distance affects the $h_{conv,}$ which in turn affects the temperature. The difference in the velocity of the air cavity did not affect the temperature trends, because the velocity would have to be an order of magnitude greater to observe significant temperature trends. Even though the differences exist the data sets are within 2.8% of each other. The data collected by MIT can represent a full-scale double skin façade, which means that the mathematical model can be used to apply to larger scale models. The error between the model and MIT data is reasonable. The model is accurate enough to give reliable estimates of temperature trends and energy consumption.

Chart 5 Comparison of MIT to Permasteelisa Data Initial Conditions

	Blinds	Heat Source	Air Velocity	Inside Temp	Outside Temp
MIT	Closed	Sun Lamp	.1 m/s	26.7° C	32.5°C
Permasteelisa	Closed	Sun	.4 m/s	25.8 °C	32.1°C

Figure 34 Comparing Inside Ventilated to Outside Ventilated Rooms of Permasteelisa

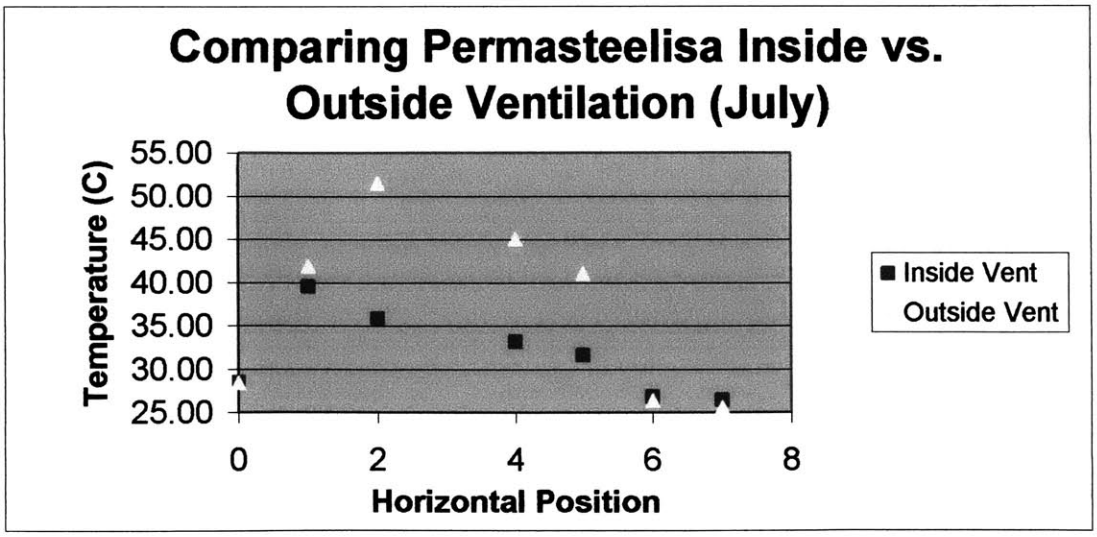

in one scenario and coming in from the inside in the other. The double glazed window is on the interior on the outside ventilated system, which is the opposite of the inside ventilated room, where the double glazed window is on the exterior. Looking at the outside and inside ventilated systems; they both achieve the same goal. They start and end with roughly the same design temperatures.

4.8 Summary

The chapter started with an explanation of the mathematical model and looked at the assumptions made to create the double skin façade window system. Some of the key assumptions were: one dimensional heat transfer in the horizontal direction, radiation, conduction, and convection were used to determine the heat transfer, and the type convective coefficient (i.e. flow over a flat plate or flow over a cylinder) was determined. The mathematical model inputs and outputs were explained in great detail. The outputs were then related to the MIT data and the MIT data was compared to the model by temperature vs. vertical height for each component and also by temperature vs. horizontal position. The accuracy of the model was calculated for various initial conditions. On average the model is within 2% to 3% of the data. The different sets of the MIT data was compared to get a better understanding of how the experiment setup responded to the parameters. A few sources of error were determined which were the heat transfer coefficient, the uncertainty of the data acquisition system, the accuracy of the measured velocity and the m factor. Finally, the data collected by Permasteelisa was compared to MIT data to see the variations between the two. The data sets were within 3%.

Chapter Five: Conclusion

The Double Skin Façade window system is unique in design and in thermal performance. Unlike traditional facades, the DSF system improves the efficiency of the building by eliminating excess energy that the environment transfers to the building. The savings are realized in the operating costs of the building through the decrease in the Heating, Cooling, and Air Conditioning system (HVAC). The Double Skin Façade system is a valuable investment, because of the long-term energy savings. This research of the Double Skin Façade window system is focused around three objectives, which were: collection of extensive data from the double skin façade window system, verification of the mathematical model and data from Permasteelisa, and application of the model to real life situations. Each of these objectives was met through the experimentation of the double skin façade system.

Extensive Data

The better part of a year was used to collect data with varying initial conditions. The data was used to compare with other data sets as well as the mathematical model. Varying the parameters such as the interior cavity length and the blind position had interesting effects to the overall performance of the system. By collecting many sets of data, a better understanding of how the double skin façade system behaves was accomplished. The temperature trends of the system were the same; in general the temperature was higher near the exterior window (closer to the heat source) and dropped off to the room temperature by the interior window, even though the cavity width or blind position changed. There were also subtle differences between temperatures with the blinds open versus closed. The data collection has been documented and can be used to educate people interested in implementing the double skin façade system into new buildings.

Comparing Model to Data

The second objective, verifying the data to the mathematical model and Permasteelisa data, was also completed. The data was thoroughly analyzed by graphing it versus time, vertical height and horizontal position. The time history graphs revealed

information about the steady state temperatures. If for example the temperature trends of the vertical height vs. temperature are extremely different for one component compared to the others in the system, the error can be traced back to the time history plots. It could be that a thermocouple fell off and was measuring the wrong temperature so that shifted the overall temperature trend.

The temperature versus vertical height illustrated that the mathematical model agreed better as the height increased. One of the factors affecting the agreement between the model and data was the convective heat transfer coefficient. The h_{conv} was constant in the model from top to bottom of the system however it should have varied with height. The agreement of the model and data would have improved if the h_{conv} decreased as the height increased. One of the next steps in improving the accuracy of the model would be to vary the h_{conv} with height.

The third type of graph, temperature versus horizontal position showed how well the entire experiment setup related to the mathematical model. Even though there may have been discrepancies in the vertical height vs. temperature, the horizontal position vs. temperature generally had very good agreement. The accuracy of the model was strongly dependant on the initial conditions. If the interior cavity width was 4.5 inches the agreement was much better than if the interior cavity width was 9 or 13.5 inches. The type of heat source also affected the accuracy of the model (using the sunlamp improved the accuracy). The temperatures were generally higher with the sun lamp compared to the modified heater, which lead to better agreement of the model. The accuracy of the model varied between 98% at its best and about 96% at its worse. Some of the error could be accounted for in the uncertainty of the data acquisition system. For instance the data acquisition system may measure a different temperature for a particular position, which can add up and create larger errors. Adding more complexity to the model such as varying h_{conv}, can help eliminate the error.

The data was also compared to the Permasteelisa results and surprisingly the two data sets were fairly close despite the change in window configuration. By comparing the data to the Permasteelisa data, the temperatures were verified. The MIT experiment was conducted indoors yet the data was comparable with the data of a life size double skin façade system implemented in a real building. This comparison was important to justify

using the experiment data for this research to compare to a mathematical model for a DSF system in a building.

Applying to Large Scale

Despite the error of the model, it still is a good representation of the double skin façade system. The model and data correspond well over the entire system, which is very important. The last objective, applying the model to large-scale systems, is possible through using the design advisor program. As mentioned in the introduction the design advisor program can model different types of DSF systems in any weather condition or global location. This research is not directly involved with the design advisor program, however it determines of the accuracy of the program, which is a preliminary step in enabling the model to predict the large-scale models. The three objectives were met: collect extensive data, compare data to model and Permasteelisa data, and apply the model to life size conditions. Overall the model predicted the behavior of the double skin façade system well. The results of the model are impressive and have the potential of convincing people involved in building construction that the double skin façade system is one worth investing because of the energy savings advantage.

Recommendations

There is room for improvement in the experiment, which will lead to a much better accuracy of the model. Two suggestions, which will improve the experimental results, are cavity insulation and a better method of measuring the air velocity. The insulation of the DSF system to its surroundings was not airtight. There were many areas for air leakages in the cavity. The heat that was supposed to be transferred vertically could leak through the sides, which could account for some of the error in the model. If the DSF system were properly insulated then temperatures would definitely increase in the cavity, windows, and blinds, which would lead to a more accurate model.

Implementing a better method to measure the air velocity would decrease the amount of the error between measured and actual value. For this research, the air velocity measurements were taken when the door to the cavity was ajar, so it was not an accurate representation of the air velocity while the experiment is running, because the door to the cavity is completely closed during experiments. The uncertainty of the air velocity

measurement could alter the predictions of the model and cause the error. It was determined from looking at the sensitivity tests on the velocity that the model was using a higher velocity than the actual value because it was predicting higher temperatures on the windows and blinds.

If the air velocity is measured while the door to the cavity remains closed than a more accurate air velocity value can be used in the model, which would in turn increase the accuracy of the model. A better method of measuring the air velocity would be to drill a hole through the door large enough for a probe to fit through. The velocity measurements could easily be taken by traversing the cavity. The height of the measurements is limited to the height of the hole; however, multiple holes can be drilled at varying levels read the velocity at different heights. These two suggestions, more insulation, and a new technique of measuring air velocities would definitely improve the results of the data.

Appendix A

A1. Graph of Fan Calibration (23 refers to the hot-film anemometer number)

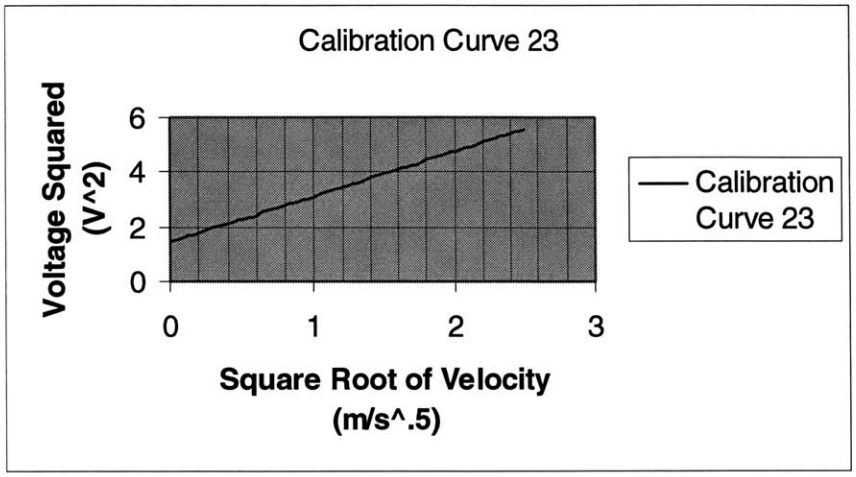

A2. Temperature vs. Time plot of Heated Box

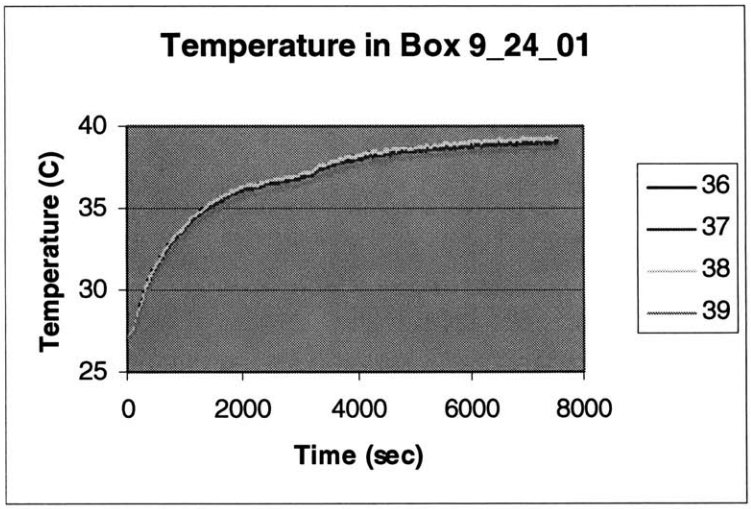

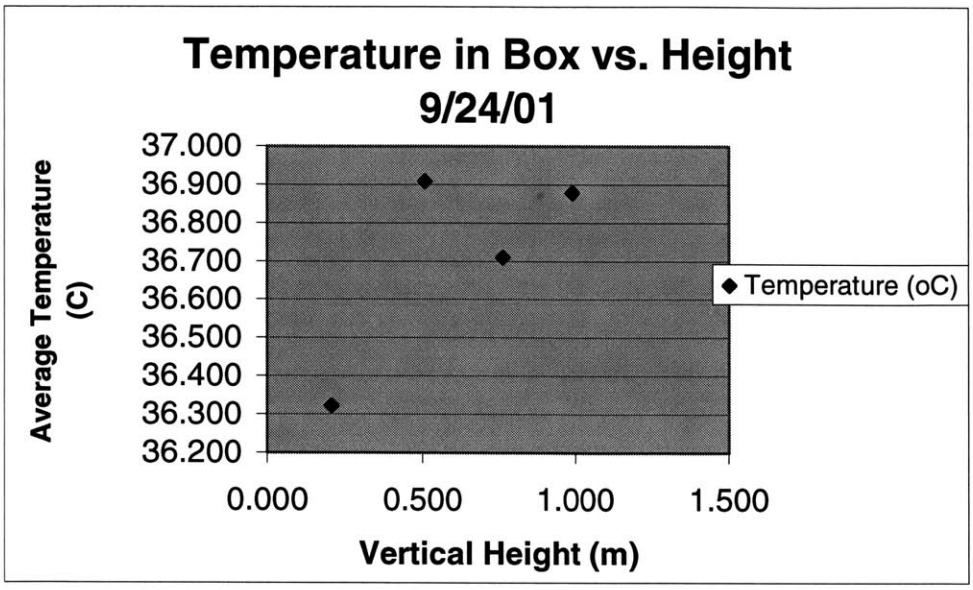

A3: Temperature vs. Vertical height of Heated Box

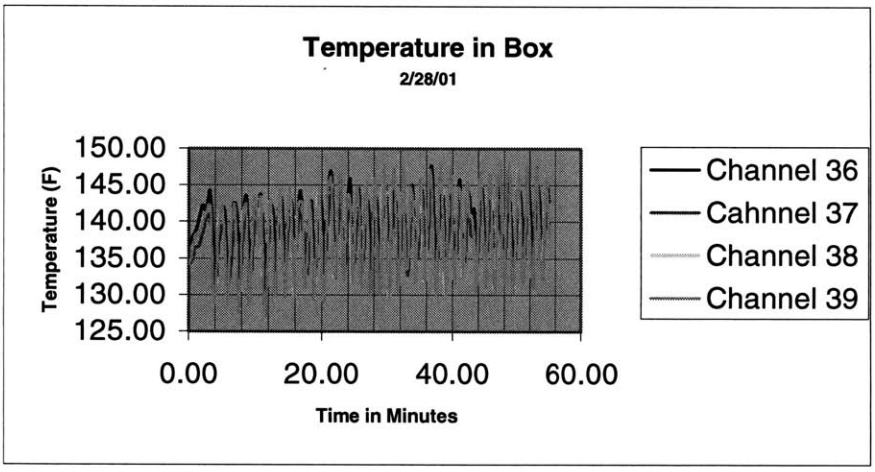

A4: Temperature vs. Time of heated box before heater modification

A5: Velocity Profiles in the exterior cavity for varying interior cavity length.

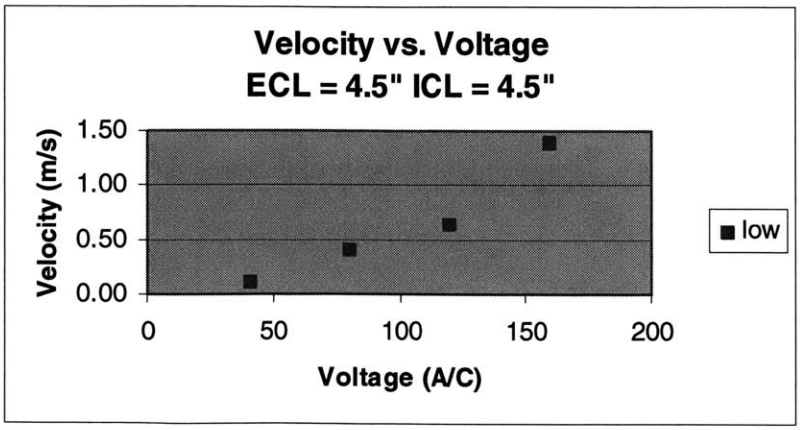

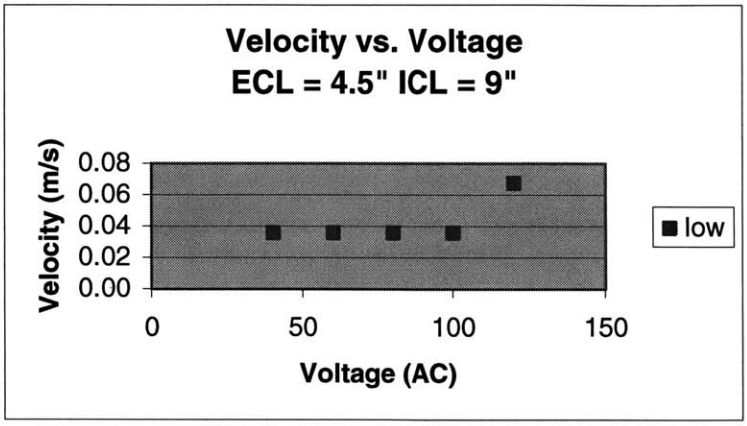

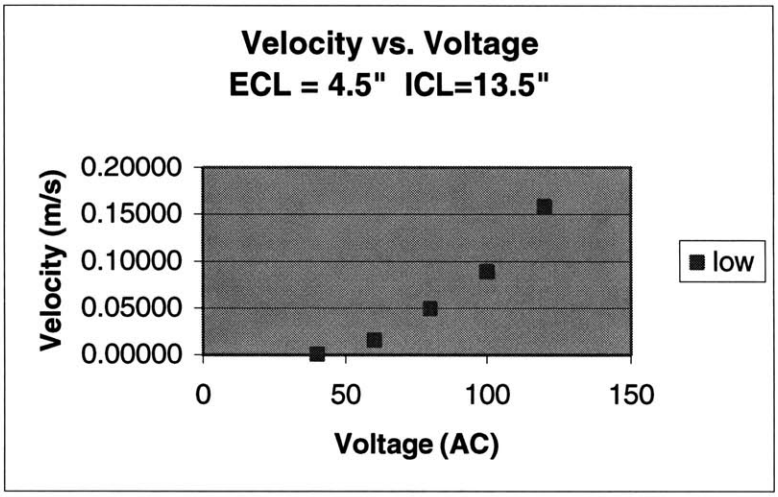

A6: Velocity Profiles in the interior cavity for varying interior cavity length.

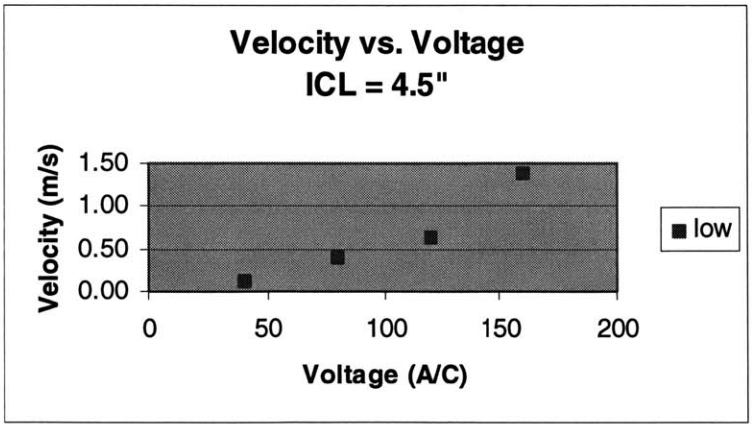

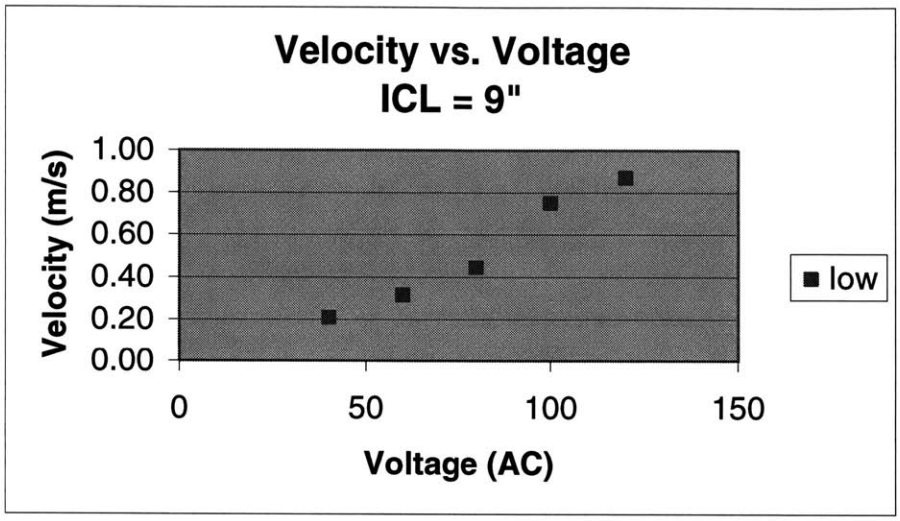
Velocity vs. Voltage
ICL = 9"
Velocity (m/s)
1.00
0.80
0.60
0.40
0.20
0.00
0
50
100
150
Voltage (AC)
low

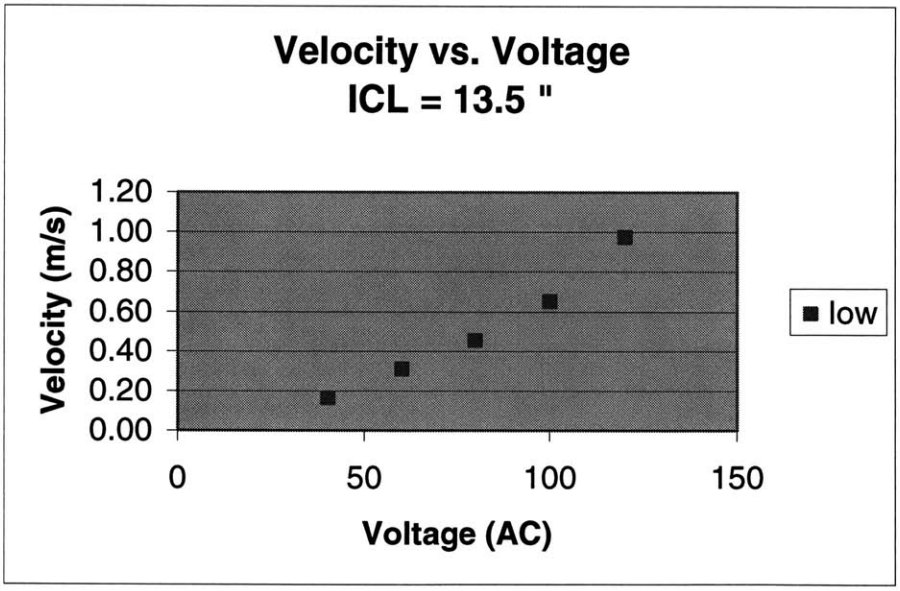
Velocity vs. Voltage
ICL = 13.5 "
Velocity (m/s)
1.20
1.00
0.80
0.60
0.40
0.20
0.00
0
50
100
150
Voltage (AC)
low

Appendix B

B1: Summary of Experiments

	Parameters					Heater = H Lamp = L Lamp out of Box = LO
Date	**Fan (ACV)**	**Blind**	**Heat (F)**	**ECL (in)**	**ICL (in)**	Heat Source
4/20/01	40 High	open	100	4.5	4.5	H
4/23/01	40 High	open	100	4.5	4.5	H
4/24/01	40 High	closed	100	4.5	4.5	H
4/26/01	40 High	open	100	4.5	4.5	H
4/27/01	25 High	open	100	4.5	4.5	H
4/28/01	25 High	closed	100	4.5	4.5	H
4/30/01_a	22.5 High	closed	100	4.5	4.5	H
4/30/01_b	22.5 High	open	100	4.5	9	H
5/1/01_a	22.5 High	open	100	4.5	9	H
5/1/01_b	22.5 High	open	100	4.5	13.5	H
5/2/01	40 Low	open	100	4.5	13.5	H
5/3/01_a	40 Low	open	100	4.5	4.5	H
5/3/01_b	40 Low	closed	100	4.5	4.5	H
5/4/01	40 Low	open	100	4.5	4.5	H
5/7/01_a	40 Low	open	100	4.5	4.5	H
5/7/01_b	40 Low	closed	100	4.5	4.5	H
5/9/01	no fan	open	100	4.5	4.5	H
5/10/01	no fan	Testing heat lamp	130	4.5	4.5	L
5/14/01_a	40 Low	open	100	4.5	9	H
5/14/01_b	40 Low	closed	100	4.5	9	H
5/15/01_a	40 Low	closed	100	4.5	9	H
5/15/01_b	40 Low	open	100	4.5	9	H
5/15/01_c	40 Low	open	100	4.5	13.5	H
5/15/01_d	40 Low	closed	100	4.5	13.5	H
5/17/01_a	40 Low	closed	100	4.5	9	H
5/17/01_b	40 Low	open	100	4.5	9	H
5/18/01	40 Low	open	100	4.5	13.5	H
5/20/01	40 Low	closed	100	4.5	13.5	H
5/21/2001_a	60 Low	open	100	4.5	4.5	H
5/21/2001_b	80 Low	open	100	4.5	4.5	H
5/22/01_a	60 Low	closed	100	4.5	4.5	H
5/22/01_b	80 Low	closed	100	4.5	4.5	H
5/23/01_a	60 Low	closed	100	4.5	9	H
5/23/01_b	60 Low	closed	100	4.5	13.5	H
9/7/2001_a	40 Low	open	100	4.5	4.5	L
9/7/2001_b	40 Low	closed	100	4.5	4.5	L
9/8/2001_a	40 Low	open	100	4.5	4.5	L
9/8/2001_b	40 Low	closed	100	4.5	4.5	L
9/10/2001_a	40 Low	closed	100	4.5	9	L
9/10/01_b	40 Low	open	100	4.5	9	L
9/10/01_c	40 Low	closed	100	4.5	9	L
9/10/01_d	40 Low	open	100	4.5	9	L
9/11/2001_a	40 Low	open	100	4.5	13.5	L
9/11/01_b	40 Low	closed	100	4.5	13.5	L
9/11/01_c	40 Low	open	100	4.5	13.5	L
9/11/01_d	40 Low	closed	100	4.5	13.5	L

9/12/2001_a	40 Low	closed	100	4.5	4.5	L
9/12/01_b	40 Low	open	100	4.5	4.5	L
9/12/01_c	40 Low	open	100	4.5	4.5	H
9/12/01_d	40 Low	closed	100	4.5	4.5	H
9/19/01_a	80 Low	open	100	4.5	4.5	L
9/19/01_b	80 Low	open	100	4.5	9	L
9/19/01_c	80 Low	open	100	4.5	13.5	L
9/19/01_d	80 Low	closed	100	4.5	4.5	L
9/20/01_a	80 Low	closed	100	4.5	9	L
9/20/01_b	80 Low	closed	100	4.5	13.5	L
9/20/01_c	80 Low	open	100	4.5	4.5	L
9/20/01_d	80 Low	open	100	4.5	9	L
9/21/01_a	80 Low	open	100	4.5	13.5	L
9/21/01_b	80 Low	closed	100	4.5	4.5	L
9/21/01_c	80 Low	closed	100	4.5	9	L
9/21/01_d	80 Low	closed	100	4.5	13.5	L
9/25/01_a	80 Low	open	100	4.5	4.5	LO
9/25/01_b	80 Low	open	100	4.5	9	LO
9/25/01_c	80 Low	open	100	4.5	13.5	LO
9/25/01_d	80 Low	closed	100	4.5	4.5	LO
9/26/01_a	80 Low	closed	100	4.5	9	LO
9/26/01_b	80 Low	closed	100	4.5	13.5	LO
9/26/01_c	80 Low	open	100	4.5	4.5	LO
9/26/01_d	80 Low	open	100	4.5	9	LO
9/27/01_a	80 Low	open	100	4.5	13.5	LO
9/27/01_b	80 Low	closed	100	4.5	4.5	LO
9/27/01_c	80 Low	closed	100	4.5	9	LO
9/27/01_d	80 Low	closed	100	4.5	13.5	LO
10/1/01_a	80 Low	open	100	4.5	13.5	LO
10/1/01_b	80 Low	open	100	4.5	9	LO
10/1/01_c	80 Low	open	100	4.5	4.5	LO
10/1/01_d	80 Low	closed	100	4.5	4.5	LO
10/2/01_a	80 Low	closed	100	4.5	9	LO
10/2/01_b	80 Low	closed	100	4.5	13.5	LO
10/2/01_c	80 Low	open	100	4.5	13.5	LO
10/2/01_d	80 Low	open	100	4.5	9	LO
10/3/01_a	80 Low	open	100	4.5	4.5	LO
10/3/01_b	80 Low	closed	100	4.5	4.5	LO
10/3/01_c	80 Low	closed	100	4.5	9	LO
10/3/01_d	80 Low	closed	100	4.5	13.5	LO
10/11/01_a	80 Low	closed	100	4.5	13.5	LO
10/11/01_b	80 Low	closed	100	4.5	9	LO
10/11/01_c	80 Low	closed	100	4.5	4.5	LO
10/11/01_d	80 Low	open	100	4.5	4.5	LO
10/15/01_a	80 Low	open	100	4.5	4.5	LO
10/15/01_b	80 Low	open	100	4.5	9	LO
10/15/01_c	80 Low	open	100	4.5	13.5	LO
10/15/01_d	80 Low	closed	100	4.5	13.5	LO
10/16/01_a	80 Low	closed	100	4.5	9	LO
10/16/01_b	80 Low	closed	100	4.5	13.5	LO
10/16/01_c	80 Low	open	100	4.5	13.5	LO
10/16/01_d	80 Low	open	100	4.5	9	LO
10/17/01_a	80 Low	open	100	4.5	4.5	LO
10/17/01_b	80 Low	closed	100	4.5	4.5	LO
10/17/01_c	80 Low	closed	100	4.5	9	LO
10/17/01_d	80 Low	closed	100	4.5	13.5	LO

10/22/01_a	80 Low	open	100	4.5	4.5	LO
10/22/01_b	80 Low	open	100	4.5	9	LO
10/22/01_c	80 Low	open	100	4.5	13.5	LO
10/22/01_d	80 Low	closed	100	4.5	13.5	LO
10/23/01_a	80 Low	closed	100	4.5	9	LO
10/23/01_b	80 Low	closed	100	4.5	4.5	LO
10/23/01_c	80 Low	open	100	4.5	4.5	LO
10/23/01_d	80 Low	open	100	4.5	9	LO
10/24/01_a	80 Low	open	100	4.5	13.5	LO
10/24/01_b	80 Low	closed	100	4.5	13.5	LO
10/24/01_c	80 Low	closed	100	4.5	9	LO
10/24/01_d	80 Low	closed	100	4.5	4.5	LO
10/26/01_a	80 Low	closed	91.4	4.5	4.5	LO

Appendix C

C1. Glass Properties (Data taken from Lawrence Berkley Lab's Window 4.1)

Glass		
Glass ID #	1	2
Glass ID Name	Float	None
k,glass1	1	1000
l,glass1	0.008	0.00001
Abs_glass1	0.08	0.000001
Ref_glass1	0.05	9E-06
Trans_glass1	0.87	0.99999
Emissivity_glass1	0.90	0.99999

WINDOW 4.1 Glass Library Format
Revision 2

ID	Name	Thick In.	Tsol	Rsol 1	Rsol 2	Tvis	Rvis 1	Rvis 2
1	None	0.008	0.99999	0.0001	0.0001	0.9999	0.0001	0.0001
700	B120.AFG	0.008	0.1386	0.4011	0.2022	0.2054	0.3219	0.2149
701	B130.AFG	0.008	0.2246	0.3196	0.1399	0.3077	0.2739	0.1505
702	B140.AFG	0.008	0.3151	0.2486	0.0913	0.4107	0.2174	0.0960
703	B220.AFG	0.008	0.0901	0.4031	0.1013	0.1782	0.3257	0.1602
704	B230.AFG	0.008	0.1379	0.3207	0.0861	0.2602	0.2755	0.1272
705	B240.AFG	0.008	0.1964	0.2496	0.0600	0.3544	0.2238	0.0779
706	B320.AFG	0.008	0.0779	0.4017	0.0956	0.1056	0.3234	0.0876
707	B330.AFG	0.008	0.1286	0.3185	0.0733	0.1603	0.2720	0.0712
708	B340.AFG	0.008	0.1795	0.2447	0.0567	0.2117	0.2120	0.0561
709	B420.AFG	0.008	0.0874	0.4022	0.1028	0.1263	0.3237	0.1019
710	B430.AFG	0.008	0.1428	0.3143	0.0783	0.1901	0.2671	0.0810
711	B440.AFG	0.008	0.2026	0.2417	0.0592	0.2548	0.2110	0.0612
712	B520.AFG	0.008	0.0839	0.3978	0.0943	0.1308	0.3189	0.1060
713	B530.AFG	0.008	0.1298	0.3216	0.0781	0.1888	0.2727	0.0862
714	B540.AFG	0.008	0.2011	0.2441	0.0604	0.2551	0.2109	0.0643
715	B620.AFG	0.008	0.0936	0.4012	0.1151	0.1771	0.3216	0.1745
716	B630.AFG	0.008	0.1501	0.3222	0.0859	0.2661	0.2757	0.1214
717	B640.AFG	0.008	0.2073	0.2473	0.0650	0.3545	0.2176	0.0841
718	B720.AFG	0.008	0.0710	0.4034	0.0873	0.1687	0.3229	0.1517
719	B730.AFG	0.008	0.1087	0.3186	0.0786	0.2489	0.2713	0.1198
720	B740.AFG	0.008	0.1485	0.2444	0.0638	0.3306	0.2122	0.0840
721	B820.AFG	0.008	0.0701	0.4015	0.0791	0.1601	0.3230	0.1370
722	B830.AFG	0.008	0.1077	0.3205	0.0699	0.2340	0.2739	0.1081
723	B840.AFG	0.008	0.1506	0.2433	0.0529	0.3174	0.2165	0.0717
724	C120.AFG	0.008	0.1107	0.6273	0.4687	0.2252	0.3326	0.3584
725	C130.AFG	0.008	0.1765	0.5750	0.4071	0.3281	0.2611	0.2532
726	C145.AFG	0.008	0.2717	0.5087	0.3347	0.4769	0.1852	0.1456
727	C155.AFG	0.008	0.3861	0.3838	0.2349	0.5851	0.1159	0.0737
728	C220.AFG	0.008	0.0752	0.6251	0.1708	0.1889	0.3160	0.2546
729	C230.AFG	0.008	0.1173	0.5726	0.1400	0.2755	0.2628	0.1801

730C245.AFG	0.008	0.1767	0.5051	0.1117	0.4000	0.1752	0.1119
731C255.AFG	0.008	0.2379	0.3725	0.0834	0.4866	0.1105	0.0661
732C320.AFG	0.008	0.0626	0.6245	0.1773	0.1203	0.3243	0.1186
733C330.AFG	0.008	0.1003	0.5609	0.1512	0.1756	0.2482	0.0887
734C345.AFG	0.008	0.1543	0.4855	0.1326	0.2518	0.1626	0.0644
735C355.AFG	0.008	0.2173	0.3650	0.1035	0.3045	0.1000	0.0477
736C420.AFG	0.008	0.0709	0.6257	0.2070	0.1441	0.3225	0.1544
737C430.AFG	0.008	0.1104	0.5586	0.1812	0.2045	0.2443	0.1160
738C445.AFG	0.008	0.1729	0.4848	0.1520	0.3013	0.1606	0.0788
739C455.AFG	0.008	0.2395	0.3674	0.1185	0.3605	0.1028	0.0541
740C520.AFG	0.008	0.0695	0.6237	0.1711	0.1445	0.3254	0.1556

C2. Air Properties

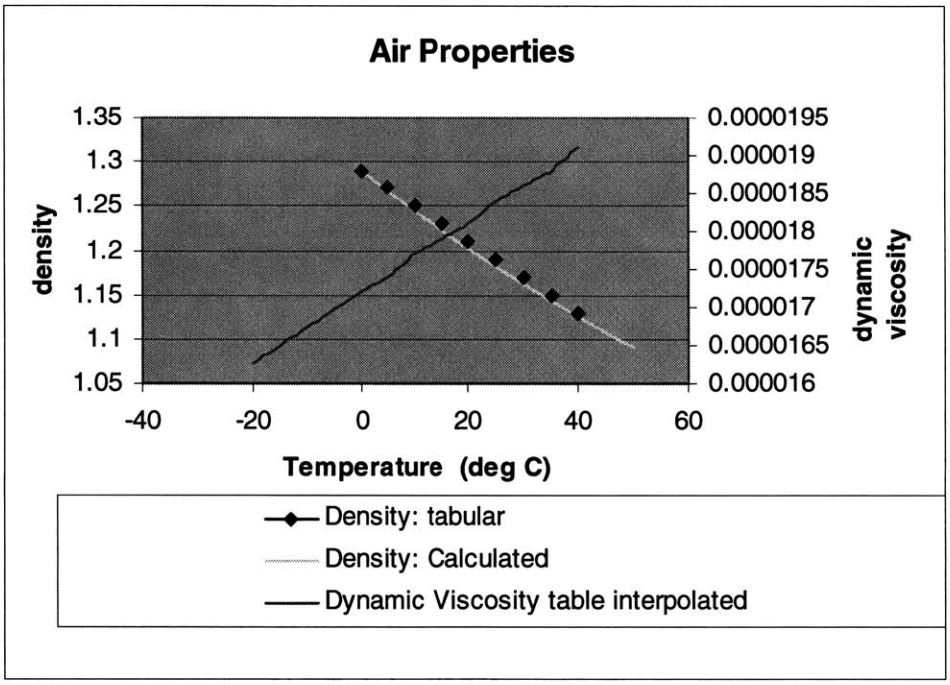

Temperature (C)	Temperature (K)	Density kg/m^3
25	298	1.181920243
25.1	298.1	1.181523758
25.2	298.2	1.18112754
25.3	298.3	1.180731587
25.4	298.4	1.180335899
25.5	298.5	1.179940477
25.6	298.6	1.179545319
25.7	298.7	1.179150426
25.8	298.8	1.178755798
25.9	298.9	1.178361433
26	299	1.177967332
26.1	299.1	1.177573495

26.2	299.2	1.177179921
26.3	299.3	1.17678661
26.4	299.4	1.176393562
26.5	299.5	1.176000776
26.6	299.6	1.175608252
26.7	299.7	1.175215991
26.8	299.8	1.174823991
26.9	299.9	1.174432252
27	300	1.174040775
27.1	300.1	1.173649558
27.2	300.2	1.173258602
27.3	300.3	1.172867907
27.4	300.4	1.172477471
27.5	300.5	1.172087296
27.6	300.6	1.17169738
27.7	300.7	1.171307723
27.8	300.8	1.170918326
27.9	300.9	1.170529187
28	301	1.170140307
28.1	301.1	1.169751685
28.2	301.2	1.169363321
28.3	301.3	1.168975215
28.4	301.4	1.168587367
28.5	301.5	1.168199776
28.6	301.6	1.167812442
28.7	301.7	1.167425364
28.8	301.8	1.167038543
28.9	301.9	1.166651979
29	302	1.16626567
29.1	302.1	1.165879617
29.2	302.2	1.16549382
29.3	302.3	1.165108278
29.4	302.4	1.164722991
29.5	302.5	1.164337958
29.6	302.6	1.16395318
29.7	302.7	1.163568657
29.8	302.8	1.163184387
29.9	302.9	1.162800371
30	303	1.162416609
30.1	303.1	1.162033099
30.2	303.2	1.161649843
30.3	303.3	1.161266839
30.4	303.4	1.160884088
30.5	303.5	1.160501589
30.6	303.6	1.160119342
30.7	303.7	1.159737347
30.8	303.8	1.159355604
30.9	303.9	1.158974111
31	304	1.15859287
31.1	304.1	1.158211879

31.2	304.2	1.157831139
31.3	304.3	1.157450649
31.4	304.4	1.157070409
31.5	304.5	1.156690418
31.6	304.6	1.156310678
31.7	304.7	1.155931186
31.8	304.8	1.155551944
31.9	304.9	1.15517295
32	305	1.154794205
32.1	305.1	1.154415708
32.2	305.2	1.154037459
32.3	305.3	1.153659458
32.4	305.4	1.153281704
32.5	305.5	1.152904198
32.6	305.6	1.152526938
32.7	305.7	1.152149926
32.8	305.8	1.15177316
32.9	305.9	1.151396641
33	306	1.151020367
33.1	306.1	1.15064434
33.2	306.2	1.150268558
33.3	306.3	1.149893021
33.4	306.4	1.14951773
33.5	306.5	1.149142683
33.6	306.6	1.148767881
33.7	306.7	1.148393324
33.8	306.8	1.14801901
33.9	306.9	1.147644941
34	307	1.147271115
34.1	307.1	1.146897533
34.2	307.2	1.146524194
34.3	307.3	1.146151098
34.4	307.4	1.145778245
34.5	307.5	1.145405634
34.6	307.6	1.145033265
34.7	307.7	1.144661139
34.8	307.8	1.144289254
34.9	307.9	1.143917611
35	308	1.143546209
35.1	308.1	1.143175048
35.2	308.2	1.142804128
35.3	308.3	1.142433449
35.4	308.4	1.14206301
35.5	308.5	1.141692812
35.6	308.6	1.141322853
35.7	308.7	1.140953134
35.8	308.8	1.140583654
35.9	308.9	1.140214414
36	309	1.139845412
36.1	309.1	1.13947665

36.2	309.2	1.139108125
36.3	309.3	1.13873984
36.4	309.4	1.138371792
36.5	309.5	1.138003982
36.6	309.6	1.137636409
36.7	309.7	1.137269075
36.8	309.8	1.136901977
36.9	309.9	1.136535116
37	310	1.136168492
37.1	310.1	1.135802104
37.2	310.2	1.135435952
37.3	310.3	1.135070037
37.4	310.4	1.134704357
37.5	310.5	1.134338913
37.6	310.6	1.133973704
37.7	310.7	1.13360873
37.8	310.8	1.133243991
37.9	310.9	1.132879487
38	311	1.132515217
38.1	311.1	1.132151181
38.2	311.2	1.131787379
38.3	311.3	1.131423811
38.4	311.4	1.131060476
38.5	311.5	1.130697375
38.6	311.6	1.130334507
38.7	311.7	1.129971872
38.8	311.8	1.129609469
38.9	311.9	1.129247298
39	312	1.12888536
39.1	312.1	1.128523654
39.2	312.2	1.128162179
39.3	312.3	1.127800936
39.4	312.4	1.127439924
39.5	312.5	1.127079144
39.6	312.6	1.126718594
39.7	312.7	1.126358274
39.8	312.8	1.125998185
39.9	312.9	1.125638327
40	313	1.125278698
40.1	313.1	1.124919299
40.2	313.2	1.124560129

Appendix D

D1. Initial Conditions of Double Skin Façade Window System

Case1	< Input case # here	
User Input and Given Parameters		
Geometry	**Case** Example One	
Height, H	Height	**1.2192** m
Num divisions	Divisions	**20**
Delta y	Dy	0.06096
Area	Area	0.06096 m^2
D_o	D_o	**1** mm
D_1	D_1	**0.114** m
D_2	D_2	**0.114** m
T_{out}	T_{out}	**37.8** Degrees C
T_{in}	T_{in}	**25.0** Degrees C
Delta T	Delta T	12.8 Degrees C
T_{mrt}	T_{mrt}	26.0 Degrees C
T_{sky}	T_{sky}	37.8 Degrees C
T_{inlet}	T_{inlet}	**25.0** Degrees C
Incident Radiation		
q_r, incident	Solar incident	**30.2** W/m^2
Glass Properties		
1/Eeff=1/E12+1/E21-1		25.19
E_{eff}		0.04
Glass #1 ID Number		CustPISARM08-1
k_{glass1}	k_{glass1}	1 W/(mK)
l_{glass1}	l_{glass1}	0.008 mm
Abs_front_glass1	Absglass1	0.19 Non-dimensional
Abs_back_glass1		0.19 Non-dimensional
Ref_front_glass1		0.07 Non-dimensional
Ref_back_glass1	Refglass1	0.07 Non-dimensional
Trans_glass1	Transglass1	0.74 Non-dimensional
Emissivity_front_glass1		0.84 Non-dimensional
Emissivity_back_glass1	Emissivityglass1	0.84 Non-dimensional
Glass #2 ID Number		CustPISARM08-2
k_{glass2}	k_{glass2}	1 W/(mK)

l_{glass2}	l_{glass2}	0.00876	m
Abs_front_glass2	Absglass2	0.18	Non-dimensional
Abs_back_glass2		0.29	Non-dimensional
Ref_front_glass2		0.31	Non-dimensional
Ref_back_glass2	Refglass2	0.2	Non-dimensional
Trans_glass2	Transglass2	0.51	Non-dimensional
Emissivity_front_glass2		0.04	Non-dimensional
Emissivity_back_glass2	Emissivityglass1	0.84	Non-dimensional
Glass # ID Number		CustPISARM08-3	
k_{glass3}	k_{glass3}	1	W/(mK)
l_{glass3}	l_{glass3}	0.008	m
Abs_front_glass3	Absglass3	0.12	Non-dimensional
Abs_back_glass3		0.12	Non-dimensional
Ref_front_glass3		0.07	Non-dimensional
Ref_back_glass3	Refglass3	0.07	Non-dimensional
Trans_glass3	Transglass3	0.74	Non-dimensional
Emissivity_front_glass3		0.84	Non-dimensional
Emissivity_back_glass3	Emissivityglass3	0.84	Non-dimensional
Heat Transfer, h_{conv}			
$h_{out}=h_1$	h_{out1}	**23**	W/m^2K
$h_{in}=h_6$	h_{in}	**8**	W/m^2K
Blinds Properties			
Emissivity, E_4	Emissivity4	0.25	Non-dimensional
Reflectivity, Ref_blind	Ref_blind	0.42	Non-dimensional
Spectral Reflectivity of blind		0.168	Non-dimensional
Diffuse Reflectivity of blind		0.252	Non-dimensional
Rho 4, tot-out		0.0805841	Non-dimensional
Alpha 4 tot		0.6643905	Non-dimensional
Rho 4, tot-in		0.245332	Non-dimensional
Absorptivity, abs_blind	Abs_blind	0.58	Non-dimensional
Length of the blind	L_{blind}	**0.025**	m
Blind Angle from horizontal (Sigma)	BL_{Angle}	**2**	Degrees
Blind Space	Blind Space	**0.02**	m
F26 (IR), geometry factor	F_IR	0.350549	Non-dimensional
F24=1-F (IR), geometry factor	1_F_IR	0.649451	Non-dimensional
F (sol), geometry factor	F_sol	0.85	Non-dimensional
1-F (sol), geometry factor	1_F_sol	0.15	Non-dimensional
Area of the blind for convection	A_{blind}	0.0762	m^2
Room Properties			
Emissivity, E_{in}	Emissivity_in	0.85	Non-dimensional
		d1	
Forced Ventilation? (Yes/No)		**Yes**	
Inlet Side		**In**	
Specific heat Cp	cp_{air_d1}	1005.00	J/kgK
Conductivity, k	k_{air_d1}	0.03	W/m^2K

Mass flow rate, m	Massflow_d1	**0.01**	kg/s
Rho, density of air	Airdensity_d1	1.20	kg/m^3
Velocity, V	Velocity_d1	0.07	M/s
Hydraulic Diameter	DH_d1	0.23	M
P_r	Pr_d1	0.69	Non-dimensional
Kinematic viscosity, air	Visc_d1	0.00	M/s^2
Re_D	ReD_d1	943.99	Non-dimensional
Laminar Nu_{DH}	NULam_d1	10.86	Non-dimensional
f	*f_d1*	0.07	Non-dimensional
Turbulent Nu_{Dh}	Nulam_d1	-0.46	Non-dimensional
Utilized Nu_{dh}	NU_d1	10.86	Non-dimensional
h_{conv} -- BLINDS	H_d1	**5.18**	W/m^2K
		d2	
Forced Ventilation? (Yes/No)		**Yes**	
Inlet Side		**In**	
Specific heat Cp	cp_{air_d2}	1005.00	J/kgK
Conductivity, k	k_{air_d2}	0.03	W/m2K
Mass flow rate, m	Massflow_d2	**0.01**	kg/s
Rho, density of air	Airdensity_d2	1.20	kg/m^3
Velocity, V	Velocity_d2	0.07	M/s
D_H	DH_d2	0.23	M
P_r	Pr_d2	0.69	Non-dimensional
Kinematic viscosity of air	Visc_d2	0.00	M/s^2
Re_D	ReD_d2	943.99	Non-dimensional
Laminar Nu_{dh}	NULam_d2	10.86	Non-dimensional
f	*f_d2*	0.07	Non-dimensional
Turbulent Nu_{Dh}	Nulam_d2	-0.46	Non-dimensional
Utilized Nu_{dh}	NU_d2	10.86	Non-dimensional
h_{conv} -- BLINDS	H_d2	**5.18**	W/m^2K
Constants			
Stefan-Boltzman	Stefan	5.70E-08	W/m^2K^4

D2: Mass flow rate Calculations

Cavity Dimension (m)	Area m^2	Mass flow rate kg/s	Volume Flow Rate m^3/s
0.11	0.07	0.0084	0.01
0.23	0.14	0.0167	0.01
0.34	0.21	0.0251	0.02

Rho, kg/m^3	Air Velocity
1.20	0.10

D1 (m)	Volume Flow Rate m^3/hr
0.11	25.08
D2 (m)	
0.23	50.17
D3 (m)	
0.34	75.25

Appendix E

E1: Temperature Distribution (°C) vs. Height (m)

Height, y	Heated	Box	Window 1	ECL	Blind	ICL	Window 5	Window 6	Room
@Bottom	Out	1	2	3	4	5	6	7	In
0	**37.78**	38.03	38.04	**25.00**	29.73	**25.00**	30.73	30.22	**25**
0.06096	37.78	38.04	38.07	25.17	29.84	25.06	30.71	30.20	25
0.12192	37.78	38.05	38.09	25.34	29.95	25.13	30.73	30.22	25
0.18288	37.78	38.06	38.12	25.50	30.06	25.19	30.75	30.23	25
0.24384	37.78	38.07	38.15	25.67	30.16	25.25	30.76	30.25	25
0.3048	37.78	38.08	38.18	25.83	30.27	25.32	30.78	30.26	25
0.36576	37.78	38.09	38.20	25.99	30.38	25.38	30.79	30.28	25
0.42672	37.78	38.10	38.23	26.15	30.48	25.45	30.81	30.29	25
0.48768	37.78	38.11	38.26	26.31	30.58	25.51	30.83	30.30	25
0.54864	37.78	38.11	38.28	26.46	30.69	25.58	30.84	30.32	25
0.6096	37.78	38.12	38.31	26.61	30.79	25.65	30.86	30.33	25
0.67056	37.78	38.13	38.33	26.76	30.89	25.71	30.87	30.35	25
0.73152	37.78	38.14	38.36	26.91	30.99	25.78	30.89	30.36	25
0.79248	37.78	38.15	38.38	27.06	31.09	25.85	30.90	30.37	25
0.85344	37.78	38.16	38.41	27.21	31.19	25.92	30.92	30.39	25
0.9144	37.78	38.17	38.43	27.35	31.29	25.98	30.93	30.40	25
0.97536	37.78	38.18	38.46	27.49	31.39	26.05	30.95	30.42	25
1.03632	37.78	38.19	38.48	27.63	31.48	26.12	30.96	30.43	25
1.09728	37.78	38.20	38.50	27.77	31.58	26.19	30.98	30.44	25
1.15824	37.78	38.20	38.53	27.91	31.67	26.26	30.99	30.46	25
1.2192	37.78	38.21	38.55	28.05	31.77	26.33	31.01	30.47	25

E2: Temperature vs. partition number

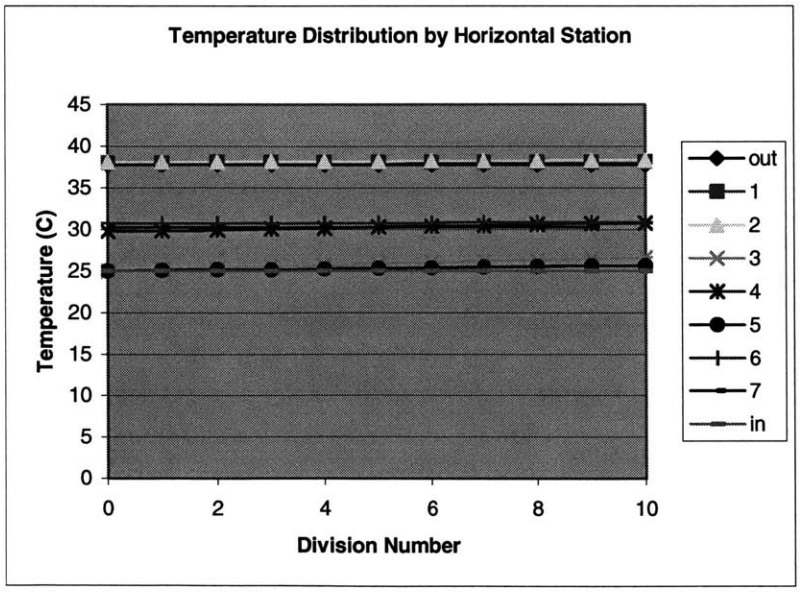

E3: Heat Transfer coefficients at different Horizontal Stations

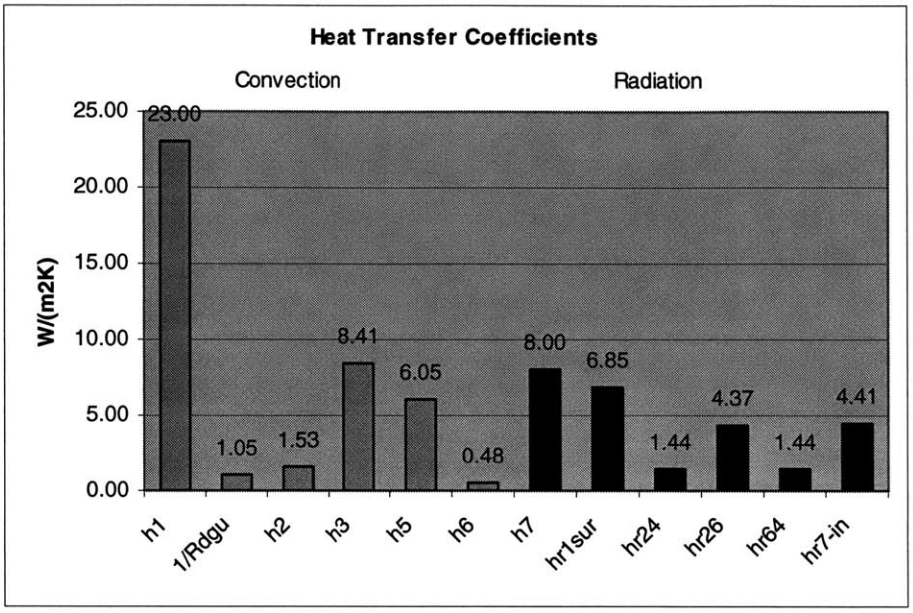

E4: Temperature vs. Horizontal Position at different vertical heights

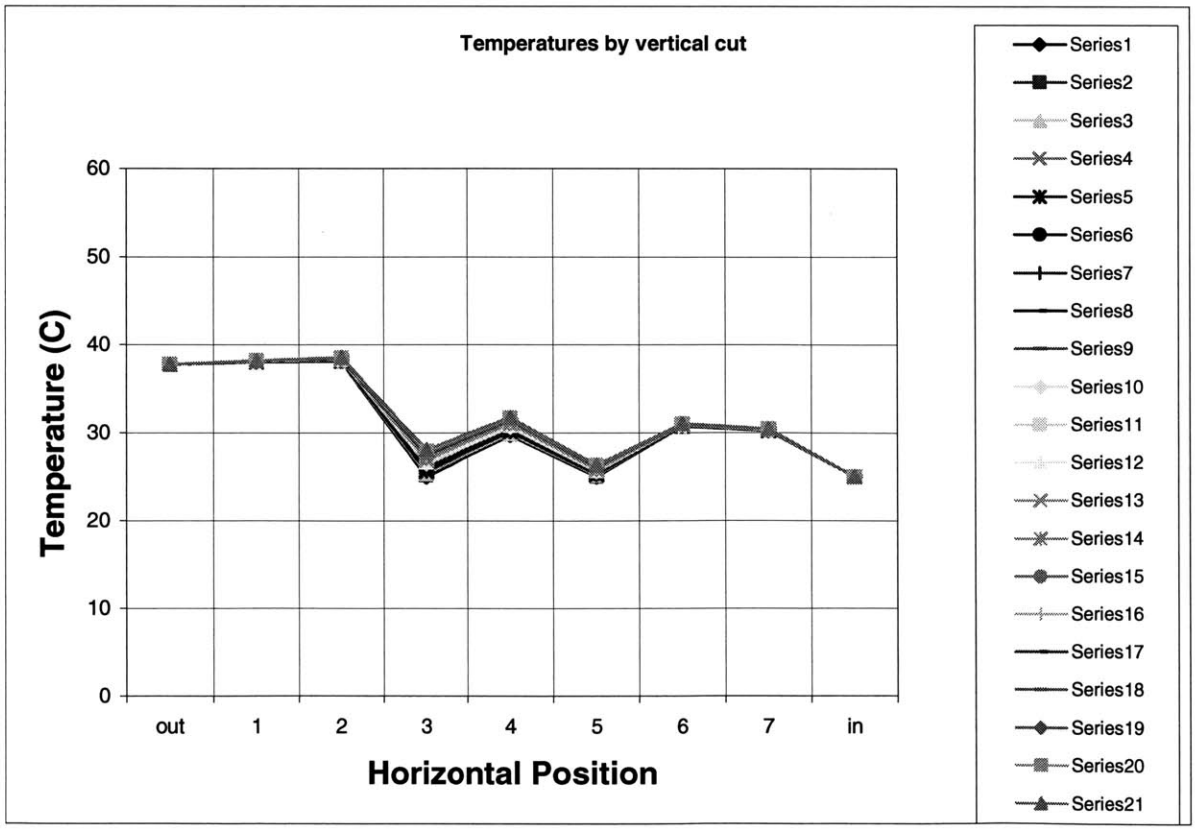

E5: Solar Heat Gain Coefficient (SHGC) vs. Air Flow Rate

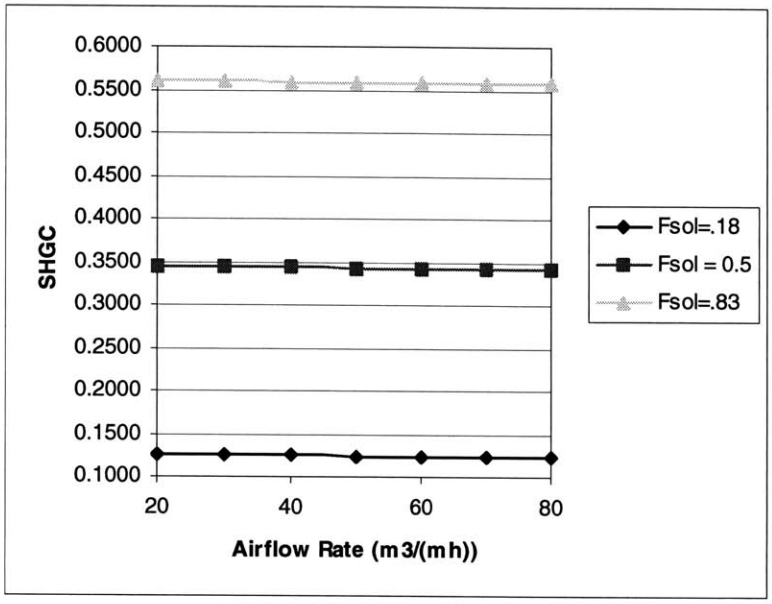

E6: Heat Transfer Coefficient (h_{conv}) vs. Air Velocity

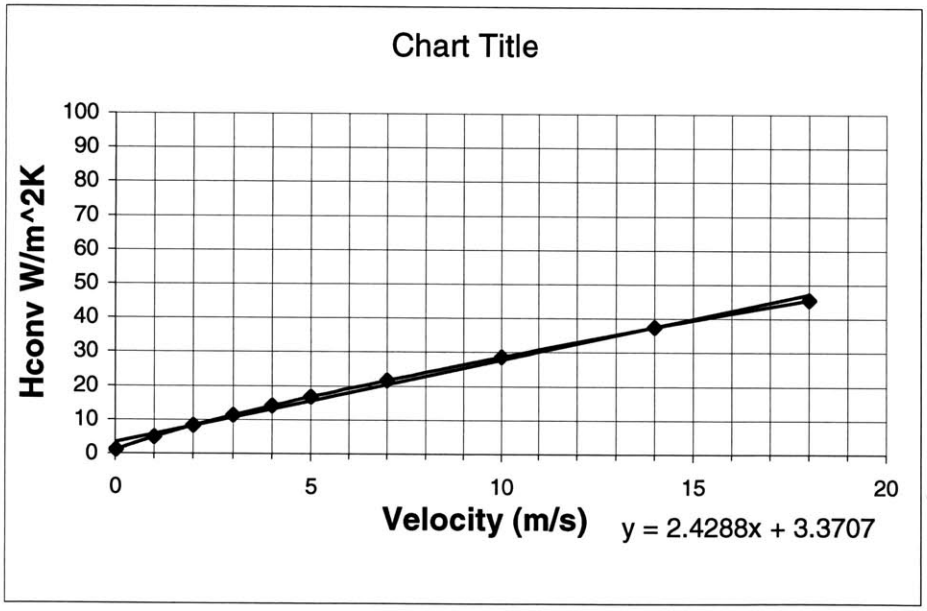

E7: Solar Altitude vs. Solar Heat Gain Coefficient

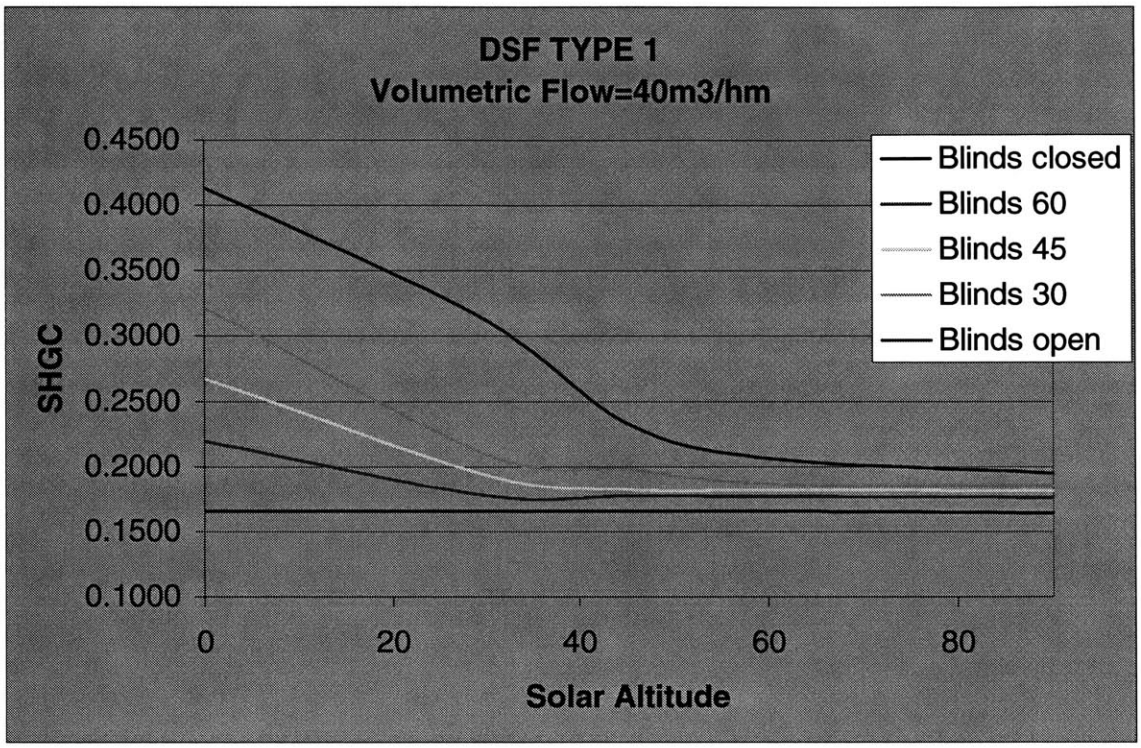

Appendix F

F1. Comparison of Model and Data of Group A (error = 2.05%)

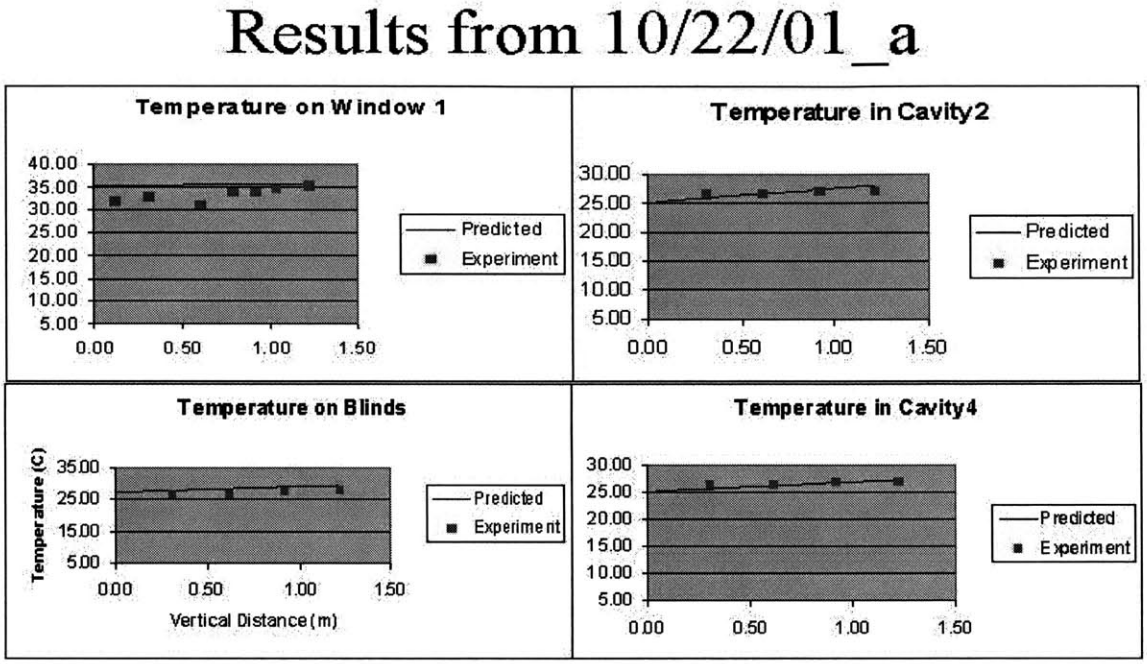

F2. Comparison of Model and Data Group A (error = 2.05%)

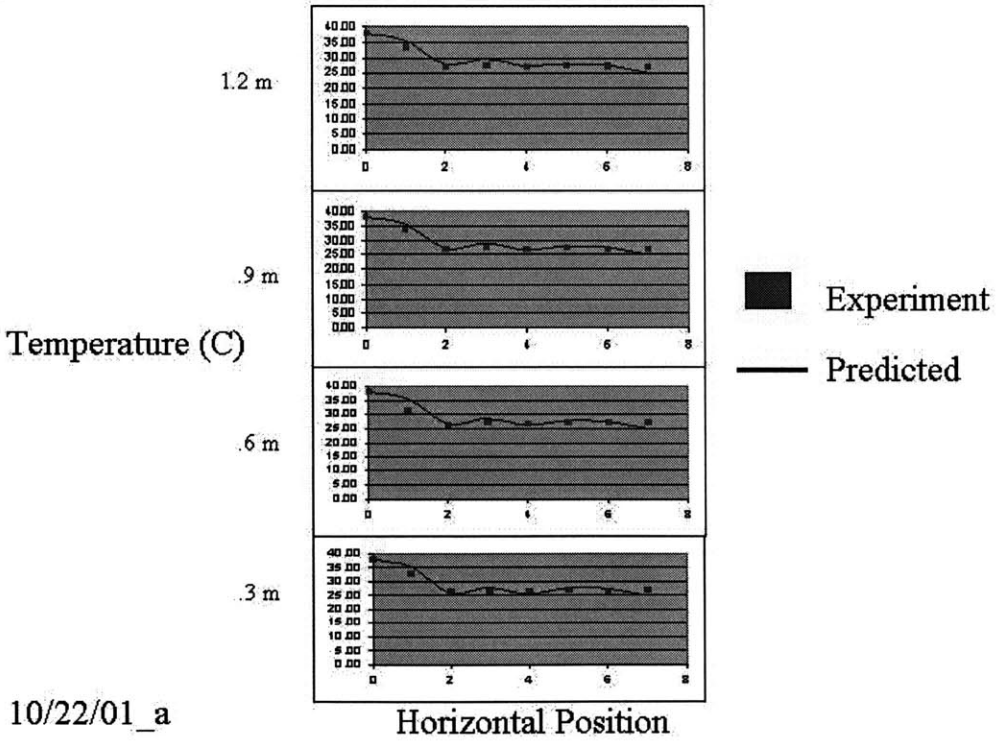

F3. Comparison of Model and Data Group B (error = 1.80%)

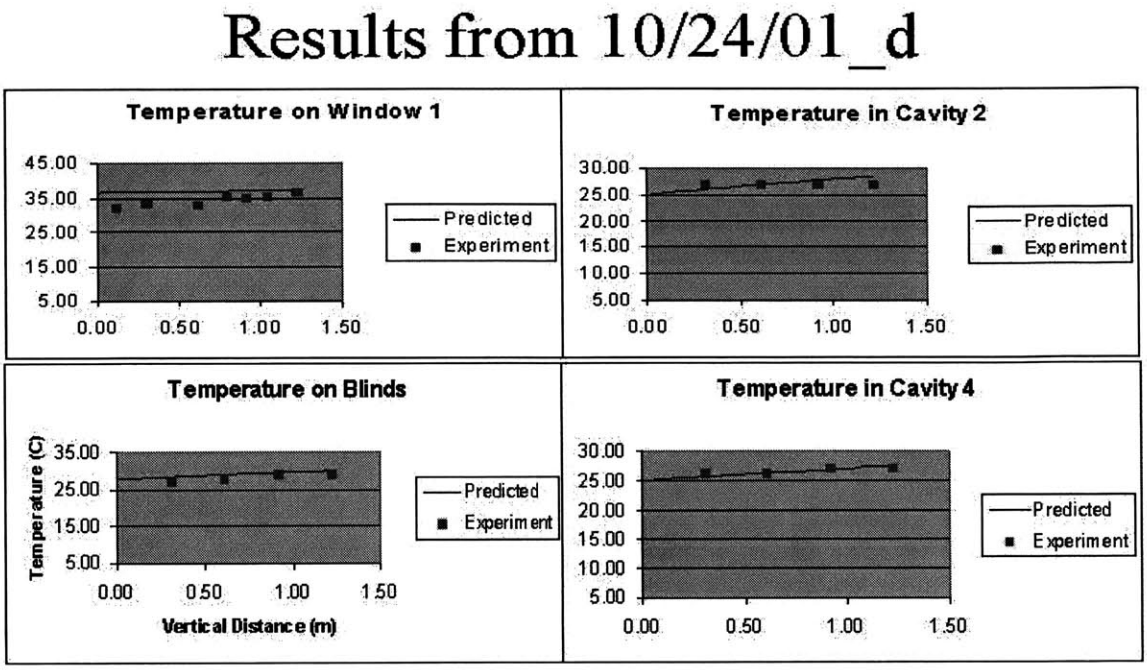

F4. Comparison of Model and Data Group B (error = 1.80%)

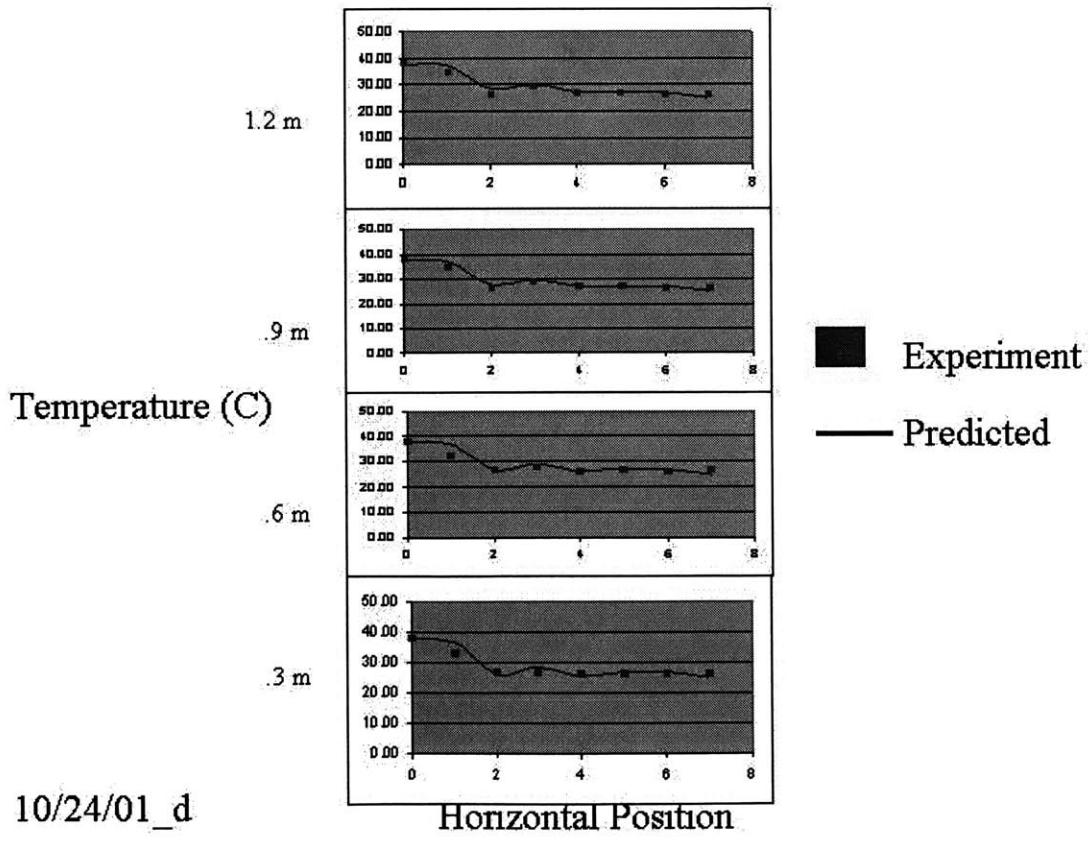

F5. Comparison of Model and Data Group C (error = 2.95%)

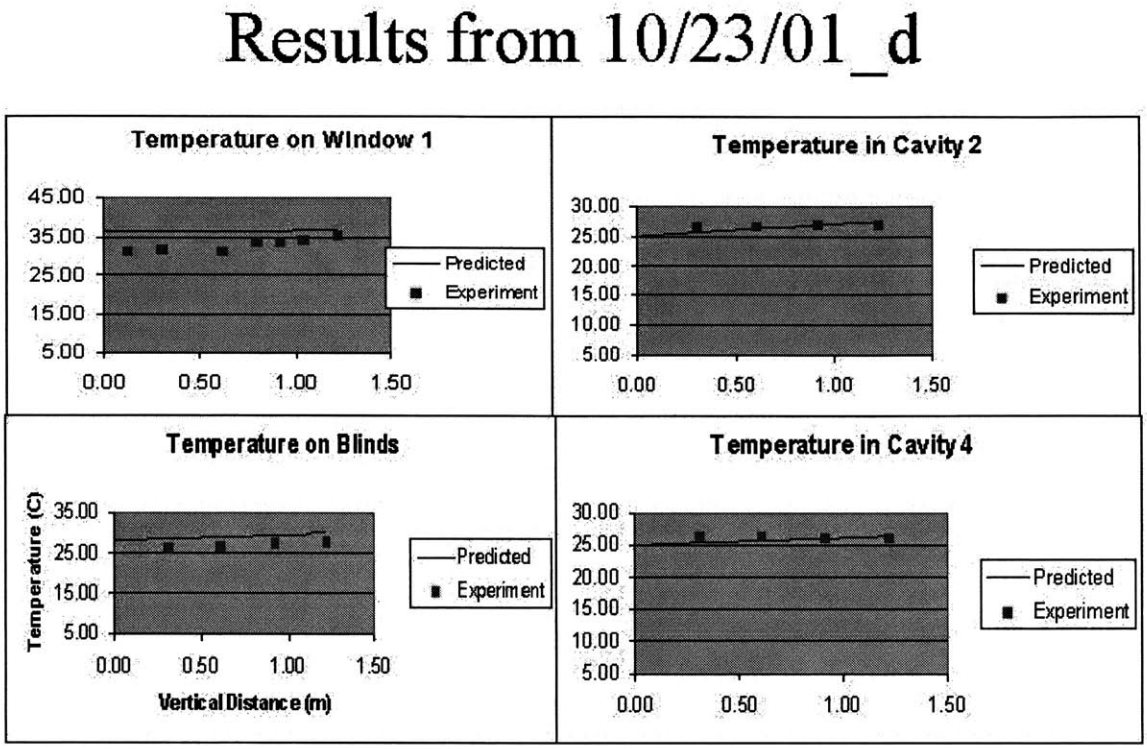

F6. Comparison of Model and Data Group C (error = 2.95%)

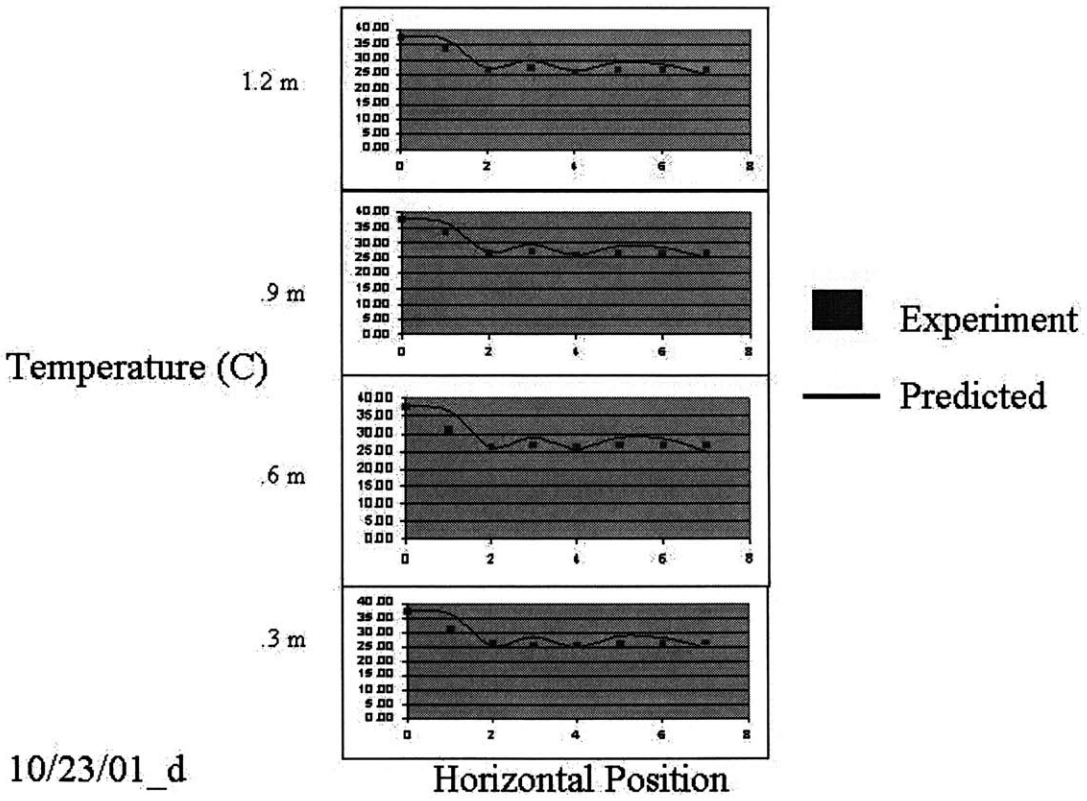

F7. Comparison of Model and Data Group D (error = 2.94%)

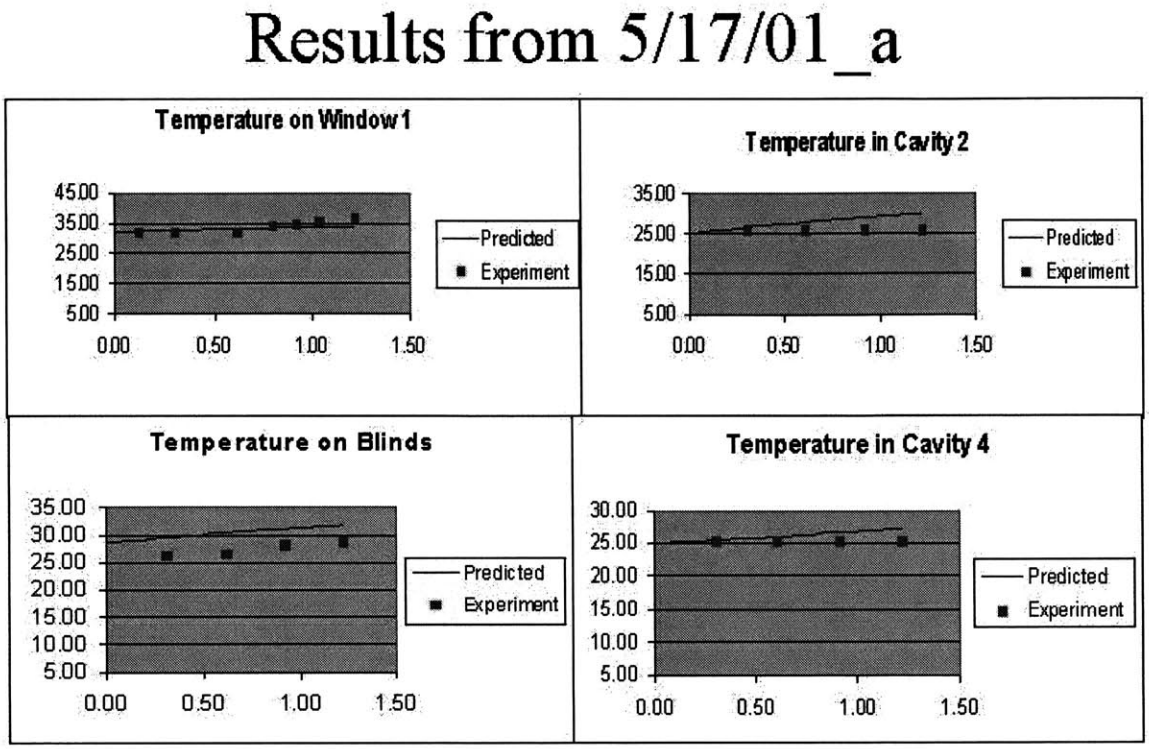

F8. Comparison of Model and Data Group D (error = 2.94%)

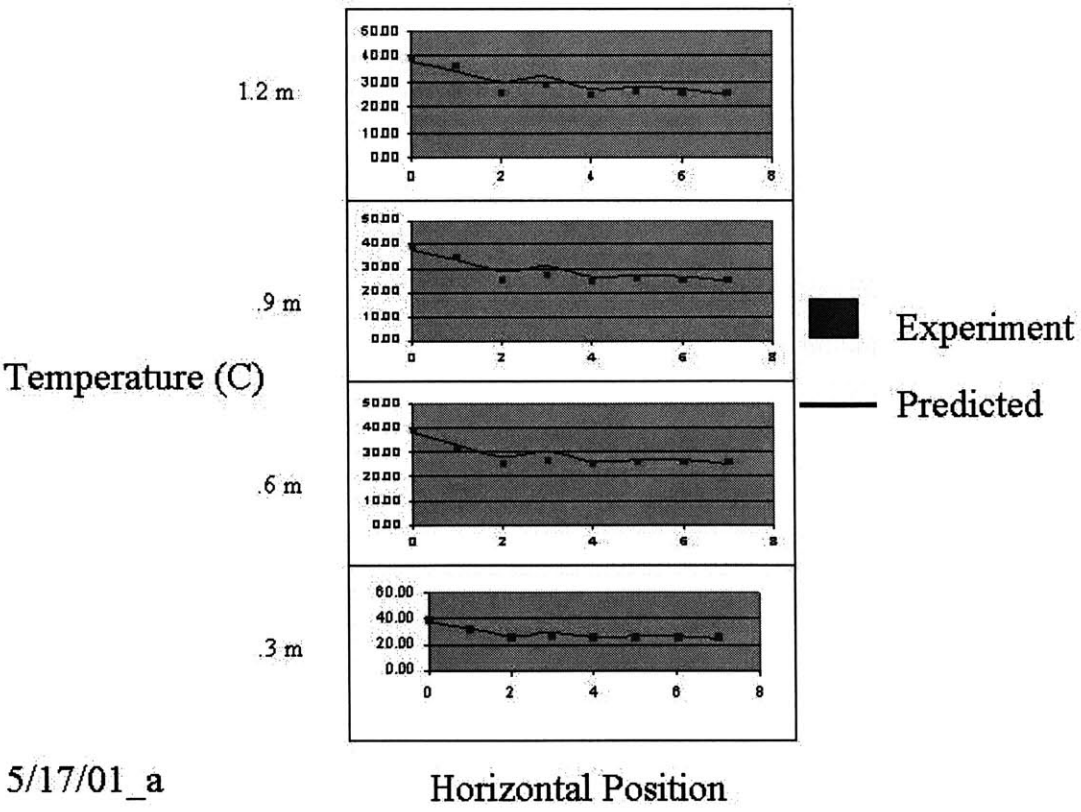

F9. Comparison of Model and Data Group E (error = 4.64%)

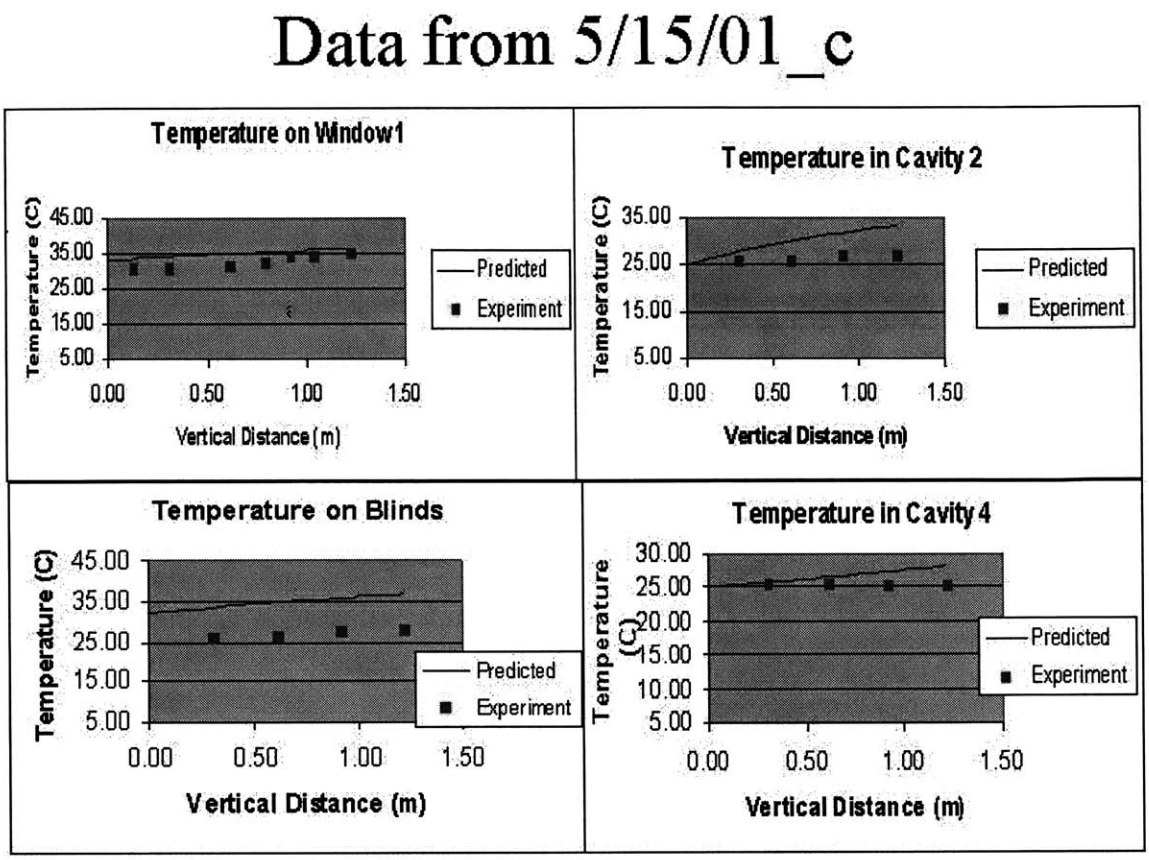

F10. Comparison of Model and Data Group E (error= 4.64%)

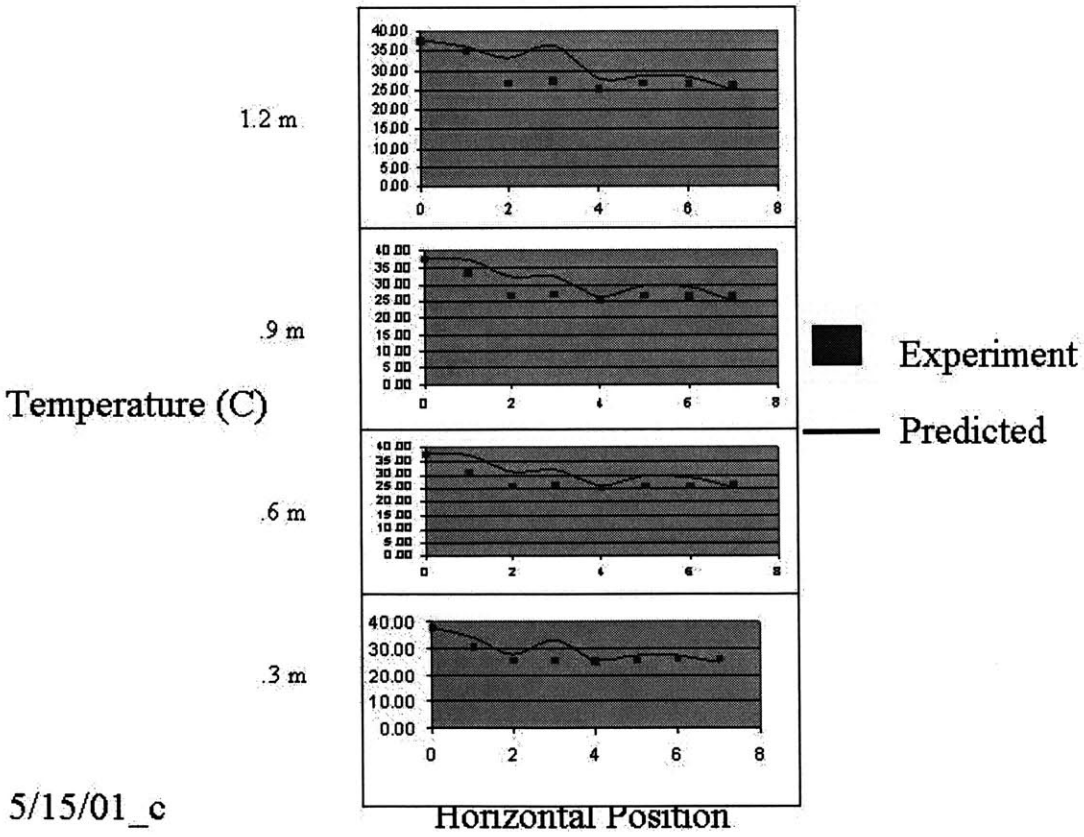

F11. Comparison of Model and Data Group F (error= 4.39%)

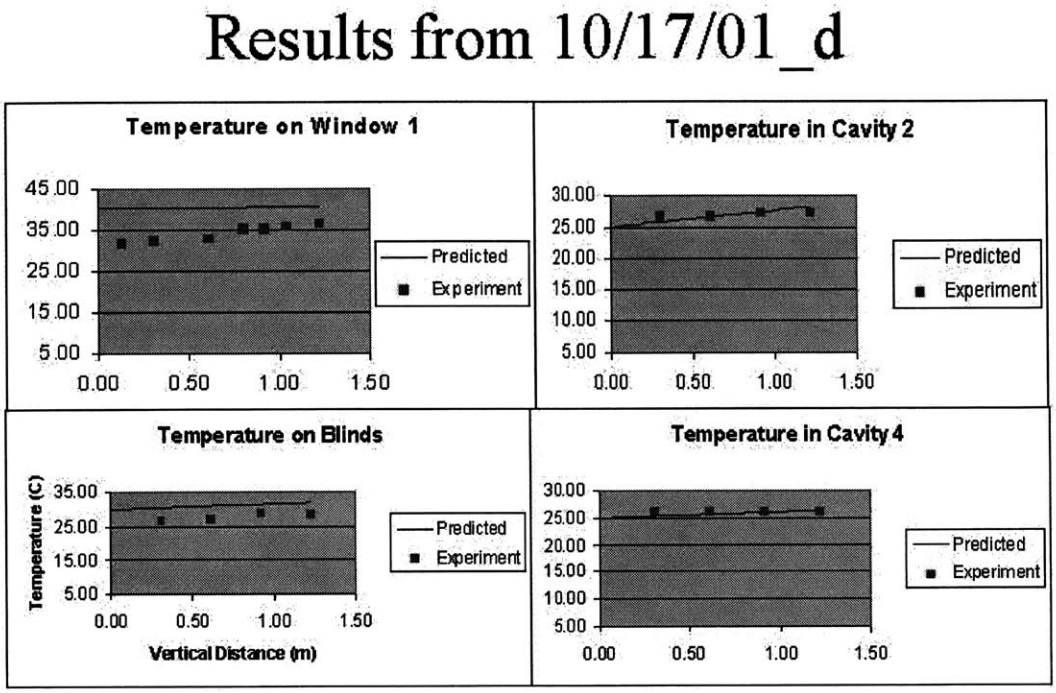

F12. Comparison of Model and Data Group F (error= 4.39%)

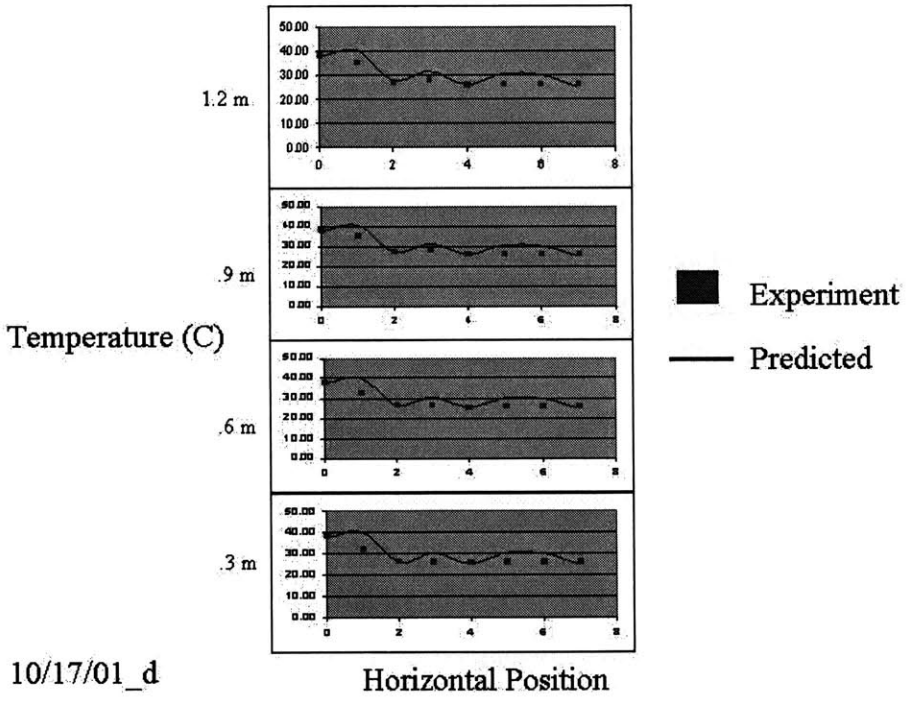

Bibliography

[Arons 2000] Arons, Daniel, " Properties and Applications of Double-Skin Facades", MIT, Cambridge, MA, June 2000.

[Blois-Brooke, Garvin, 1995] Blois-Brooke, TRE, Garvin, SL. Double Glazing units: a BRE guide to improved durability. CRC Ltd. Watford, Herts, 1995.

[Fischer, Gruneis, 1997] Fischer, Volker, Gruneis Horst, Commerzbank, Frankfurt am Maim. Axel Menges, London, 1997 pp. 17-25.

[Hens, Saelens, 1999] Hens, Hugo, Saelens, Dirk, " Low Energy Design and Airflow Windows, some Considerations Illustrated with case study", 10th International Symposium for Building Physics and Building Climatology, 9/1999. Dresden, Germany. 1999.

[Keithley, 2000] Keithley Instruments Inc., " Model 2700 Multimeter/Data Acquisition System User Manual", Cleveland, Ohio, 2/200. A-1.

[Lee, Vine, Selkowitz, DiBartalomeo, 1998] Lee, E., Vine, E., Selkowitz, S., DiBartalomeo, D., "Integrated Performance of an Automated Venetian Blind/ Electric lighting System in a Full Scale Private Office", Thermal Performance of the Exterior Envelope Building VII, 1998.

[Mahan, 1998] Mahan, M., "Strategies for Use of the Building Envelope as a Dynamic Element in Thermal Performance", Thermal Performance of the Exterior Envelope Building VII, 1998.

[Pearson, 1997] Pearson, James, "Delicate Essen", Architectural Review, July 1997, pp. 40-45.

[Robinson, 1970] Robinson, Henry," An Exploratory Study of Laboratory Testing Methods and Standards for Factory-Sealed Double Glazed Window Units", Building Science Series 20: Durability of insulating glass. National Bureau Standards, Washington D.C. February 1970, pp. 45-58.